February 13, 2019

MASTER THESIS

FRAMEWORK FOR COMPARING AND OPTIMIZING OF FULLY ACTUATED MULTIROTOR UAVS

Jelmer Goerres (s1381644)

Faculty of Engineering Technology (CTW)
Mechanics of Solids, Surfaces and Systems (MS3)

Exam committee:
Prof. Dr. Ir. A. de Boer
R.A.M. Rashad Hashem MSc
Dr. Ir. R.G.K.M. Aarts
Dr. Ir. J.B.C. Engelen

Document number:
Mechanics of Solids, Surfaces and Systems (MS3)– ET.18/TM-5843

UNIVERSITY OF TWENTE.

Abstract

Multirotor UAVs (unmanned aerial vehicles) have seen a great growth in popularity in the past years. However the application of these UAVs has been limited to simple flying tasks. For these tasks the optimal UAV design is very straightforward: an in-plane rotor configuration with parallel rotors. Although this design is inherently underactuated, it is able to fly in all required directions by tilting itself towards the desired direction. The application of multirotor UAVs could be expanded when full actuation of the six degree's of freedom (DoFs) could be achieved by the UAV. These applications include: object manipulation, assembly, contact inspection tasks, etcetera.

To achieve full actuation, the UAV needs to be able to produce thrust in all directions and the thrust generated by only parallel rotors will no longer suffice. The optimal rotor configuration is no longer straightforward, but depends on the requirements of the application. In order to find the optimal rotor configuration for any application, a framework is presented that compares available fully actuated UAV concepts with a set of qualitative criteria, such as: design complexity and flying stability, as well as a set of quantitative criteria that compare the wrench and accelerations of the concepts. These criteria are general and are used to evaluate the strengths and weaknesses of a number of concepts found in literature. In this way the framework can be applied for any application, as a first step to determine the optimal rotor configuration. To demonstrate the usability of the framework, two UAVs have been developed for two different applications that require full actuation.

The first application is a large crop spraying UAV. Due to the great width and low flying height, this UAV can only roll very little before colliding with the ground. To be able to withstand side-wind disturbance, this UAV needs to be able to translate in sideways direction without changing orientation, so horizontal actuation is required. The optimization of this UAV yielded a UAV with optimized rotor positions and a number of rotor tilt configurations that can be applied for different wind speeds. This optimization shows how the framework can be used to create a multirotor design with very specific requirements and limitations.

The second application is a human interacting UAV. This UAV needs to be omnidirectional to response to any wrench applied to it by humans. The optimization of the rotor configuration of this UAV has been done for six, eight and ten rotors, using a scalar measure for the entire achievable acceleration called the dynamic manoeuvrability. The optimization yielded a number of solutions for coupled and decoupled dynamic manoeuvrability, as well as a solution with high thrust efficiency. These solutions have been compared extensively, resulting in a UAV with high flying efficiency and high omnidirectional accelerations, as well as a better insight in the applicability of dynamic manoeuvrability in the optimization of UAVs.

The optimization for the crop spraying UAV and the the human interacting UAV shows that the framework can be applied for a wide range of applications.

Contents

Chapter 1

Introduction

Unmanned aerial vehicles (UAVs) have seen a great growth in popularity in the past years. A UAV is an aircraft without human pilot, as the name suggest. To categorize UAVs, Nonani et al. [1] suggested three categories:

- Fixed wing UAVs: UAVs use the lift produced by the airflow around its fixed wings to fly, as shown in figure 1.1a. This type of UAV is able to fly with low power consumption, similar to an airplane.
- Rotary wing UAVs: UAVs that can fly due to the lift produced by rotating its wings, also known as propellers, as shown in figure 1.1b. This type of UAV is able to take of and land vertically (VTOL).
- Lighter than air UAVs: UAVs that fly because the density is lower than air, as shown in figure 1.1c. This type of UAV reaches the highest endurance, however the speed is very limited and the size is generally very large.

A fourth category can be specified as a combination of any of these categories: hybrid UAVs, as shown in figure 1.1d, where a fixed wing is combined with a rotary wing to fly with low power consumption while allowing VTOL.

(a) Fixed wing UAVs

(b) Rotary wing UAVs

(c) Lighter than air UAVs

(d) Hybrid UAVs

Figure 1.1: Different categories of UAVs

This report will focus on a special type of rotary wing UAVs: multirotor UAVs. These UAVs consist of a number of rotors that can create wrench in multiple directions by rotation of the different propellers. By far the most common multirotor UAV is the quadrotor UAV, which consists of four parallel rotors placed around the axis transverse to the plane of the rotors. The UAV moves in vertical direction if all rotors create the same thrust and tilts if the rotor thrust varies. Because all rotors are parallel, this UAV is inherently underactuated and cannot actuate the horizontal translation. However, coupled translation is possible if the UAV rotates itself in an orientation where the rotors are not facing upward. In this orientation the rotors will produce some horizontal thrust and the UAV will move in the direction the rotors are facing, enabling it to fly forward and sideways despite the underactuation. This UAV design is the simplest design that is able to fly in all required directions and is applicable in a wide range of application due to this simple design and low costs. These applications consist of, but are not limited to: Photography, military scouting, delivery and even racing.

The underactuated nature of this type of UAV is allowed for these application. However, the applicability of UAVs could be expanded if full actuation of the degrees of freedom (DoFs) could be achieved:

- Physical interaction: object manipulation [2], assembly [3], contact inspection tasks [4] and wall contact [5]
- Applications that do not allow rotations: transport of payload that is not allowed to move (liquids, injured passengers, organs), peg in hole operation [6]
- Application that require flight a specific orientation: landing on an inclined surface [7].

1.1 Problem description

Recently, a lot of research is done to find ways of achieving the horizontal actuation required for these applications. The difficulty of this is the increase in design variables. For underactuated concepts, the orientation of the rotors is already specified to be vertical and the optimal rotor position is an in-plane symmetric configuration.When full actuation is required the orientation of the rotors needs to be altered, which results in a wide range of possible rotor configurations. Depending on the requirements of the application, this results in a wide range of different possible concepts. Since these concept are so vastly different and designed for different application, the difficulty is finding a general set of criteria to consider when designing a fully actuated UAV. Although fully actuated UAVs are currently considered complex, it is expected that, as with all new developments, the complexity will decrease as they are investigated and applied more. To stimulate the application of fully actuated drone, this study is done to create a framework that compares fully actuated UAVs and can be used to design a new UAV for any application that requires full actuation, which is not yet done in literature. This results in the following research question:

How to optimize the rotor configuration of a UAV for any application requiring full actuation based on a framework of existing fully actuated multirotor concepts?

1.2 Contributions

The research question consists of two parts: creating the framework for comparing fully actuated concepts and showing how to optimize the rotor configuration of a UAV for an application that requires full actuation based on this framework. Before the framework can be made a literature study is required to determine which fully actuated UAVs are available and what the significant differences between these concepts are. Based on this study the UAVs have been separated into two groups: fixed tilt concepts and variable tilt concepts. Due to a different type of actuation it is considered that making an objective and unbiased comparison between these groups of concepts is very difficult. The framework is split up into two categories: Fixed tilt rotor concepts and variable tilt rotor concepts. It should be noted that there are a number of hybrid concepts that achieve full actuation, as shown in appendix A, however this type of UAV is not considered in this thesis.

For the development of the framework, a set of quantitative and qualitative criteria has been developed that cover the criteria an application might have. The qualitative criteria consist of observable properties that can be compared based on a grading. This grading is based on the information given by the designer of the concepts. These criteria are chosen such that they can be graded independent of the application of the UAV. The quantitative criteria are based on the statics and dynamics of the concepts and give an insight in the so-called manoeuvrability. The different criteria can be given different importance based on the application in order to find the best performing concept for that application. In this comparison only the design of UAVs is considered. The actual control will not be discussed. To compare the performance of different UAVs it is assumed that the control is sufficient for reaching the maximum possible performance.

The resulting framework can be used as a first step for determining the optimal rotor configuration for any application that requires horizontal actuation. After the best concept is found the rotor configuration can be optimized based on this concept. To show the usability of the framework two UAVs have been developed for two applications that require horizontal actuation: a crop spraying UAV and a human interacting UAV.

1.3 Organization

This report is divided into 8 chapters. In chapter 2, general background for multirotor UAVs is presented. This background has been referred to throughout the report. This background consists of the static and dynamic description of any UAV and a number of general considerations, all based on earlier work done on UAVs.

In chapter 3 a large number of different fully actuated UAV concepts that are found in literature are introduced. The concepts are described with a brief summary of the specifics as given in the quoted reference, the rotor configuration and the mapping matrix, which is explained in chapter 2.

In chapter 4 the qualitative and quantitative criteria that are used in the framework to compare the concepts are considered. For the quantitative criteria the accompanying mathematics are given.

In chapter 5 the framework is presented. This framework compares the fully actuated UAV concepts described in chapter 3 based on the qualitative- and quantitative criteria specified in chapter 4.

In chapter 6 the first application of the framework is demonstrated: A crop spraying UAV. This chapter consists of a description of the problem, specific requirements and a concept choice based on the framework of chapter 5. This chosen concept has then been optimized such that it will be able perform optimally while fulfilling all requirements for this application.

In chapter 7, the optimization of a UAV for a second application of the framework is shown. In this chapter the complete rotor configuration of the UAV is optimized for human interaction. This rotor configuration is based on the framework and optimized using a scalar measure for omnidirectional acceleration called dynamic manoeuvrability, which is described in chapter 2.

Lastly, in chapter 8, a conclusion of the entire study is given based on the conclusions from all the earlier chapters.

Chapter 2

Background

In this chapter, the calculations used to quantitative describe the performance of any UAV are explained. These calculations have been used throughout the report to compare different fully actuated UAV designs and to optimize the rotor configuration of a UAV. In this chapter the static wrench analysis of a UAV in section 2.3, as well as the dynamic measure in section 2.4. Next an alternative method used to determine the static and dynamic performance for variable tilt concepts is described, followed by a description of a method to describe the entire kinematic or dynamic performance with a single scalar measure; The kinematic and dynamic manoeuvrability, in section 2.5.1. Lastly a method to determine the airflow interference between rotors is given in section 2.6.

2.1 Coordinate Frame

There are a number of relevant coordinate frames that are defined in $\mathbb{R}^3$. The first coordinate frame is the inertial world frame: $\mathcal{F}_\mathcal{W} = \{O_W, x_W, y_W, z_W\}$ where O_W is the origin, which is placed arbitrarily. The principle directions z_W is placed parallel to the direction of the gravity and x_W and y_w are the two directions in the horizontal plane.

Next to $\mathcal{F}_\mathcal{W}$, the body fixed frame is defined as the $\mathcal{F}_\mathcal{B} = \{O_B, x_B, y_B, z_B\}$. Origin O_B coincides with the center of mass (CoM) of the UAV. z_B is the vertical direction, which is the defined direction the UAV will ascend, x_B is the longitudinal direction, which is the direction where the horizontal force is the highest and y_B is the direction transverse to the longitudinal and the vertical direction. These directions are depicted in figure 2.1a, along with the three principle rotation directions: pitch (rotation around the y-axis), roll (rotation around the x-axis) and yaw (rotation around the z-axis). Note that x_B and y_B can be chosen arbitrarily if the horizontal direction is not actuated. For convenience it is advised to coincide the body fixed frame with the inertial world frame, as shown in chapter 4.2.1.

Lastly the rotor fixed frame is defined as $\mathcal{F}_{r,i} = \{O_{r,i}, x_{r,i}, y_{r,i}, z_{r,i}\}$, where $O_{r,i}$ coincides with the CoM of rotor i. The principle axes z_i is in vertical direction, equal to z_B. $x_{r,i}$ is parallel to the axis between O_B and $O_{r,i}$ and $y_{r,i}$ is transverse to $x_{r,i}$ and $z_{r,i}$, as shown in figure 2.1b.

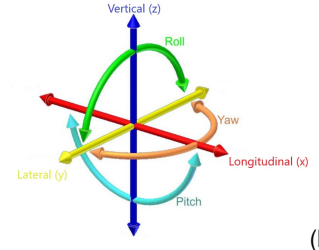

(a) Definition of $\mathcal{F}_\mathcal{B}$ [8]

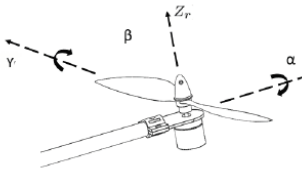

(b) Definition of tilting angles α and β [9]

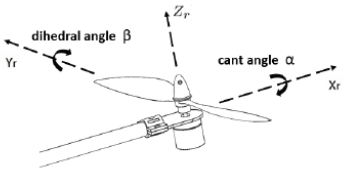

(c) Definition of cant angle and dihedral [9]

Figure 2.1: Definition of the principle directions of the coordinate frames

2.2 Rotor Configuration

The rotor configuration in $\mathcal{F}_\mathcal{W}$ of any UAV can be expressed with two matrices: the orientation of the rotors, given by **u**, and the position of the CoM of the rotor, given by **r**, given by:

$$\mathbf{u} = \begin{bmatrix} \vec{u_1} & \vec{u_2} & ... & \vec{u_n} \end{bmatrix} \tag{2.1}$$

$$\mathbf{r} = \begin{bmatrix} \vec{r_1} & \vec{r_2} & ... & \vec{r_n} \end{bmatrix} \tag{2.2}$$

where $\vec{u_i}$ and $\vec{r_i}$ give the $\mathbb{R}^3$ rotor orientation and position respectively and n is the amount of rotors the UAV consists of. The orientation vector of rotor i ($\vec{u_i}$) can be described with two angles. A third angle is not necessary, because the rotor rotates around its axis, making this angle irrelevant for the orientation. The two angles can be defined a number of ways. In this report they are defined as the rotation around the x-axis and the rotation around the y-axis, as shown in figure 2.1c. Here α defines the rotation around the x-axis and β defines the rotation around the y-axis of the body fixed frame. The position of the CoM of rotor i ($\vec{r_i}$), is given in Cartesian coordinates in the body fixed frame. With this definition $\vec{u_i}$ and $\vec{r_i}$ are given by:

$$\vec{u_i} = \begin{Bmatrix} \sin(\beta_i) \\ -\cos(\beta_i)\sin(\alpha_i) \\ \cos(\beta_i)\cos(\alpha_i) \end{Bmatrix}, \qquad \vec{r_i} = \begin{Bmatrix} x_i \\ y_i \\ z_i \end{Bmatrix} \tag{2.3}$$

2.2.1 Cant and Dihedral Angle

An alternative definition of the orientation that is often used for UAVs with planar rotor positions, is the two rotation angles around the axis between the CoM and the rotor, referred to as x_r, instead of the x-axis of $\mathcal{F}_\mathcal{W}$. In this definition α is the rotation angle around x_r, referred to as cant angle, and β is the rotation angle around the axis perpendicular to x_r; y_r, referred to as dihedral angle. This definition is shown in figure 2.1b. This definition is often advantageous, as the rotor arm often coincides with the axis between the CoM and the rotors, resulting in clear definition of the rotation around the rotor arm. If the rotor is placed in the xy-plane of $\mathcal{F}_\mathcal{W}$, this definition results in the orientation vector given by:

$$\vec{u_i} \begin{Bmatrix} \sin(\beta_i)\cos(\phi_i) + \cos(\beta_i)\sin(\alpha_i)\sin(\phi_i) \\ \sin(\beta_i)\sin(\phi_i) - \cos(\beta_i)\cos(\phi_i)\sin(\alpha_i) \\ \cos(\alpha_i)\cos(\beta_i) \end{Bmatrix} \tag{2.4}$$

where the ϕ_i is the angle between the positive x-axis of $\mathcal{F}_\mathcal{W}$ and the axis between the CoM and the rotor. This definition can be used for any rotor position, however for out-of-plane rotor configurations, the axis between the CoM and the rotor requires two angles to describe and the definition becomes less attractive to use. Obviously the orientation vector $\vec{u_i}$ should remain the same for any definition of the orientation angles.

2.3 Static Wrench Analysis

After the orientation of the UAV is defined, the static wrench it can produce in $\mathcal{F}_\mathcal{W}$ is given. The wrench a UAV produces depends on the thrust λ produced by each rotor. Based on the vector of all rotor thrust $\vec{\lambda}$ and the position and orientation of the rotor, a static wrench analysis can be done.

$$\vec{W} = \begin{Bmatrix} \vec{f} \\ \vec{\tau} \end{Bmatrix} = \mathbf{M}\vec{\lambda} \tag{2.5}$$

where $\vec{W}$ is the wrench, consisting of three forces (F_x, F_y and F_z) and three torques (τ_x, τ_y and τ_z) around the CoM of the UAV in $\mathcal{F}_\mathcal{W}$. $\vec{\lambda}$ is a n-by-1 vector that gives the thrust produced by each rotor. The 6-by-n matrix $\mathbf{M}$ is the so called mapping matrix that transforms $\vec{\lambda}$ into the three forces, and the rotational mapping matrix this combination of thrust produces. The mapping of the forces is very straightforward, since the torques only need to be rotated to the orientation of the rotor. This part of the mapping matrix is referred to as the translational mapping matrix $\mathbf{M_t}$. Mapping the torque is a bit more complicated: to determine the torque produced by the thrust it needs to be rotated to the orientation of the rotor and multiplied by the arm between the CoM of the rotor and the rotor. This part of the mapping matrix is called the translational mapping matrix, $\mathbf{M_r}$. Next to the torque produced by the rotors, the rotors produce a small torque due to the drag from the rotating propellers. This drag torque depends on the ratio between the rotor thrust and its drag torque, given by γ_i. For multirotor UAVs γ is generally around 0.02 m. The direction of the drag torque depends on the rotation direction of the rotor, given by σ_i. For clockwise rotating rotors σ_i=1 and for counterclockwise rotation σ_i=-1. The mapping matrix is given by:

$$\mathbf{M} = \begin{bmatrix} \mathbf{M_t} \\ \mathbf{M_r} \end{bmatrix} = \begin{bmatrix} \vec{u_1} & ... & \vec{u_n} \\ \vec{r_1} \times \vec{u_1} + \gamma_i\sigma_1\vec{u_1} & ... & \vec{r_n} \times \vec{u_n} + \gamma_n\sigma_n\vec{u_n} \end{bmatrix} \tag{2.6}$$

It should be noted that the mapping matrix has a different unit in the top and bottom part: the first three rows, referred to as the translational part of the mapping matrix,$\mathbf{M_t}$, translates the thrust from the rotors (N) into exerted forces (N), so it is dimensionless, while the last three rows of the mapping matrix, referred to as the rotational part of the mapping matrix,$\mathbf{M_r}$, transforms the thrust (N) into torques (Nm), so this part of the matrix has unit m.

2.3.1 Rotor Thrust generation

The thrust generated by the rotors, λ, depends on the rotation speed of the rotor and the propeller. Two types of rotors are specified: one-directional rotors and two-directional rotors. One-directional rotors can only produce thrust in one direction. λ is defined as:

$$0 \leq \lambda \leq \lambda_{max} \tag{2.7}$$

where λ_{max} is the maximum thrust the rotor can produce, which depends on the maximum rotation speed of the rotor with propeller. This maximum thrust can be determined experimentally and is mostly given by the manufacturer of the motor. Bi-directional rotors are rotors that can produce thrust in positive and negative direction, so λ becomes:

$$-\lambda_{max} \leq \lambda \leq \lambda_{max} \tag{2.8}$$

Bi-directional thrust can be obtained in two ways: variable propeller pitch and variable motor rotation direction. Variable pitch rotors are rarely applicable to the considered UAVs due to the high complexity, costs and the fact that they are not very applicable at small scale.

is mechanically very challenging on generally small scaled UAVs, so for all bi-directional rotors considered in this report motors with variable rotation direction are used.

Although bi-directional rotors provide more actuation possibility than one-directional rotors, there are a number of disadvantages to bi-directional rotors: lower energetic efficiency, lower controllability of the exerted force at low speeds and higher mechanical complexity [10].

Furthermore for bi-directional rotors, so called "ESC-induced singularity" can occur: *"temporary loss of thrust when the reversible rotor changes its rotating direction due to the lack of position sensing (i.e., sensor-less BLDC), which, if not treated properly, makes the UAV behave fairly shaky"* [6]. It should be noted that using variable pitch rotors resolves this problem, because the rotation speed does not need to be changed to change direction, but as mentioned these rotors are generally not used.

2.3.2 Redundancy

The mapping matrix can be used to determine the redundancy of a UAV. Redundancy is defined as the amount of actuators minus the amount of DoFs that are actuated. The columns of the mapping matrix depicts the amount of actuators. The amount of DoFs of the UAV can also be determined using the mapping matrix. When a row of the mapping matrix is empty, it means that this direction is not actuated, so amount of DoFs is given as the amount of non-zero rows of $\mathbf{M}$.

2.3.3 Omnidirectional

A special case of fully actuated UAVs is an Omnidirectional UAV. The difference between the two is that an omnidirectional UAV is able to exert wrench in all DoFs in all directions, while a full actuation only specifies that all DoFs are actuated. An example is a Fully actuated UAV that ascends using the rotor thrust and descends using gravity. This UAV may be able to actuate all DoFs, but not in all directions, so it is not omnidirectional.

2.4 Accelerations

The accelerations achievable by any UAV can be described by the general dynamic equation:

$$\begin{Bmatrix} \vec{a} \\ \vec{\alpha} \end{Bmatrix} = \mathbf{A}\vec{\lambda} \tag{2.9}$$

where a and α are the translational - and angular acceleration of the UAV. The matrix $\mathbf{A}$ is the acceleration mapping matrix, which is a 6-by-n matrix for the 6 DoFs. Note that in this definition the acceleration

is instantaneous: effects of gravity, wind drag etc. are not considered. The acceleration mapping matrix can be written as a function of the mapping matrix:

$$\mathbf{A} = \mathbf{I}^{-1}\mathbf{M} \tag{2.10}$$

Where $\mathbf{I}$ is the inertia matrix, given by:

$$\mathbf{I} = \begin{bmatrix} m_{tot} & 0 & 0 & 0 & 0 & 0 \\ 0 & m_{tot} & 0 & 0 & 0 & 0 \\ 0 & 0 & m_{tot} & 0 & 0 & 0 \\ 0 & 0 & 0 & I_{xx} & I_{xy} & I_{xz} \\ 0 & 0 & 0 & I_{yx} & I_{yy} & I_{yz} \\ 0 & 0 & 0 & I_{zx} & I_{zy} & I_{zz} \end{bmatrix} \tag{2.11}$$

where m_{tot} is the total mass of the UAV and I_{xx} is the mass inertia in x-direction . The mass of a UAV can easily be measure, but this is not the case for the inertia. In most references the inertia is estimated based on a 3D generated model of the UAV. The inertia of the UAV can be approximated as the inertia of a number of mass points. The inertia of these mass points is given by:

$$\mathbf{I} = \sum_{i=1}^{n} m_{mp,i} \begin{bmatrix} r_{2,i}^2 + r_{3,i}^2 & -r_{1,i}r_{2,i} & -r_{1,i}r_{3,i} \\ -r_{1,i}r_{2,i} & r_{1,i}^2 + r_{3,i}^2 & -r_{2,i}r_{3,i} \\ -r_{1,i}r_{3,i} & -r_{2,i}r_{3,i} & r_{1,i}^2 + r_{2,i}^2 \end{bmatrix} \tag{2.12}$$

where $m_{mp,i}$ is the mass of the mass point i and $r_{j,i}$ the position of the mass point i. Similar to $\mathbf{M}$, $\mathbf{A}$ can be separated in the translational accelerations mapping $\mathbf{A_t}$, with unit kg^{-1}, and the angular acceleration mapping $\mathbf{A_r}$, with unit kg^{-1}m^{-1}.

2.5 Variable Tilt Rotors

For concepts that actively actuate the tilt angle of the rotor, the mapping matrix is constantly changing. A variable mapping matrix very undesirable, since the overall performance of the UAV cannot be measured independent of the tilt angle. This calls for another formulation of the mapping matrix for these concepts:

$$W = \mathbf{M}\vec{\lambda} = \mathbf{M}^*\vec{\lambda^*} \tag{2.13}$$

Where $\vec{\lambda^*}$ is the thrust produced by the rotor expressed in Cartesian coordinates and $\mathbf{M}^*$ is the mapping matrix independent of the tilt angle of the rotors. With the notation of $\vec{\lambda^*}$, the tilting of the rotor is included in the expression of the thrust. For one variable tilting angle α, $\vec{\lambda^*}$ becomes:

$$\vec{\lambda^*} = \begin{Bmatrix} \lambda_1 \cos(\alpha_1) \\ \lambda_1 \sin(\alpha_1) \\ \lambda_2 \cos(\alpha_2) \\ \lambda_2 \sin(\alpha_2) \\ \vdots \\ \lambda_N \cos(\alpha_N) \\ \lambda_N \sin(\alpha_N) \end{Bmatrix} \tag{2.14}$$

By defining it in the thrust vector, the variable angle α is omitted from the mapping matrix. The non-variable mapping matrix $\mathbf{M}^*$ should be adapted to $\vec{\lambda^*}$, such that the resulting wrench is correct for all tilt angles. As an example, consider a canted rotor given by:

$$\vec{u_i} = \begin{Bmatrix} \sin(\alpha_i)\sin(\phi_i) \\ -\cos(\phi_i)\sin(\alpha_i) \\ \cos(\alpha_i) \end{Bmatrix}, \qquad \vec{r_i} = l \begin{Bmatrix} \cos(\phi) \\ \sin(\phi) \\ 0 \end{Bmatrix} \tag{2.15}$$

where ϕ is the angle around the z-axis of the rotor position. This configuration yields a wrench of:

$$\vec{W_i} = \vec{M^i}\lambda_i = \begin{bmatrix} \sin(\alpha_i)\sin(\phi_i) \\ -\cos(\phi_i)\sin(\alpha_i) \\ \cos(\alpha_i) \\ \sin(\phi_i)(l\cos(\alpha_i) + \gamma\sigma_i \sin(\alpha_i)) \\ -\cos(\phi_i)(l\cos(\alpha_i) + \gamma\sigma_i \sin(\alpha_i)) \\ \gamma\sigma_i \cos(\alpha_i) - l\sin(\alpha_i) \end{bmatrix} \lambda_i \tag{2.16}$$

where $\vec{M^i}$ is the mapping matrix of the rotor. Based on this definition of $\vec{M^i}$ and $\vec{\lambda}^*$ in equation 2.14, the non-variable mapping matrix of this rotor $\mathbf{M^{i^*}}$ can be determined:

$$\mathbf{W} = \mathbf{M^{i^*}}\vec{\lambda}^* = \begin{bmatrix} 0 & \sin(\phi_i) \\ 0 & -\cos(\phi_i) \\ 1 & 0 \\ l\sin(\phi_i) & \gamma\sigma_i\sin(\phi_i) \\ -l\cos(\phi_i) & -\gamma\sigma_i\cos(\phi_i) \\ \gamma\sigma_i & -l \end{bmatrix} \begin{Bmatrix} \lambda_i\cos(\alpha_i) \\ \lambda_i\sin(\alpha_i) \end{Bmatrix} = \begin{bmatrix} \sin(\alpha_i)\sin(\phi_i) \\ -\cos(\phi_i)\sin(\alpha_i) \\ \cos(\alpha_i) \\ \sin(\phi_i)(l\cos(\alpha_i) + \gamma\sigma_i\sin(\alpha_i)) \\ -\cos(\phi_i)(l\cos(\alpha_i) + \gamma\sigma_i\sin(\alpha_i)) \\ \gamma\sigma_i\cos(\alpha_i) - l\sin(\alpha_i) \end{bmatrix} \lambda_i \tag{2.17}$$

Note that with this notation each rotor now adds two columns to the mapping matrix instead of one. This means that each variable tilt rotor contributes double to the redundancy, as discussed in section 2.3.2. The extra redundancy results from the addition of an actuator, the tilt actuator, which is used to actively tilt the rotors. For two tilting angles $\hat{\lambda}$ becomes:

$$\{\hat{\lambda}\} = \begin{Bmatrix} \lambda_1\cos(\alpha_1)\sin(\beta_1) \\ \lambda_1\cos(\alpha_1)\cos(\alpha_1) \\ \lambda_1\sin(\alpha_1) \\ \lambda_2\cos(\alpha_2)\sin(\beta_2) \\ \lambda_2\cos(\alpha_2)\cos(\beta_2) \\ \lambda_2\sin(\alpha_2) \\ \vdots \\ \lambda_n\cos(\alpha_n)\sin(\beta_n) \\ \lambda_n\cos(\alpha_n)\cos(\alpha_n) \\ \lambda_n\sin(\alpha_n) \end{Bmatrix} \tag{2.18}$$

Again the amount of columns this rotor adds to the mapping matrix increases by one. With two tilt rotors each rotor adds three actuators to the redundancy. For the tilting, two types of actuator are available: brushless motors and servo motors. Brushless motors are more expensive, while servo actuators have a limited rotation angles, which limits the possible tilting angles. In this report, it is assumed that tilt angle of the rotors is not constrained by the tilt actuator type for an unbiased comparison between variable tilt concepts. This effectively signifies brushless motors are used for all concepts.

2.5.1 Manoeuvrability

In this section a scalar measure for the performance of a system based on the mapping matrix is presented: the manoeuvrability. This measure has been proposed by Yoshiwada [11] to assess the kinematic manipulability of robotic arms and extended the measure to the dynamic manipulability [12]. Kiso et al. [13] showed that this measure can also be applied in the optimization of the a fully actuated hexarotor. The measure could be used to compare the kinematic performance of any fully actuated UAV. The measure is given in this report as manoeuvrability instead of manipubility, because UAVs are not designed for manipulating but for manoeuvring. The different naming does not change the definition of the measure.

The manoeuvrability is a measure of the volume spanned by the attainable wrench or accelerations of the system. For kinematic manoeuvrability (w_K) this is the volume of the mapping matrix $\mathbf{M}$, while the dynamic manoeuvrability (w_D) is the volume of the acceleration matrix $\mathbf{A}$. To derive the volume of any $\mathbf{M}$ and $\mathbf{A}$, first the derivation of the manoeuvrability of a square matrix is shown, because in this case the volume is equal to the determinant of the matrix [14]. Consider a UAV with six rotors and six DoFs with a 6-by-6 $\mathbf{M}$. w_K can be written as:

$$w_K = |\det(\mathbf{M})| \tag{2.19}$$

This definition is not generally applicable, because if $\mathbf{M}$ is not a square matrix, which is the case for a redundant UAV, the determinant of the $\mathbf{M}$ cannot be defined with this definition. To be able to determine w_K for redundant UAVs, equation 2.19 can be extended to a general form using two properties that apply for a determinant of a square matrix:

$$\det(\mathbf{M}) = \det(\mathbf{M}^T) \tag{2.20}$$

$$\det(\mathbf{M})\det(\mathbf{M}) = \det(\mathbf{M}\mathbf{M}) \tag{2.21}$$

With these properties the definition of w_K can be extended to:

$$w_K^2 = \det(\mathbf{M})\det(\mathbf{M}) = \det(\mathbf{M}^T\mathbf{M}) = \det(\mathbf{M}\mathbf{M}^T) \tag{2.22}$$

Using this definition the determinant of a non-square matrix can be determined, since $\mathbf{M}\mathbf{M}^T$ and $\mathbf{M}^T\mathbf{M}$ yield a square matrix for any UAV. To prove that this method yields the correct result, any 2-by-2 matrix $\mathbf{P}$ is defined:

$$\mathbf{P} = \begin{bmatrix} p_{11} & p_{12} \\ p_{21} & p_{22} \end{bmatrix} \tag{2.23}$$

(2.24)

The determinant of $\mathbf{P}$ can be determined by the three methods:

$$(\det(\mathbf{P}))^2 = (p_{11}p_{22} - p_{12}p_{21})^2 = p_{11}^2p_{22}^2 - 2p_{11}p_{22}p_{12}p_{21} + p_{12}^2p_{21}^2 \tag{2.25}$$

$$\det(\mathbf{P}^T\mathbf{P}) = (p_{11}^2 + p_{21}^2)(p_{12}^2 + p_{22}^2) - (p_{12} + p_{21}p_{22})(p_{11}p_{12} + p_{21}p_{22}) \tag{2.26}$$

$$= p_{11}^2p_{22}^2 - 2p_{11}p_{12}p_{21}p_{22} + p_{12}^2p_{21}^2 \tag{2.27}$$

It should however be noted that this proof is not general for all matrices, as $\mathbf{P}^T\mathbf{P} \neq \mathbf{P}\mathbf{P}^T$ for non-square matrices. If $\mathbf{P}$ is a 3-by-2 matrix, the inverse will be a 2-by-3 matrix and $\mathbf{P}^T\mathbf{P}$ yields a 2-by-2 matrix with rank two, while $\mathbf{P}\mathbf{P}^T$ yields a 3-by-3 matrix with rank two. In the latter case, the the matrix is rank deficient and the determinant of this matrix will be zero. For a 2-by-3 matrix the opposite is true: $\mathbf{P}^T\mathbf{P}$ is rank deficient and yields a determinant of zero. The following conclusion can be taken from this for any m-by-n matrix $\mathbf{P}$:

$$if \quad m = n, \qquad (\det(\mathbf{P}))^2 = (\det(\mathbf{P}))^2, \tag{2.28}$$

$$if \quad m < n, \qquad (\det(\mathbf{P}))^2 = (\det(\mathbf{P}\mathbf{P}^T))^2, \tag{2.29}$$

$$if \quad m > n, \qquad (\det(\mathbf{P}))^2 = (\det(\mathbf{P}^T\mathbf{P}))^2 \tag{2.30}$$

In the case that $\mathbf{P}$ is the mapping matrix, m is 6 and n is the amount of rotors. So when the amount of rotors $n \geq 6$ equation 2.29 is applicable. When the amount of rotors is lower than 6 the amount of DoFs will always be lower than 6 as well. In that case the mapping matrix will contain rows with only zeros and the determinant will always equal zero. That is why the unactuated rows have to be removed from the mapping matrix for determining the manoeuvrability and m is always lower than or equal to n. The kinematic manoeuvrability for any UAV is thus given by:

$$w_K = \sqrt{\det(\mathbf{M}\mathbf{M}^T)} \tag{2.31}$$

When there is no redundancy, the definition of the kinematic manoeuvrability can still be reduced to equation 2.19. The dynamic manoeuvrability (w_D) is very similar to w_K, but instead of $\mathbf{M}$, the acceleration mapping matrix $\mathbf{A}$ is used:

$$w_D = \sqrt{\det(\mathbf{A}\mathbf{A}^T)} \tag{2.32}$$

When there is no redundancy, the definition of the dynamic manoeuvrability can also be reduced to:

$$w_D = |\det(\mathbf{A})| \tag{2.33}$$

A very important remark is that the volume given by the dynamic manoeuvrability is the entire volume of attainable wrench or accelerations, so for both the positive and the negative thrust λ. For concepts with one-directional rotors, the dynamic manoeuvrability gives a manoeuvrability that unrealizable.

2.5.2 Decoupling

It is often advantageous to decouple the translational and rotational part of the manoeuvrability, as shown by Tadokoro et al. [15]. The dynamic manoeuvrability is separated into translational dynamic manoeuvrability ($w_{A,t}$) and rotational dynamic manoeuvrability ($w_{A,r}$), given by:

$$w_{D,t} = \sqrt{\det(\mathbf{A_t}{\mathbf{A_t}}^T)} \tag{2.34}$$

$$w_{D,r} = \sqrt{\det(\mathbf{A_r}{\mathbf{A_r}}^T)} \tag{2.35}$$

The total dynamic manoeuvrability can be expressed by these two decoupled dynamic manoeuvrability measures:

$$w_D = \sqrt{\det(\mathbf{A}\mathbf{A}^T)} = \sqrt{\det(\begin{bmatrix} \mathbf{A_t} \\ \mathbf{A_r} \end{bmatrix} \begin{bmatrix} {\mathbf{A_t}}^T & {\mathbf{A_r}}^T \end{bmatrix})} \tag{2.36}$$

This can be rewritten using the definition of the determinant of a block matrix [16]:

$$\det(\begin{bmatrix} A & B \\ C & D \end{bmatrix}) = \det(AD - BD^{-1}CD) \tag{2.37}$$

Based on this definition, equation 2.36 can be rewritten to:

$$w_D^2 = \det(\begin{bmatrix} \mathbf{A_t}\mathbf{A_t}^T & \mathbf{A_t}\mathbf{A_r}^T \\ \mathbf{A_r}\mathbf{A_t}^T & \mathbf{A_r}\mathbf{A_r}^T \end{bmatrix}) \tag{2.38}$$

$$= \det(\mathbf{A_t}\mathbf{A_t}^T\mathbf{A_r}\mathbf{A_r}^T - \mathbf{A_t}\mathbf{A_r}^T(\mathbf{A_r}\mathbf{A_r}^T)^{-1}\mathbf{A_r}\mathbf{A_t}^T\mathbf{A_r}\mathbf{A_r}^T) \tag{2.39}$$

$$= \det((\mathbf{A_t} - \mathbf{A_t}\mathbf{A_r}^T(\mathbf{A_r}\mathbf{A_r}^T)^{-1}\mathbf{A_r})\mathbf{A_t}^T)\det(\mathbf{A_r}\mathbf{A_r}^T) \tag{2.40}$$

$$w_D = \sqrt{\det((\mathbf{A_t} - \mathbf{A_t}\mathbf{A_r}^T(\mathbf{A_r}\mathbf{A_r}^T)^{-1}\mathbf{A_r})\mathbf{A_t}^T)} \quad w_{D,r} \tag{2.41}$$

The first part of this definition consists of $w_{D,t}$ and a coupling between the rotation and translation. This coupling term is given by:

$$\mathbf{A_t}\mathbf{A_r}^T(\mathbf{A_r}\mathbf{A_r}^T)^{-1}\mathbf{A_r} \tag{2.42}$$

According to Tadokoro et al. this term depends on the distance between the origin of $\mathcal{F}_\mathcal{W}$ and the point where the wrench is exerted, which is the CoM. When the CoM is defined at the origin of $\mathcal{F}_\mathcal{W}$, as discussed in section 2.1 the whole term is zero and equation 2.41 becomes:

$$w_D = w_{D,t}w_{D,r} \tag{2.43}$$

2.5.3 Unit

The physical interpretation of the dynamic manoeuvrability does require some attention. One inconsistency is the unit of this equation. For the kinematic manoeuvrability the unit depend on the unit of the mapping matrix $\mathbf{M}$. $\mathbf{M_t}$ is unitless, so $w_{K,t}$ is unitless as well. The rotational part $\mathbf{M_r}$ has unit m. Because $w_{K,r}$ is the determinant of $\mathbf{M_r}$, its unit depends on the row size of mapping matrix. For this reason the unit of $w_{K,r}$ depend on the amount of DoFs: m^{n_r}, where n_r is the number of the rotational DoFs. Since $w_{K,t}$ is dimensionless, w_K has the same unit as $w_{K,r}$.

Similarly the unit of the dynamic manoeuvrability is determined. The translational part of the acceleration matrix, A_t has the unit kg^{-1}, so the unit of $w_{D,t}$ is kg^{-n_t}. The rotational part, A_r has unit $\text{kg}^{-1}\text{m}^{-1}$, so the unit of $w_{D,r}$ is $\text{kg}^{-n_r}\text{m}^{-n_r}$, where n_r is the amount of rotational DoFs. This results in a w_D with unit $\text{kg}^{-(n_t+n_r)}\text{m}^{-n_r}$. From this unit inconsistency it could be argued that comparing concepts with different amounts of DoFs yields a biased comparison. The inconsistency in unit will not be a problem when the number of DoFs is equal.

2.6 Airflow Interference

The thrust a rotor produces depends on the airspeed around the rotor. If a rotor is placed in the airflow resulting from the thrust of another rotor, the thrust of this rotor will depend on the the thrust of the other rotor. This coupling between thrust of rotors will make the control of the UAV significantly more complex and will result in a decrease in performance if it is not tackled sufficiently in the control algorithm. For this reason considering the airflow interference between rotors is important in the design of a UAV.

To prevent airflow interference, the minimal required distance from the rotor's airflow for which the effects of the airflow on other rotors can be neglected needs to be determined. This distance can be determined experimentally. This has been done by Park [6] for the optimization of a fully actuated octorotor UAV. This minimal distance from the airflow, called d_{aero}, has been determined experimentally by measuring the wind velocity downstream of a rotor, as shown in figure 2.2a. The airspeed for which the influence of the airflow can be neglected, called the interference-threshold wind speed, is assumed to be 4 m/s. This yields a d_{aero} of 0.125 m, which is almost equal to the rotor diameter. The distance where the downstream air speed is sufficiently low is around 2.4 m, so the rotors should not be placed below each other unless the distance between the rotors is very high.

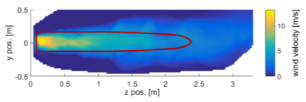

(a) *"Anemometer measurement of wind velocity distribution downstream the rotor generating thrust required for hovering, also marked with interference-threshold wind speed to be 4 m/s."* [6]

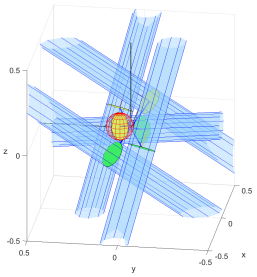

(b) Visualization of the airflow interference from rotor 1. There is no airflow interference, since the (blue) cylinder depicting the airflow and the (red) sphere around the rotors do not intersect.

Figure 2.2: Airflow interference

In order to check whether the rotors are placed inside the airflow from another rotor, first the airflow produced by the rotors is specified as a line between the upper and lower limit of the airflow of the rotor, $\vec{f_r}^u$ and $\vec{f_r}^l$ respectively. These limits are given for rotor i, :

$$\vec{f_{r,i}}^u = \vec{r_i} + \delta d_{aero,z}\vec{u_i} \tag{2.44}$$

$$\vec{f_{r,i}}^l = \vec{r_i} - d_{aero,z}\vec{u_i} \tag{2.45}$$

where $d_{aero,z}$ is the z-distance from the rotor where the airflow is below 4 m/s (see figure 2.2a). The variable δ is used to specify the difference between one-directional and bi-directional rotors: For bi-directional rotors δ=1, because these rotors can produce airflow in two directions. For one-directional rotors the only direction airflow is produced is downward, so δ=0. Note that the orientation $\vec{u}$ is defined as the direction the rotors produce thrust in, so the airflow will be in negative direction in this case.

Next the distance between a rotors and the airflow from another rotor is given as the line crossing the position of rotor j transverse to the line between the upper and lower limit of the airflow from the other rotor i, which is give by:

$$a = \vec{f_{r,i}}^u - \vec{f_{r,i}}^l \tag{2.46}$$

$$b = r_j - \vec{f_{r,i}}^l \tag{2.47}$$

$$d = \frac{||a \times b||}{||a||} \tag{2.48}$$

where r_j is the position of the rotor j and d the minimum distance between rotor j and the airflow of rotor i. To make sure there is no airflow interference, this distance should be higher than the sum of d_{aero} and the radius of the rotor. In This way the sphere around the rotor i does not intersect the cylinder around the line between the limits of the airflow, as visualized in figure 2.2b. Note that in this visualization the UAV has bi-directional rotors, as the airflow is observed in both positive and negative direction.

Chapter 3

Fully Actuated UAV Concepts

In this chapter, an overview of available fully actuated UAV concepts is presented. For each concept a brief description and the mapping matrix, as explained in chapter 2.3, is provided. The concept descriptions are complemented with an illustration of the prototype from the specific reference, as well as an illustration of the top view and, if necessary, side view of the rotor configuration. The numbering of the rotors in this illustration agrees with the numbering in the mapping matrix. The rotation direction of the rotors is displayed with an arrow, as well as a coloring: clockwise rotating rotors are yellow, while the counterclockwise rotating rotors are green. In most concepts there is some kind of symmetry in the rotor configuration, which is exploited to abbreviate the notation mapping matrix, which yields a much clearer overview of the total mapping matrix.

In section 3.1 the different types of fully actuated UAVs are explained, in section 3.2 the fixed tilt concepts are described and in section 3.3 the variable tilt rotors are described.

3.1 Fully Actuated UAV Categories

The UAV concepts can be separated into two categories: fixed tilt UAVs and variable tilt UAVs.

3.1.1 Fixed Tilt UAVs

Fixed tilt UAVs consist of rotors that are placed in a fixed orientation. Full actuation is achieved by altering the relative rotation speed of the nonparallel rotors. These concepts have low complexity relative to variable tilt concepts. These concepts are very dexterous, since the flying direction can be altered by changing the rotor speed. Airflow interference between the rotors, as discussed in chapter 2.6 can be prevented by configuring the rotors such that the airflow of the rotors do not intersect other rotors. For these concepts bi-directional rotors are used, unless it is specifically stated otherwise. As mentioned in chapter 2.3.1, using bi-directional rotors increase the wrench in all directions, which is advantageous for fully actuated UAVs.

3.1.2 Variable Tilt UAVs

Variable tilt UAVs are UAVs that can actively actuate the orientation of the rotors with added tilt actuators. Full actuation of the UAV is achieved by changing the orientation of the rotors, as well as the rotation speed of the different rotors. Full actuation is possible with as little as 4 rotors. Variable tilt UAVs are very effective at hovering at a non-zero roll or pitch angle, as the rotors can be tilted such that they still produce vertical thrust when the UAV is rotated. However, when following a trajectory, the variable tilt UAVs perform less than fixed cant UAVs, as position disturbance cannot be countered directly like the fixed cant UAVs by changing the rotor speed. Instead the cant angle needs to be changed first and then the rotor speed needs to be adjusted to maintain altitude, which takes more time. Airflow interference between the rotors is not prevented by the design, because the orientation of the rotor is not fixed. Instead it should be prevented with the control algorithm. For these concepts bi-directional are not necessary, because the tilt actuators can be used to produce thrust in any direction (within the limitation of the specific concept). As mentioned in chapter 2.3.1, the concepts have been illustrated by a top view of the rotor configuration. In this figure only the rotors have been numbered, not the tilt actuators. The tilt actuators are illustrated with a torque arrow indicating the axis of rotation. Note that the orientation and position matrix are defined differently from the fixed cant concept, as discussed in chapter 2.5.

3.2 Fixed Tilt Concepts

A number of fixed tilt concepts found in literature are summarized in this section.

3.2.1 Quadrotor with four horizontal rotors

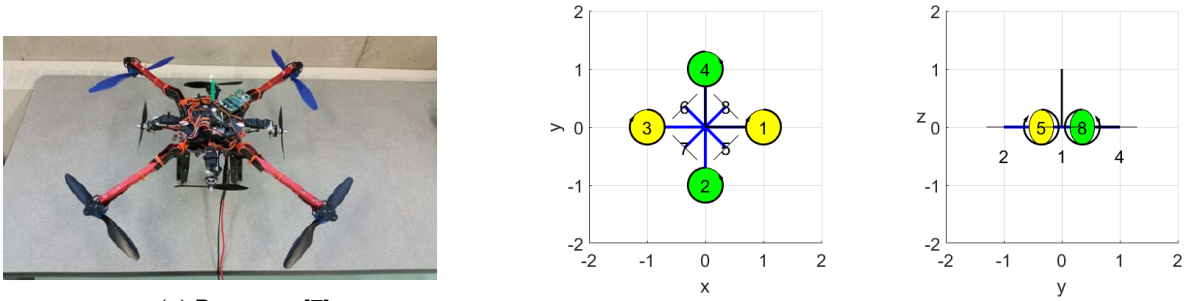

(a) Prototype [7]

(b) Rotor configuration, top view

(c) Rotor configuration, front view

Figure 3.1: Quadrotor with 4 horizontal rotors

This concept (figure 3.1), by Frankenberg and Nokleby [7], consist of four bi-directional horizontal rotors (rotors 5-8 in figure 3.1b) that are added to a traditional quadrotor to make it omnidirectional. The additional rotors are positioned between the quadrotor rotor arms, such that these added rotors do not create tilting moment and the airflow interference between the rotors is minimized. A similar concept by Salazar [17] with horizontal rotors placed on the arm of the vertical rotors showed that the interference of airflow has very negative effects on controllability of the UAV, as discussed in chapter 2.6. Rotor 1, 3, 5 and 6 rotate clockwise, while rotor 2, 4, 7 and 8 rotate counterclockwise. In this way the drag torque from rotor 5 is countered by rotor 6, which rotates at the same speed. The same applies for rotor 7 and 8. This concept is an extension of the quadrotor with one horizontal rotor, designed by Albers et al. [5]. This UAV utilizes the added DoF to climb walls and is considered as one of the earliest attempts to obtain horizontal actuation with a multirotor UAV.

Mapping Matrix

The mapping matrix is separated into vertical $\vec{M}^{v,i}$ and horizontal rotors $\vec{M}^{h,i}$, given by:

$$\vec{M}^{v,i} = \begin{bmatrix} 0 \\ 0 \\ 1 \\ l\sin(\phi_i) \\ -l\cos(\phi_i) \\ \gamma\sigma_i \end{bmatrix}, \qquad \phi_{v,i} = (i-1)\frac{\pi}{2}, \quad \vec{M}^{h,i} = \begin{bmatrix} \cos(\phi_i) \\ \sin(\phi_i) \\ 0 \\ \gamma\sigma_i \frac{l}{2}\sin(\phi_i) \\ \gamma\sigma_i \frac{l}{2}\cos(\phi_i) \\ 0 \end{bmatrix}, \quad \phi_{h,i} = (i-1)\frac{\pi}{2} + \frac{\pi}{4} \tag{3.1}$$

The total mapping matrix is:

$$\mathbf{M} = \begin{bmatrix} \vec{M}^{v,\{1,\dots 4\}} & \vec{M}^{h,\{1,\dots 4\}} \end{bmatrix} \tag{3.2}$$

3.2.2 Hexarotor with Canted Rotors

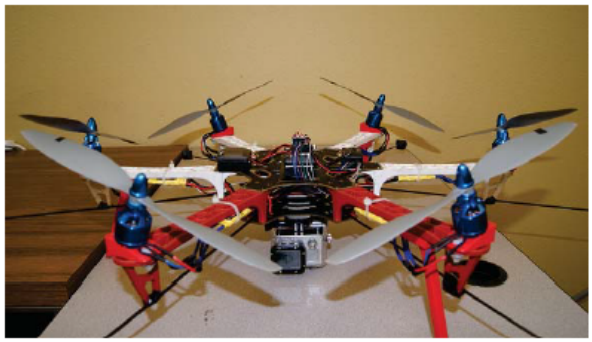

(a) Prototype [18]

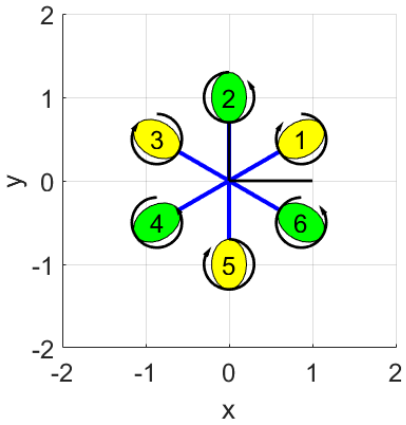

(b) Rotor configuration, top view

Figure 3.2: Hexarotor with canted rotors

This concept (3.2a), first proposed by Voyles et al. [18], is the most commonly used and investigated design for fully actuated UAVs. The rotor positioning is equal to that of a traditional hexarotor, with all 6 rotors placed in the horizontal plane one the vertices of a hexagon. Full actuation is achieved by tilting the rotors around the axis of the rotor arm. This rotation, referred to as canting, is denoted by α, as discussed in chapter 2.2. By canting the rotors, they will not only produce thrust in vertical, but also in horizontal direction. The canting angle of all rotors are equal and the canting direction and rotation direction of the rotors is alternating ($\alpha_2 = -\alpha_1$ etc.), resulting in three symmetric rotor pairs with opposite rotation direction. Due to this symmetry, the drag torque of the rotors can be counteracted easily and control is very straightforward. The amount of canting depends on the application: when high vertical acceleration is required, a small cant angle is required and if high horizontal acceleration is required, a large cant angle is required. The angle is limited by the minimum required upward thrust for overcoming gravity. The cant angle is optimized for maximum total dynamic manoeuvrability, discussed in chapter 2.5.1, by Tadokoro [15]. The optimal angle is found to be $35.3°$. This design will be used in the concept comparison in chapter 3. The UAV has bi-directional rotors, which allows omnidirectional wrench.

Mapping Matrix

The mapping matrix for rotor i is given by:

$$\vec{M}^i = \begin{bmatrix} \sin(\alpha_i)\sin(\phi_i) \\ -\sin(\alpha_i)\cos(\phi_i) \\ \cos(\alpha_i) \\ \sin(\phi_i)(l\cos(\alpha_i) + \gamma\sigma_i \sin(\alpha_i)) \\ -\cos(\phi_i)(l\cos(\alpha_i) + \gamma\sigma_i \sin(\alpha_i)) \\ \gamma\sigma_i \cos(\alpha_i) - l\sin(\alpha_i) \end{bmatrix}, \qquad \phi_i = (i-1)\frac{\pi}{3} + \frac{\pi}{6} \tag{3.3}$$

where l is the length of the rotor arm and ϕ is the angle of the rotor relative to the positive x-axis in the xy-plane. The total mapping matrix is:

$$\mathbf{M} = \left[\vec{M}^{\{1,\dots,6\}}\right] \tag{3.4}$$

3.2.3 Hexarotor with canted and dihedral rotors

(a) Prototype [19]

(b) Rotor configuration, top view

Figure 3.3: Hexarotor with canted and dihedral rotors

For this concept (figure 3.3a), by Rajappa et al. [19], the rotors of a hexarotor are not only canted, like the hexarotor cant in section 3.2.2, but also tilted along the axis perpendicular to the cant angle, called dihedral angle (β), as discussed in section 2.2. There are multiple studies (e.g. by Jyang et al. [9] and Rashad et al. [20] that showed that adding dihedral angle is always unfavourable because it reduces the torque contribution of a rotor, while canting the rotors adds yaw torque, as shown by the mapping matrix in equation 3.5. For that reason an optimization to the maximum wrench of a hexarotor will yield canted rotors. However, Rajappa performed a different optimization to minimize the required total thrust for full UAV controllability in position and orientation for different trajectories. The optimal orientation is shown to depend heavily on the trajectory and for stationary yawing and pitching the optimal dihedral angles is actually nonzero. To account for the different optimal orientations, the prototype, shown in figure 3.3a, has been outfitted with manually tiltable rotors. The direction of the dihedral angle (positive or negative) does not influence the performance of the UAV. However, the maximum dihedral angle is more limited by the frame when the rotor is tilted inward. For that reason the rotors that are tilted outward, which corresponds to a positive β. Like the hexarotor with canted rotors in section 3.2.2, α is alternating. Since the prototype by Rajappa lacks UAV specifics required for a comparison, the design of this concept by Staub et al. [14] with $\alpha = 35°$ and $\beta = 10°$ has been used for the comparison in chapter 5. The tilting angles were determined similar to Rajappa's method.

Mapping Matrix

The mapping matrix for rotor i is:

$$\vec{M}^i = \begin{bmatrix} \sin(\beta_i)\cos(\phi_i) + \cos(\beta_i)\sin(\alpha_i)\sin(\phi_i) \\ \sin(\beta_i)\sin(\phi_i) - \cos(\beta_i)\cos(\phi_i)\sin(\alpha_i) \\ \cos(\alpha_i)\cos(\beta_i) \\ \gamma\sigma_i(\sin(\beta_i)\cos(\phi_i) + \cos(\beta_i)\sin(\alpha_i)\sin(\phi_i)) + l\cos(\alpha_i)\cos(\beta_i)\sin(\phi_i) \\ \gamma\sigma_i(\sin(\beta_i)\sin(\phi_i) - \cos(\beta_i)\sin(\alpha_i)\cos(\phi_i)) - l\cos(\alpha_i)\cos(\beta_i)\cos(\phi_i) \\ -l\cos(\beta_i)(\sin(\alpha_i) - \gamma\sigma_i\cos(\alpha_i)) \end{bmatrix}, \quad \phi_i = (i-1)\frac{\pi}{3} + \frac{\pi}{6} \tag{3.5}$$

The total mapping matrix is:

$$\mathbf{M} = \left[\vec{M}^{\{1,\dots,6\}}\right] \tag{3.6}$$

3.2.4 Coaxial Hexagon with Twelve Canted Rotors

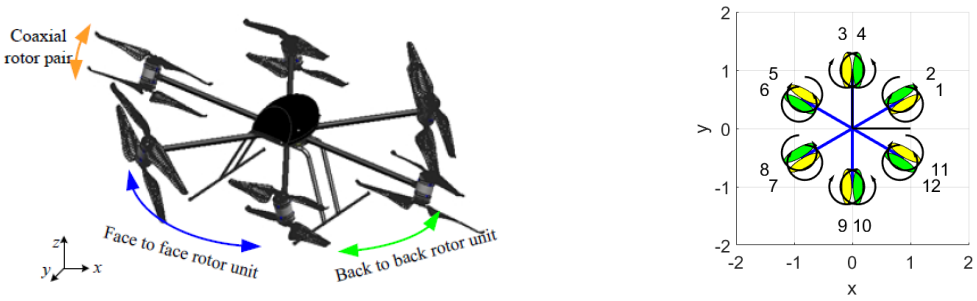

(a) Prototype [21]

(b) Rotor configuration, top view

Figure 3.4: Coaxial hexagon (12 rotors) with canted rotors

This concept (figure 3.4a), by Lei et al. [21], consists of twelve rotors that are positioned in pairs of two in a hexagonal configuration. These pairs are called coaxial rotor pairs, since the rotors rotate around the same axis. The rotors have an opposing rotation direction, such that the drag torque from one rotor is counteracted by the drag from the other rotor. Since both rotors rotate at the same speed there will be no resultant drag torque from the coaxial pair. The advantage of coaxial rotor pairs is that the amount of thrust that can be produced increases compared to a single rotor. A disadvantage is that the airflow from the top rotor influences the performance of the bottom rotor. Although the performance is reduced, the controllability of this drone is not influenced like discussed in section 2.6. The reason is that the airflow interference only changes when the rotor itself changes rotation speed itself, rather than when another rotor does, because the coaxial rotors have the same rotation speed. Since the reference does not give the cant angle of the rotors, the coaxial rotor pairs have been placed at the optimized cant angle for maximum dynamic manoeuvrability, defined for the hexarotor with canted rotors in section 3.2.2 of $35.3°$. This optimal cant angle does not change when the amount of rotors is doubled.

Mapping matrix

If the distance between the coaxial rotors, which has a limited influence on the torque, is neglected, the mapping matrix of the rotors is equal to the rotor mapping matrix $\vec{M}^i$ of the hexarotor with canted rotors, given by equation 3.3. For one coaxial pair the mapping matrix, $\mathbf{M}^{\mathbf{c},i}$, is given by:

$$\mathbf{M}^{\mathbf{c},i} = \begin{bmatrix} \vec{M}^i & \vec{M}^i \end{bmatrix} \tag{3.7}$$

The total mapping matrix is:

$$\mathbf{M} = \begin{bmatrix} \mathbf{M}^{\mathbf{c},\{1,\dots,6\}} \end{bmatrix} \tag{3.8}$$

3.2.5 Double Tetrahedron Hexarotor

(a) Prototype [22]

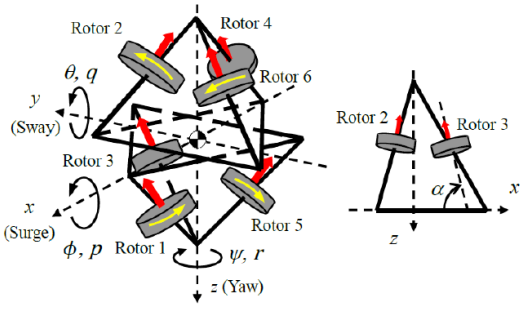

(b) Rotor configuration [22]

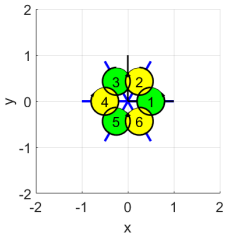

(c) Rotor configuration, top view

Figure 3.5: Double tetrahedron hexarotor

This concept (figure 3.5a) is proposed by Toratani [22]. It is the result of an optimization of the orientation and position of six rotors restricted to the shape of two tetrahedrons (figure 3.5b). Rotors 2, 4 and 6 (in figure 3.5c) rotate in clockwise direction and rotors 1, 3 and 5 rotate in counterclockwise direction. The

size and angle of the two tetrahedrons on which the rotors are placed are optimized based on numerical optimization: the edge length of the tetrahedron, l, equals 0.6 m and the elevation angle, α, equals 75°. Note that this α does not refer to the cant angle but in fact relates to the dihedral angle $(\alpha = 90° - \beta)$, as shown in figure 3.5b. The reference does not specified for which criterion these variable are optimized.

Mapping Matrix

The mapping matrix per rotor is:

$$\vec{M}^i = \begin{bmatrix} \cos(\alpha_i)\cos(\phi_i) \\ \cos(\alpha_i)\sin(\phi_i) \\ -\delta_i \sin(\alpha_i) \\ \gamma\sigma_i \cos(-\delta_i\alpha_i)\cos(\phi_i) - \delta_i l \sin(\alpha_i)\sin(\phi_i) - (\delta_i l \cos(-\delta_i\alpha_i)\sin(\alpha_i)\sin(\phi_i)) \\ \gamma\sigma_i \cos(-\delta_i\alpha_i)\sin(\phi_i) + \delta_i l \cos(\phi_i)\sin(\alpha_i) + (\delta_i l \cos(-\delta_i\alpha_i)\cos(\phi_i)\sin(\alpha_i)) \\ -\gamma\sigma_i\delta_i \sin(\alpha_i) \end{bmatrix}, \quad \phi_i = (i-1)\frac{\pi}{3} \tag{3.9}$$

where δ_i is either 1, if rotor is placed on the top of the UAV, or -1, if it is placed on the bottom. In this case $\delta_i = \sigma_i$.

The total mapping matrix is:

$$\mathbf{M} = \left[\vec{M}^{\{1,\ldots,6\}}\right] \tag{3.10}$$

3.2.6 Heptarotor with Minimized Frame

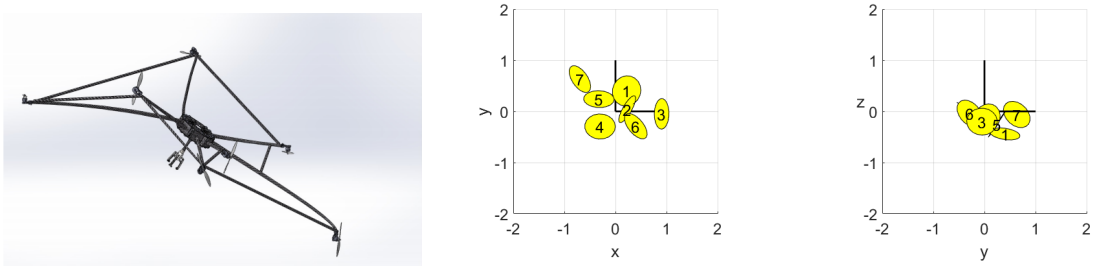

(a) Prototype [23]

(b) Rotor configuration, top view

(c) Rotor configuration, front view

Figure 3.6: Fixed cant angle heptarotor with minimized frame

This concept (figure 3.6a) is designed by Nikou et al. [23], who created an omnidirectional UAV with one-directional rotors. He showed that a minimum of seven rotors is required to achieve this. The rotor configuration has been optimized to minimize the mass of the frame. The airflow interference between rotors, as discussed in chapter 2.6, has been taken into account in the optimization by imposing the minimum distance d_{aero} between the rotors, based on CFD-analysis (computational fluid dynamics), for which airflow interference can be neglected. All rotors are rotating clockwise, so the rotation direction arrows are omitted in figure 3.6 for readability.

Mapping matrix

Because there is no symmetry in the rotor configuration, the total mapping matrix is given:

$$\mathbf{M} = \begin{bmatrix} 0.40 & -0.94 & -0.84 & 0.16 & 0.23 & 0.47 & 0.53 \\ -0.02 & 0.19 & -0.26 & -0.54 & -0.81 & 0.74 & 0.67 \\ 0.92 & 0.29 & -0.48 & 0.82 & -0.55 & -0.49 & -0.51 \\ 0.40\gamma - 0.42 & -0.94\gamma & 0.06 - 0.84\gamma & 0.16\gamma + 0.31 & 0.23\gamma - 0.13 & 0.47\gamma - 0.05 & 0.53\gamma + 0.24 \\ -0.02\gamma - 0.096 & 0.19\gamma + 0.19 & -0.26\gamma - 0.25 & -0.54\gamma - 0.16 & 0.15 - 0.81\gamma & 0.74\gamma - 0.25 & 0.67\gamma + 0.40 \\ 0.92\gamma + 0.18 & 0.29\gamma - 0.14 & 0.03 - 0.48\gamma & 0.82\gamma - 0.17 & -0.55\gamma - 0.28 & -0.49\gamma - 0.42 & 0.78 - 0.51\gamma \end{bmatrix} \tag{3.11}$$

3.2.7 Heptarotor with Maximized Wrench

(a) Prototype [24]

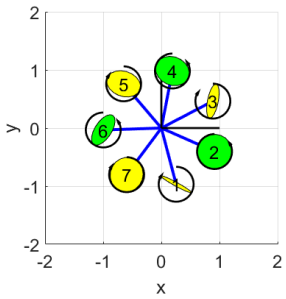

(b) Rotor configuration, Top view

Figure 3.7: Heptarotor with maximized wrench

This concept (figure 3.7a), by Tognon and Franchi [10], achieves omnidirectional wrench with seven one-directional rotors, just like the heptarotor with optimized frame in section 3.2.6. The rotors are placed on the vertices of a heptagon in the horizontal plane. The rotors rotate in alternating direction. The orientation of the rotors is optimized for maximum omnidirectional wrench.

Mapping matrix

Because there is no symmetry in the rotor orientation, the total mapping matrix is given:

$$\mathbf{M} = \begin{bmatrix} -0.94 & 0.078 & -0.042 & 0.55 & 0.68 & -0.29 & -0.026 \\ 0.25 & 0.087 & 0.94 & -0.099 & -0.064 & -0.81 & -0.31 \\ 0.11 & -0.98 & 0.31 & 0.81 & -0.72 & -0.48 & 0.94 \\ 0.11l - 0.82\gamma & 0.014\gamma - 0.77l & -0.73\gamma & -0.44\gamma - 0.63l & 0.5\gamma + 0.7l & 0.21l - 0.42\gamma & 0.21\gamma + 0.4l \\ -0.54\gamma - 0.025l & -0.12\gamma - 0.61l & 0.59\gamma + 0.31l & 0.51l - 0.35\gamma & 0.47\gamma + 0.15l & 0.76\gamma + 0.43l & -0.23\gamma - 0.85l \\ 0.11\gamma + 0.67l & 0.98\gamma - 0.061l & 0.31\gamma - 0.59l & 0.12l - 0.81\gamma & 0.59l - 0.72\gamma & 0.48\gamma - 0.49l & 0.94\gamma - 0.3l \end{bmatrix} \tag{3.12}$$

where the rotors are placed at a distance l from the CoM.

3.2.8 Octorotor Cube

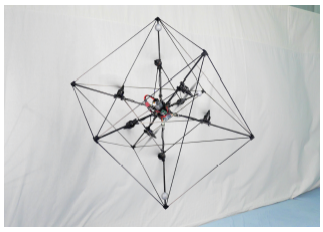

(a) Prototype [25]

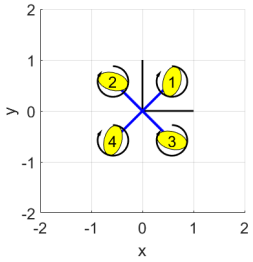

(b) Rotor configuration, top view

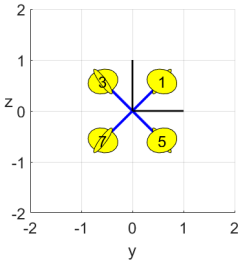

(c) Rotor configuration, Front view

Figure 3.8: Octorotor cube

This concept (figure 3.8a) is designed by Brescianini and D'Andrea [25]. The position and orientation of the rotors are optimized for maximum omnidirectional wrench with bi-directional rotors. The rotor positions are fixed to the vertices of a cube. All rotors are rotating in the same direction. The UAV is surrounded by a cage-like frame to allow human interaction without risk of injury from collision with the propellers.

Mapping Matrix

The total mapping matrix is:

$$\vec{M} = \begin{bmatrix} -a & b & -b & a & a & -b & b & -a \\ b & a & -a & -b & -b & -a & a & b \\ c & -c & -c & c & c & -c & -c & c \\ cd-bd-a\gamma & b\gamma-cd-ad & ad+cd-b\gamma & bd-cd+a\gamma & cd-bd+a\gamma & -ad-cd-b\gamma & ad+cd+b\gamma & bd-cd-a\gamma \\ b\gamma-cd-ad & bd-cd+a\gamma & cd-bd-a\gamma & ad+cd-b\gamma & -ad-cd-b\gamma & bd-cd-a\gamma & cd-bd+a\gamma & ad+cd+b\gamma \\ ad+bd+c\gamma & -ad-bd-c\gamma & -ad-bd-c\gamma & ad+bd+c\gamma & c\gamma-bd-ad & ad+bd-c\gamma & ad+bd-c\gamma & c\gamma-bd-ad \end{bmatrix} \tag{3.13}$$

With:

$$a = \frac{1}{2} + \frac{1}{\sqrt{12}}, \qquad b = \frac{1}{2} - \frac{1}{\sqrt{12}}, \qquad c = \frac{1}{\sqrt{3}}, \qquad d = \frac{1}{\sqrt{3}} \tag{3.14}$$

3.2.9 Octorotor Beam

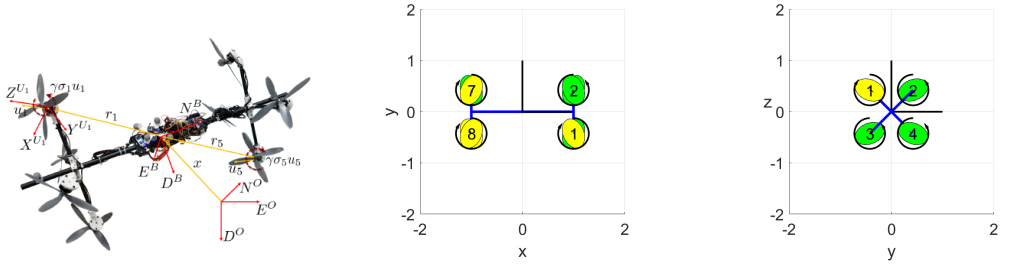

(a) Prototype [6]

(b) Rotor configuration, top view

(c) Rotor configuration, front view

Figure 3.9: Beam Octorotor rotor configuration

This concept (figure 3.9a), by Park et all. [6], is an extension of the beam hexarotor [26] with a similar design with 8 rotors placed on a beam. Each side of the beam contains four rotors placed on the vertices of a square, as shown in figure 3.9c. Rotor 1 and 6-8 rotate clockwise and rotor 2-5 rotate counterclockwise. The rotor position and orientation are optimized for omnidirectional wrench, while imposing the minimum distance for which airflow interference can be neglected, as discussed in chapter 2.6. Weighing factors have been added to distinguish which directions require most force or torque in the optimization.

Mapping Matrix

The translational mapping matrix $\mathbf{M^t}$ of rotor 1 to 4 is:

$$\mathbf{M}^{\mathbf{t},\{1\ldots4\}} = \begin{bmatrix} a & a & a & a \\ b & b & -b & -b \\ a & -a & a & -a \end{bmatrix} \tag{3.15}$$

where a and b give the orientation of the rotors. The rotational mapping matrix $\mathbf{M^r}$ of rotor 1 to 4 is:

$$\mathbf{M}^{\mathbf{r},\{1\ldots4\}} = \begin{bmatrix} a(\gamma-l_2)-bl_2 & a(-\gamma-l_2)-bl_2 & a(-\gamma-l_2)-bl_2 & a(-\gamma-l_2)-bl_2 \\ b\gamma+a(l_2-l_1) & -b\gamma+a(l_2+l_1) & b\gamma+a(-l_2-l_1) & b\gamma+a(-l_2+l_1) \\ a(\gamma+l_2)+bl_1 & a(\gamma-l_2)+bl_1 & a(-\gamma+l_2)-bl_1 & a(\gamma-l_2)-bl_1 \end{bmatrix} \tag{3.16}$$

where l_1 is the length of the center beam and l_2 the length of the square where the rotors are placed on. For the optimized rotor configuration, the values of the variables are:

$$l_1 = 0.40, \qquad l_2 = 0.17, \qquad a = 0.68, \qquad b = 0.28 \tag{3.17}$$

The total mapping matrix is:

$$\mathbf{M} = \begin{bmatrix} \mathbf{M}^{\mathbf{t},\{1\ldots4\}} & \mathbf{M}^{\mathbf{t},\{1\ldots4\}} \\ \mathbf{M}^{\mathbf{r},\{1\ldots4\}} & -\mathbf{M}^{\mathbf{r},\{1\ldots4\}} \end{bmatrix} \tag{3.18}$$

3.3 Variable Tilt Concepts

A number of variable tilt UAV concepts found in literature are presented in this section.

3.3.1 Trirotor with One Horizontal Rotor

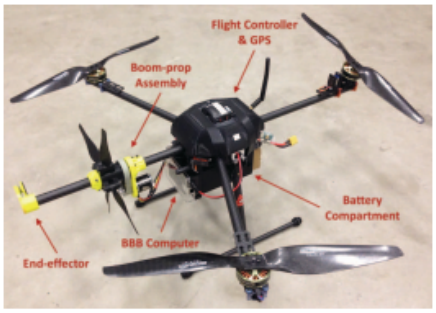

(a) Prototype [27]

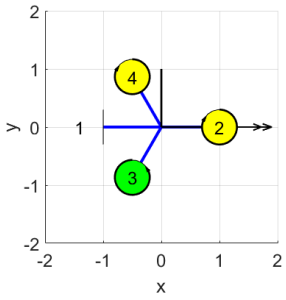

(b) Rotor configuration, top view

Figure 3.10: Trirotor with one horizontal rotor rotor configuration

This concept (figure 3.10a), by Mc. Arthur et al. [27], consists of a trirotor UAV with a single reversible horizontal rotor added to it. The axis of the horizontal rotor (rotor 1 in figure 3.10b) is aligned with the axis of the arm of rotor 2, which enables it to translate directly and without changing its attitude. This yields a total of 5 DoFs. A trirotor consists of three rotors placed in a triangular configuration. Rotor 2 and 4 rotate clockwise and rotor 3 rotates counterclockwise. The drag torque generated by the rotors results in a yaw torque, which is countered by actively canting rotor 2. Due to this canting, the y-direction is actuated and the vertical direction is rotated slightly with respect to the $\mathcal{F}_\mathcal{W}$ z-axis, but this difference between the vertical direction and the z-axis in $\mathcal{F}_\mathcal{W}$ is neglected. The drag torque from the horizontal rotor causes roll of the UAV, which can be rejected by rotor 3 and 4.

Mapping Matrix

The total mapping matrix is given by:

$$\mathbf{M} = \begin{bmatrix} 1 & 0 & 0 & 0 & 0 \\ 0 & 0 & 1 & 0 & 0 \\ 0 & 1 & 0 & 1 & 1 \\ \gamma & 0 & 0 & -l\sin(\phi) & l\sin(\phi) \\ 0 & -l & \gamma & l\cos(\phi) & l\cos(\phi) \\ 0 & \gamma & l & -\gamma & \gamma \end{bmatrix}, \quad \phi = \frac{\pi}{3} \tag{3.19}$$

Note that the mapping matrix of rotor 2 consists of two columns, since it has a variable tilt angle. The other rotors consist of only one column in $\mathbf{M}$.

3.3.2 Quadrotor with Variable Cant Rotors

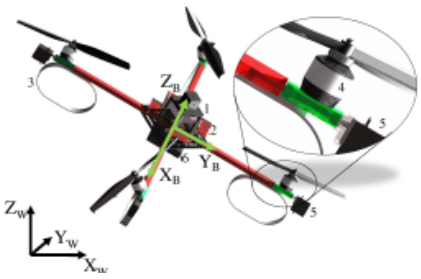

(a) Prototype [28]

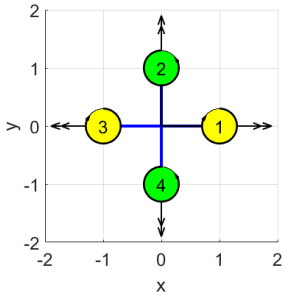

(b) Rotor configuration, top view

Figure 3.11: Quadrotor with variable cant

This concept (figure 3.11a), by Ryll et al. [28], adds four tilting actuators to the rotors of a conventional quadrotor. These actuators actively cant each rotor around the rotor arm axes individually, enabling it to fly in any orientation.

Mapping Matrix

The mapping matrix of rotor i is given by:

$$\mathbf{M^i} = \begin{bmatrix} 0 & \sin(\phi_i) \\ 0 & -\cos(\phi_i) \\ 1 & 0 \\ l\sin(\phi_i) & \gamma\sigma_i \sin(\phi_i) \\ -l\cos(\phi_i) & -\gamma\sigma_i \cos(\phi_i) \\ \gamma\sigma_i & -l \end{bmatrix}, \qquad \phi_i = (i-1)\frac{\pi}{2} \tag{3.20}$$

The total mapping matrix is given by:

$$\mathbf{M} = \begin{bmatrix} \mathbf{M}^{\{1,\dots,4\}} \end{bmatrix} \tag{3.21}$$

3.3.3 Quadrotor with Variable Dihedral Rotors

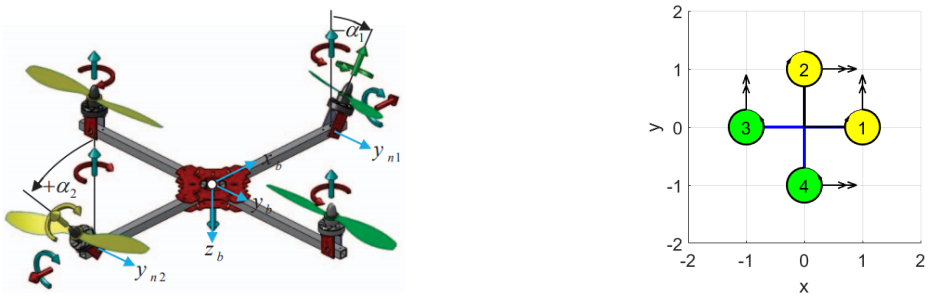

(a) Prototype [29]

(b) Rotor configuration, top view

Figure 3.12: Quadrotor with variable dihedral

This concept (figure 3.12a), by Badr et al. [29], resembles the variable cant UAV. Instead of the cant angle, the dihedral angle is variable. Contrary to the cant angle, the inward dihedral angle is limited by the frame, which interferes with the rotor blades at large dihedral angle. Another difference with variable cant rotors is that dihedral angle does not contribute to the yaw torque (as discussed in section 3.2.3), effectively reducing the total torque. The rotation direction of the rotors is non-alternating, as shown in figure 3.12, unlike the other quadrotor concepts. According to the reference, this is required to counteract the drag torque from the rotors when they are tilted.

Mapping Matrix

The mapping matrix of rotor i is given by:

$$\mathbf{M^i} = \begin{bmatrix} 0 & \cos(\phi_i) \\ 0 & \sin(\phi_i) \\ 1 & 0 \\ l\sin(\phi_i) & \gamma\sigma_i \cos(\phi_i) \\ -l\cos(\phi_i) & \gamma\sigma_i \sin(\phi_i) \\ \gamma\sigma_i & 0 \end{bmatrix}, \quad \phi_i = (i-1)\frac{\pi}{2} \tag{3.22}$$

The total mapping matrix is given by:

$$\mathbf{M} = \begin{bmatrix} \mathbf{M}^{\{1,\dots,4\}} \end{bmatrix} \tag{3.23}$$

3.3.4 Quadrotor with Variable Cant and Dihedral Rotors

(a) Prototype [30]

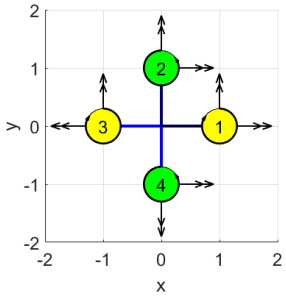

(b) Rotor configuration, top view

Figure 3.13: Quadrotor with variable cant and dihedral

This concept (figure 3.13a), by Segui-Gasco et al. [30], has two actuators added to the each rotor of a conventional quadrotor to actively tilt the rotors around cant and dihedral angle. This allows the rotors to be redirected into almost any directions, enabling it to produce full vertical thrust in almost all orientations. For the dihedral actuation, a push pull mechanism is used, which limits the maximum dihedral angle. Ryll et al.[31], However, showed an alternative actuation method for the cant and dihedral angle that can be used to obtain complete cant and dihedral angle.

Mapping Matrix

The mapping matrix of rotor i is given by:

$$\mathbf{M^i} = \begin{bmatrix} \sin(\phi_i) & 0 & \cos(\phi_i) \\ -\cos(\phi_i) & 0 & \sin(\phi_i) \\ 0 & 1 & 0 \\ \gamma\sigma_i \sin(\phi_i) & l\sin(\phi_i) & \gamma\sigma_i \cos(\phi_i) \\ -\gamma\sigma_i \cos(\phi_i) & -l\cos(\phi_i) & \gamma\sigma_i \sin(\phi_i) \\ -l & \gamma\sigma_i & 0 \end{bmatrix}, \quad \phi_i = (i-1)\frac{\pi}{2} \tag{3.24}$$

The total mapping matrix is given by:

$$\mathbf{M} = \left[\mathbf{M}^{\{1,\dots,4\}}\right] \tag{3.25}$$

3.3.5 Quadrotor with Coupled Variable Cant and Dihedral Rotors

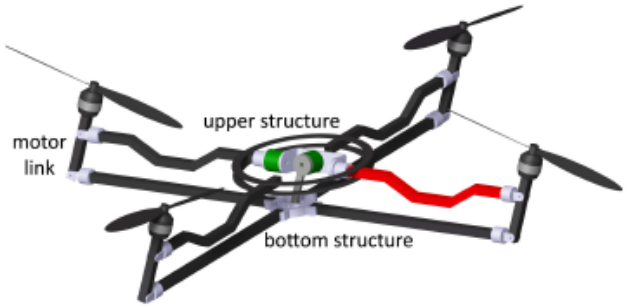

(a) Prototype [32]

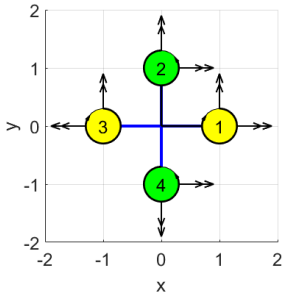

(b) Rotor configuration, top view

Figure 3.14: Quadrotor with coupled variable cant and dihedral

This concept (figure 3.14a) is by Odelga et al. [32], who proposed to actuate the angle of all rotors with a single actuator using parallelogram linkage mechanism, instead of actuating each rotor separately. This linkage mechanism tilts all rotors in the same direction. For a second rotation direction another similar linkage is used. In this way all rotors always have the same orientation and cannot be orientated individually. Due to this coupling, the maximum tilting angle of all rotors in all directions is now limited by the maximum inward dihedral angle. This actuation method reduces the amount of actuators required for cant and dihedral actuation from eight to two. It should be noted that this article is only a conceptual proposition of the concept and a working prototype has not yet been made.

Mapping Matrix

The mapping matrix of this concept is equal to the mapping matrix of the uncoupled quadrotor with variable cant and dihedral is section 3.3.4, given by equation 3.24 and 3.25.

3.3.6 Hexarotor with Variable Cant Rotors

(a) Prototype [33]

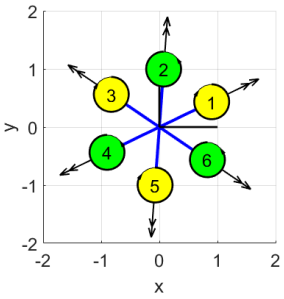

(b) Rotor configuration, top view

Figure 3.15: Hexarotor with variable cant

This concept (figure 3.15a) was produced by a number of students from Swiss Federal Institute of Technology (ETH Zurich) and Zurich University of the Arts [33]. It has been described by Kamel et al. [34]. The concepts adds a canting actuator to all the rotor of a conventional hexarotor to achieve omnidirectional flight with one-directional rotors.

Mapping Matrix

The mapping matrix of rotor i is given by:

$$\mathbf{M^i} = \begin{bmatrix} 0 & \sin(\phi_i) \\ 0 & -\cos(\phi_i) \\ 1 & 0 \\ l\sin(\phi_i) & \gamma\sigma_i \sin(\phi_i) \\ -l\cos(\phi_i) & -\gamma\sigma_i \cos(\phi_i) \\ \gamma\sigma_i & -l \end{bmatrix}, \qquad \phi_i = (i-1)\frac{\pi}{3} + \frac{\pi}{6} \tag{3.26}$$

The total mapping matrix is given by:

$$\mathbf{M} = \left[\mathbf{M}^{\{1,\dots,6\}}\right] \tag{3.27}$$

3.3.7 Hexarotor with Coupled Variable Cant Rotors

(a) Prototype [35]

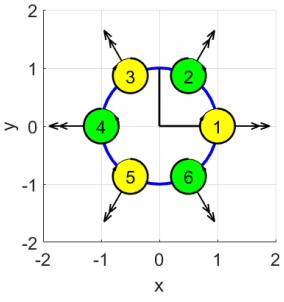

(b) Rotor configuration, top view

Figure 3.16: Hexarotor with coupled variable cant

This concept (figure 3.16a), by Ryll et al. [35], uses a single actuator to cant all six rotors of a hexarotor. This coupled rotor tilting is achieved using a wire mechanism. Different from other variable tilt angle concepts, the rotors are not actively tilted to control the UAV. Instead the variable tilt is used to change to ratio between horizontal and vertical acceleration during flight. The cant angle is alternating, equal

to hexarotor canted in section 3.2.2. If horizontal actuation is required the cant angle can be increased and if vertical actuation is required the cant angle can be decreased. The maximum cant angle is limited by the frame. The advantage of a single actuator instead of six actuators to cant the rotors is that the energy consumption and total mass of the system reduce, however the manoeuvrability of the UAV does reduce by the limited cant angle and coupling between the cant angles. Furthermore it should be noted that the actuation of the propeller groups, additional mechanics and tilt actuator, increases the mass of the UAV compared to a hexarotor with canted rotors.

Mapping Matrix

The mapping matrix of this concept is equal to that of the hexarotor with variable cant (section 3.3.6), as given by equation 3.26 and 3.27.

3.3.8 Ducted Pentarotor with Two Coaxial Rotors and Three Variable Dihedral Rotors

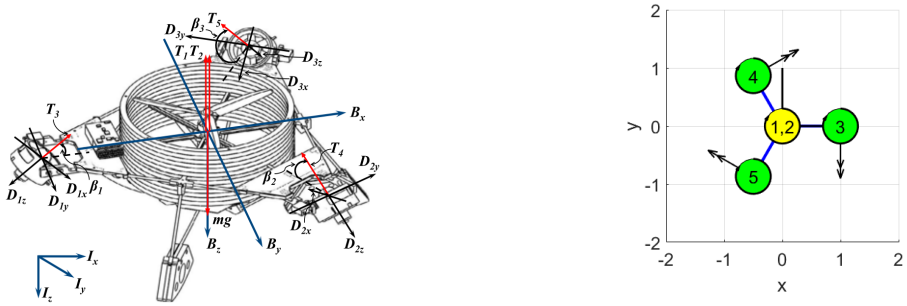

(a) Prototype [36]

(b) Rotor configuration, top view

Figure 3.17: Ducted pentarotor with two coaxial rotors and three variable dihedral rotors

This concept (figure 3.17a) by Long et al. [36] combines a number of design aspects. The main thrust is generated by two large counter rotating coaxial propellers (figure 3.17b rotor 1 and 2) and the full actuation of the UAV is achieved by three smaller rotors (rotor 3, 4 and 5) that are actively tilted in dihedral direction. Yaw torque is generated by differentiating the speed of the coaxial rotors. As mentioned in section 3.2.4, the advantage of the coaxial rotor pair is this is that the drag moment from the rotors is counteracted by the other rotor and the disadvantage is that there is a lot of interference between the airflow from the rotors. Furthermore a duct is placed around the propellers, which channels the airflow and increases the lift generated by the propellers. The tilting rotors are also ducted, with fins placed in the duct that counteract the drag torque from the rotors.

Mapping matrix

The mapping matrix of the coaxial rotor pair M^c and the variable dihedral rotor i $M^{d,i}$ is given by:

$$\mathbf{M^c} = \begin{bmatrix} 0 & 0 \\ 0 & 0 \\ 1 & 1 \\ 0 & 0 \\ 0 & 0 \\ \gamma & -\gamma \end{bmatrix}, \qquad \mathbf{M^{d,i}} = \begin{bmatrix} 0 & \cos(\phi_i) \\ 0 & \sin(\phi_i) \\ 1 & 0 \\ l\sin(\phi_i) & 0 \\ -l\cos(\phi_i) & 0 \\ 0 & 0 \end{bmatrix}, \qquad \phi_i = (i-1)\frac{2\pi}{3} \tag{3.28}$$

The total mapping matrix is given by:

$$\mathbf{M} = \begin{bmatrix} \mathbf{M^c} & \mathbf{M^{d\{1,\ldots,3\}}} \end{bmatrix} \tag{3.29}$$

Chapter 4

Criteria for Comparing Fully Actuated UAVs

In order to make a sensible and general comparison between the concepts, a number of comparison criteria is specified. These criteria are separated into qualitative and quantitative criteria. Next to these criteria there are some other criteria that are non-graded, but can be required for certain applications. These criteria can be used to limit the number of concepts to those that fulfill the criteria.

4.1 Qualitative Criteria

The qualitative criteria are graded with a score between very poor (- - -) and excellent (+++). The grading is based on interpretation of the information given in the references. The qualitative criteria consist of:

4.1.1 Flying stability

The Flying stability gives an indication of the ability to follow a trajectory with minimal error in position and orientation. This is mainly determined by the speed at which disturbances can be rejected. As an example, the disturbance rejection of a standard quadrotor to a horizontal position error is given: first the UAV needs to be tilted and then the position error can be rejected by increasing the total thrust. This is a very slow method of disturbance rejection. The flying stability depends on the ability to directly reject external disturbance, as well the amount of susceptibility to disturbances. these disturbances consist of: airflow interference, as discussed in chapter 2.6), and side wind disturbance, which depends on the body drag coefficient is high. The speed at which disturbances are rejected also depends on the acceleration that can be achieved by the UAV, however this is not considered in depth for this criteria, because it will be considered in the quantitative comparison.

4.1.2 Design complexity

The design complexity gives an indication of the effort that has to be done to design and manufacture the UAV. This criteria consists of two two parts: optimization complexity and manufacturing complexity. Optimization complexity indicates the effort required to optimize the rotors configuring. This effort depends on the amount of design parameters required to describe the orientation and position of the rotors. Fewer design parameters results in less optimization effort. The amount of parameter decreases, for example, if there is symmetry in the UAV design. Manufacturing complexity indicates the effort required to manufacture the UAV. An aspects that influences this complexity is the frame design, e.g. a standard quadrotor only consists of four bars connecting the rotors; the manufacturing complexity is low. If an existing frame can be used, the manufacturing complexity is minimal. A high amount of moving parts, e.g. actively tiling rotors, increases the manufacturing complexity as well.

4.1.3 Downscaling Ability

The downscaling ability gives an indication of the problems that occur when scaling down. The main problem with scaling down, is fitting all the required parts on the UAV. There is a lower limit to the rotor size, so the downscaling ability is limited by the amount of rotors. A large required frame also has a negative effect on the downscaling.

4.1.4 Upscaling Ability

The upscaling ability gives an indication of the complexities that occur when scaling up. Just like a lower limit, there is an upper limit to the propeller size: at very large scale the existing brushless motors cannot rotate the propellers fast enough. This limits the possible available thrust per rotor and thus the total available thrust. Another issue is the higher frame stiffness requirement. Lastly, the practical usability of the UAV at large scale is incorporated into this criteria: if the proportions of the UAV are such that the height is extremely high at large scale, the practical application will be limited.

4.1.5 Redundancy

The redundancy is given as the amount of actuators minus the amount of required DoFs, as discussed in chapter 2.3.2. Redundancy is an indication of the amount of rotors or actuators may fail before the UAV becomes uncontrollable and eventually crashes. Provided that the control scheme can handle it, UAVs with redundancy should remain controllable after rotor failure, albeit with reduced degrees of freedom. Redundancy also results in an abundance of control possibilities, which can be exploited to maximize the thrust efficiency.

4.1.6 Costs

are an indication of how much the UAV will cost to be produced. The costs mainly depend on the costs of the motors for the rotors and tilt actuation. For the rotors, the brushless motors are assumed equal in price for of all concepts and therefore the total costs of the rotor motors depend only on the amount of rotors. Apart from that the type of rotors (one-directional or bi-directional) have to be considered, where bi-directional rotors are more expensive than one-directional rotors. Similar to the rotor motor, the cost of a tilt actuators is considered equal for all concept, because it is assumed that all concepts contain brushless motors for tilt actuators, as discussed in section 2.5. Lastly, the manufacturing costs of the frame are considered. For concepts with simple frames or frames that are already commercially available these costs are significantly lower. It should be noted that the manufacturing costs correlate to the manufacturing complexity. Other aspects that determine the total costs, like the wiring, battery and other electronics are assumed to be similar for all concepts and are thus not included in the comparison.

4.2 Quantitative Criteria

For the quantitative criteria, two comparisons have been defined. First a static comparison is done based on the mapping matrix $\mathbf{M}$ for the considered concepts given in the concept description in chapter 3. The static comparison is done, because it is easy to derive for any concept and can be done very general without any assumption. This comparison shows the maximum static wrench a concept can produce. However, the performance of the UAV for all applications, except for a physical interaction application, does not depend on the wrench, but on the acceleration it can achieve. For this reason the static comparison is complemented by a dynamic comparison, based on the acceleration mapping matrix $\mathbf{A}$, defined in chapter 2.4. In order to determine the acceleration mapping matrix $\mathbf{A}$, the inertia matrix $\mathbf{I}$ is required. The dynamic analysis is often disregarded in the design of a UAV, because determining the rotational part of this inertia matrix is not straightforward, as discussed in chapter 2.4. To establish whether the extra effort of determining the inertia is required to determine which UAV concept performs best, the static and dynamic performance of the concepts has been compared.

4.2.1 Static Comparison

There are a number of methods to compare fully actuated UAVs based on the mapping matrix. The most general comparison method would be to compare the maximum possible uncoupled wrench the UAVs can attain in all directions. Here, uncoupled wrench means that there is only wrench allowed in the desired direction and vertical direction. The vertical force is allowed, because for UAVs with fixed one-directional rotors, no thrust is possible without actuating it. Wrench in other directions should be zero for this comparison, because the applications that require full actuation often require this full actuation, because the UAV is not allowed to tilt during horizontal flight. When a fully actuated UAV would produce a torque alongside horizontal force, this UAV is essentially similar to an underactuated UAV. To determine the maximum uncoupled wrench in any direction, the combination of rotor thrusts given by $\vec{\lambda}$ that yields this maximum wrench is required. Determining $\vec{\lambda}$ is not a problem for UAVs with parallel rotors. For example, maximum vertical force is achieved if all rotors produce maximum force. For fully actuated UAVs, however, determining $\vec{\lambda}$ is far more complex due to the nonparallel and, in some cases, nonsymmetric rotor configuration.

To overcome the difficulty of finding the set of required $\vec{\lambda}$ for all wrench directions, an alternative static comparison measure is presented: manoeuvrability. This measure is described in chapter 2.5.1 and could be used to compare the kinematic performance of fully actuated UAVs. The advantage of using this method for the comparison is that it can easily be applied to any concept if the position and orientation of the rotor is known. The main disadvantage of using this measure is that the scalar representation of all wrench makes comparing the concepts for wrench in individual directions impossible. Furthermore, the manoeuvrability is only valid for rotors that produce bi-directional thrust, which is not the case for all concepts. For these reasons this measure is considered unfit and the maximum wrench will have to be used. As mentioned, a method to determine the $\vec{\lambda}$ has to be provided.

In order to make this comparison as general as possible, all UAVs are scaled to fit inside a unit sphere (radius is 1 m). Furthermore a generalized maximum thrust λ_{max} of 1 N is specified for all concepts.

Maximum Uncoupled Wrench

To determine the wrench resulting from any rotor thrust, the static wrench analysis of chapter 2.3 is used. The required mapping matrix is given in the concept description in chapter 3 for each of the considered concepts. As mentioned, determining $\vec{\lambda}$ for maximum uncoupled wrench is not straightforward for fully actuated UAVs. Some references use the brute force method to achieve this, trying all possible combinations of rotor thrust to find the maximum wrench [26]. However, in order to find uncoupled wrench, the amount of considered thrust combinations will need to be very high, so this method is disregarded here. An alternative method to find $\vec{\lambda}$ is to optimize the wrench in the required direction using an optimization algorithm, where $\vec{\lambda}$ is taken as the variable. This optimization is done with the MATLAB *fmincon* optimization function. For the optimization, the following objective function is used:

$$f(\lambda_1, ..., \lambda_n) = -|\mathbf{M_i}\vec{\lambda}| \tag{4.1}$$

where $\mathbf{M_i}$ is the i^{th} row of the mapping matrix, corresponding to the direction for which the wrench is maximized ($1 \leq i \leq 6$). The absolute value of this wrench is used, because for the maximum wrench it can be either positive or negative. The minus sign is used, because the *fmincon* function minimizes the objective function. The boundary conditions of the variables, $\vec{\lambda}$, depend on the type of rotors used. For a one directional rotor, the boundaries are defined as:

$$0 \leq \lambda \leq \lambda_{max} \tag{4.2}$$

For bi-directional rotors the thrust is reversible. Assuming that the maximum thrust in both directions is equal, the boundary conditions are:

$$-\lambda_{max} \leq \lambda \leq \lambda_{max} \tag{4.3}$$

To make sure the wrench is uncoupled, all wrench in other directions is required to be zero by additional constraints:

$$\mathbf{M_i}'\vec{\lambda} = \vec{0} \tag{4.4}$$

where $\mathbf{M_i}'$ consists of the rows of the mapping matrix for which the wrench needs to be zero, which is all rows except the i^{th} and third row, corresponding to the vertical force. This optimization yields the thrust of the n rotors that is yield the maximum wrench in direction i.

Orientation of UAV in World Inertial Frame

Before the maximum wrench in $\mathcal{F}_\mathcal{W}$ can be determined, the orientation of the UAV in $\mathcal{F}_\mathcal{W}$ needs to be considered. As mentioned in chapter 2.1, the principle axes of $\mathcal{F}_\mathcal{B}$ are in the direction of the longitudinal, lateral and vertical direction. to make sure the directions of the maximum wrench, defined in $\mathcal{F}_\mathcal{W}$, coincides with these directions, the axes of $\mathcal{F}_\mathcal{B}$ need to coincide with the axes of $\mathcal{F}_\mathcal{W}$. For the concepts considered in chapter 3, the maximum vertical force does always coincide with the z-axis of $\mathcal{F}_\mathcal{W}$. However, for the longitudinal and lateral force, this is not always the case. In these cases, the UAV needs to be rotated around the z-axis in $\mathcal{F}_\mathcal{W}$. To determine the amount of rotation required, the direction of the longitudinal force in $\mathcal{F}_\mathcal{W}$ in the current orientation needs to be determined. The longitudinal force F_l is given as the resultant force in x- and y-direction in $\mathcal{F}_\mathcal{W}$ and is found by adaption of the objective function of the optimization in section 4.2.1, given by:

$$F_l(\lambda_1, ..., \lambda_n) = -||\mathbf{M_h}\vec{\lambda}|| \tag{4.5}$$

where $\mathbf{M_h}$ represents the horizontal translational part of the mapping matrix, given by the first two rows of $\mathbf{M}$. By optimizing the norm of these two forces, the maximum resultant force is found. The angle (ψ) between the x-axis of $\mathcal{F}_\mathcal{W}$ and the direction of the resultant force is given by the angle between the x- and y-components of the resultant force:

$$\psi = \tan^{-1}\left(\frac{\vec{M}_2\vec{\lambda}}{\vec{M}_1\vec{\lambda}}\right) \tag{4.6}$$

where $\vec{M}^1$ and $\vec{M}^2$ are the first and second row of the mapping matrix, respectively. The Body fixed frame is rotated around the z-axis with this angle ψ using the rotation matrix around the z-axis:

$$R_z = \begin{bmatrix} \cos(-\psi) & -\sin(-\psi) & 0 \\ \sin(-\psi) & \cos(-\psi) & 0 \\ 0 & 0 & 1 \end{bmatrix} \tag{4.7}$$

The matrix is rotated with $-\phi$ in order to rotate it towards the correct position. After the rotation the maximum wrench can be determined using the optimization of equation 4.5.

Note that the forces are now in the maximum direction, but the maximum torque can be in a different direction. It is possible to perform a similar rotation for the maximum roll and pitch and yaw directions instead of the maximum force direction. However, rotating the UAV based on the forces is favoured, because actuation of the horizontal forces is the distinctive advantage of fully actuated UAVs over underactuated UAVs, so this actuation should be emphasized. This does result in rotational wrench that does not necessarily coincide with the roll, pitch and roll direction of the UAV and the torque will therefore not referred to as such. Instead, the rotations are called: x-rotation, y-rotation and z-rotation, which refers to the rotation axis in $\mathcal{F}_\mathcal{W}$.

Thrust Efficiency

Next to the ability to fly fast, many applications require the UAV to fly with minimal power consumption, referred to as efficient flight. Efficient flight is defined as flying with minimal thrust requirement. A measure of this flying efficiency of a UAV during hovering is the thrust efficiency η_F, which is defined as the ratio between the maximum vertical force produced by the UAV and the sum of the thrust of all rotors:

$$\eta_F = \frac{F_z}{n\lambda_{max}} \tag{4.8}$$

where F_z is the vertical force resulting from the optimization of equation 4.5 in vertical direction (i=3) and n is the amount of rotors. This ratio gives insight in how much vertical force is 'lost' due to horizontal actuation. As an example, a horizontally flying UAV with parallel rotors has an η_F of 1.

4.2.2 Dynamic Comparison

The dynamic comparison is done similar to the static comparison, with the only difference that $\mathbf{A}$ is used instead of $\mathbf{M}$. The comparison yields uncoupled accelerations in all directions. The different $\vec{\lambda}$ that yield these accelerations are derived the same way as the $\vec{\lambda}$ is derived for maximum wrench. The inertia matrix prohibits the scaling of the concepts for the dynamic comparison to a general size similar to the static comparison in section 4.2.1, since the mass and inertia of different parts scales differently. In order to scale the UAVs they would all need to be completely redesigned and the new mass and inertia would have to be determined. Instead of redesigning each UAV to a general scale, the concept are not scaled and remain as they are presented by their respective reference. It is assumed that each concept is optimized by its designer. By using these designs the mass and inertia specified in the references can be used for this comparison. For a number of concepts the inertia is not given. An estimation of the inertia has been proposed in appendix E, but this estimation based on the rotor mass was not accurate enough to make a fair comparison. For that reason the rotational dynamics of the concept without a specified inertia are not included in the comparison. Although this limits the comparability, it should be stressed that the main objective of horizontal actuated UAVs is the translational part of the dynamics. A number of specifications of the concepts are required for the dynamic comparison. These specifications are:

- The length of UAV, given as the distance between the position of the rotors that are furthest away from each other.
- The rotational inertia, as defined in chapter 2.4.
- The total mass of the UAV, including rotors, frame, battery and electronics
- The rotor mass, including the mass of the motor and the propellers, given in appendix B. This mass is not necessary to determine the maximum accelerations, but is used for comparing the rotor thrust to weight ratio.
- Thrust: the maximum thrust the rotor can produce. This value is either given in the reference or based on data given by the manufacturer of the motor specified in the reference.

Prior to the dynamic comparison, the design of the concepts are compared independently of the rotor configuration with the thrust to weight ratio to determine the differences resulting from design considerations like the rotor choice.

Thrust to weight ratio

The translational dynamic performance of a UAV is defined as the ratio between the wrench it can produce and the total mass , so the highest acceleration is obtained if the total mass is low relative to the thrust. That is why, before the concepts are compared based on actual acceleration they can produce they are compared purely on the ratio between the thrust they can produce and the weight (given as mass times gravity constant). This ratio,$(T/w)_{tot}$, yields an indication of the influence of a number of design considerations done for the concepts on their dynamic performance. These design considerations include all choices that influence the thrust and weight of the UAV, including: rotor choice, battery choice and frame design. It is clear that, when the available rotor thrust increases, the total weight of the UAV increases as well, due to an increase in rotor weight, required frame weight and battery weight. If the ratio between the total thrust and weight of a concept is high, the dynamic performance will be high compared to the static comparison, relative to the other concepts.

Next to $(T/w)_{tot}$, the thrust to weight ratio of a single rotor, $(T/w)_{rotor}$, is given. This ratio shows how well the design of the rotor has been done rather than the entire design of the UAV. The thrust a rotor produces, as well as the weight, depends on the propeller diameter and the motor power. Different combination of rotors and propellers yield different thrust and weight. High $(T/w)_{rotor}$ means that the combination of the motor and the propeller is effective. The relation between rotor thrust and the weight has been investigated in Appendix D.

Flying Thrust

Similar to the thrust efficiency, a dynamic measure of the flying efficiency is presented: the flying thrust λ_f, which is defined as the minimal total rotor thrust required for forward accelerating flight without changing orientation. The required forward acceleration is chosen to be 5 m/s^2 and the vertical acceleration is equal to the gravitational acceleration (g=9.81 m/s^2). This forward flight needs to be achieved without rotation. This measure gives an insight into how efficient the UAV can fly using the horizontal actuation. λ_f is found with an optimization similar to the maximum wrench optimization in section 4.2.1, but instead of maximizing the acceleration, the total thrust, which is the sum of $\vec{\lambda}$, is minimized. The objective function is:

$$\lambda_f(\lambda_1, ..., \lambda_n) = \sum_i^n \lambda_i \tag{4.9}$$

To make sure the required accelerations for the forward fight are obtained, a number of constraints are added:

$$||\mathbf{A_h}\vec{\lambda}|| \geq 5 \text{ m/s}^2 \tag{4.10}$$

$$\vec{A_v}\vec{\lambda} = 9.81 \text{ m/s}^2 \tag{4.11}$$

$$\vec{A_r}\vec{\lambda} = \vec{0} \tag{4.12}$$

where A_h is the horizontal translational part $\mathbf{A}$ and $\vec{A_v}$ is the vertical translational part of $\mathbf{A}$. By optimizing the norm of the horizontal flying direction, the UAV will fly in most flying efficient direction, which is not per definition the longitudinal direction. Furthermore, the horizontal acceleration is allowed to be above 5 m/s^2, but the vertical acceleration needs to be exactly 9.81 m/s^2 to prevent the UAV from

ascending. The third constraint is used to make sure the UAV does not rotate during the flight, as required. This measure yields an indication of the efficiency of fully actuated flight of the UAVs, where a high λ_f indicates low flight efficiency. For some concepts the maximum horizontal acceleration is less than 5m/s^2. In these cases, λ_{max} is increased such that the acceleration can be achieved. Since this acceleration is not actually obtainable by the actual UAV, the flying efficiency is referred to as virtual flying thrust in this cases.

Chapter 5

Comparison of Fully Actuated UAVs

In this chapter, the concepts from chapter 3 have been compared in order to create a framework that can be used as a first step in designing a UAV for any application. This framework should be as general as possible, such that the specific requirements of said application can be applied to it. In chapter 4 the criteria used for the comparison are specified. The framework is separated into two categories: fixed tilt concepts and variable tilt concepts. As mentioned, an unbiased comparison between fixed and variable tilt is difficult, since the concepts are fundamentally different. In order to specify which UAV category to use, a general comparison between fixed and variable tilt concept is given prior to the framework to specify which framework should be used for which applications.

In section 5.1, the concepts from chapter 3 have been abbreviated to improve the readability of the report. In section 5.2, the limitations and assumptions that are required to make the framework are discussed. In section 5.3 the choice between fixed and variable tilt rotors is discussed. This choice needs to be made before the accompanying framework can be used. A number of design considerations that can be made before using the framework have been discussed in section 5.4. The framework of the fixed tilt concepts is given in section 5.5 and the framework for the variable tilt concepts is given in section 5.6. These frameworks are based on the criteria declared in chapter 4.

5.1 Abbreviations

In order to improve the readability of the report, the compared concepts described in chapter 3 have been given an abbreviation to refer to them. The abbreviations of all concepts are shown in table 5.1, along with the section in chapter 3 where the concept can be found.

Concept	Abbreviation	Chapter
Quadrotor with four horizontal rotors	Quad4Hor	3.2.1
Hexarotor with canted rotors	HexC	3.2.2
Hexarotor canted and dihedral rotors	HexCD	3.2.3
Coaxial Hexagon with 12 canted rotors	CoHexC	3.2.4
Double tetrahedron hexarotor	HexDTet	3.2.5
Heptarotor with minimized frame	HeptF	3.2.6
Heptarotor with maximized wrench	HeptW	3.2.7
Octorotor cube	OctCu	3.2.8
Octorotor beam	OctB	3.2.9
Trirotor with one horizontal rotor	Tri1Hor	3.3.1
Quadrotor with variable cant rotors	QuadvC	3.3.2
Quadrotor with variable dihedral rotors	QuadvD	3.3.3
Quadrotor with variable cant and dihedral rotors	QuadvCD	3.3.4
Quadrotor with coupled variable cant and dihedral rotors	QuadvCDc	3.3.5
Hexarotor with variable cant rotors	HexvC	3.3.6
Hexarotor with coupled variable cant rotors	HexvCc	3.3.5
Ducted Pentarotor with coaxial and variable dihedral rotors	PentvD	3.3.8

Table 5.1: Abbreviations of the concepts described in chapter 3

5.2 Comparison Limitations

There are a number of specifications that do influence the performance of the UAV, but that are not taken into account in this comparison, either because they do not uniquely specify the concept or because determining these specifications is outside of the scope of this report.

- The rotors are considered as a black box with a certain mass that produces a certain thrust and drag torque in accordance with the specifications from the articles. The required rotor speed, motor torque etc. is considered sufficient to produce the required thrust and is therefore not considered.
- For the quantitative analysis the influence of aerodynamic interference on the rotor thrust, as discussed in chapter 2.6, is neglected, as these aerodynamics are outside of the scope of this report. In the Qualitative comparison the negative effect of the airflow interference on the flying stability is considered however.
- For the static comparison, the concepts are scaled to fit inside a unit sphere. However, some of the concepts considered are optimized for a specific dimensions and optimization for this unit sphere might result in a different design. This inconsistency in optimization is neglected in this comparison.
- The dynamic performance has only been determined for the concepts for which the required specifications are given in the reference.

5.3 Fixed Tilt versus Variable Tilt Concepts

In the framework a clear distinction has been made between the fixed and variable tilt concepts. Before the framework can be applied for the optimization of a UAV, the consideration between fixed and variable tilt has to be made. For this choice a few general considerations has been given.

- Changing rotor speed is a faster than changing rotor tilt angle, so fixed tilt concept are faster than variable tilt concepts at rejecting disturbances, resulting in a higher flying stability.
- Variable tilt concepts generally have higher design complexity, as the active tilting of the rotor adds a lot of complexity to the manufacturing of the UAV.
- Variable tilt concepts generally have a higher redundancy than fixed tilt concepts, while the amount of rotors is generally lower. As a result of the low amount of rotors failure has a larger impact on the flyability of the UAV, despite the higher redundancy.
- Variable tilt concepts can achieve higher wrench and acceleration than fixed tilt concepts in all direction, because the rotors can be positioned such that the wrench in the desired direction is maximized. Since the rotors can also be positioned vertically, the thrust efficiency is 1 for all variable tilt concepts.

After the choice between fixed- and Variable tilt concepts is made, the appropriate Framework can be used. These frameworks of the Fixed tilt concepts is given in chapter 5.5 and the framework for the Variable Tilt concept is given in chapter 5.6.

5.4 Preliminary Design Considerations

There are a number of specific considerations that can be done before the framework is applied. When a certain design specific is required, the framework can be limited to the concepts that can fulfill this requirement. The design considerations include:

- **Number of rotors**. The framework can be subdivided in concepts with a certain amount of rotors. For fixed concepts a minimum of six rotors is required for full actuation.
- **Number of tilt actuators**. For variable tilt concepts, the number of tilt actuators can be defined next to the amount of rotors.
- **Design variables**. The amount of variables required to optimize the UAV. A low amount of design variables yields a faster optimization. This specific is directly related to the design complexity.
- **Bi-directional rotors**. Whether or not the UAV will have bi-directional rotors, which produce thrust in positive as well as negative direction, rather than one-directional rotors, as discussed in chapter 2.3.1.

- **Omnidirectionality**. The ability to exert wrench in all direction, both positive and negative. If a UAV is omnidirectional, it can produce wrench in any orientation. Omnidirectionality can be seen as an extension of full actuated concepts.

Note that some of these considerations will not directly result from requirements of the UAV, however all these considerations can be used to limit the concept choice in the framework.

5.5 Comparison of Fixed Tilt Concepts

In this section the qualitative and quantitative criteria from chapter 4 have been applied to the fixed tilt concepts from chapter 3.2. The design consideration for these concepts are shown in table 5.2.

Concept	Number of rotors	Design variables	Bi-directional rotors	Omnidirectional
Quad4Hor	8	1	Yes	No
HexC	6	2	Yes	Yes
HexCD	6	3	Yes	Yes
CoHexC	12	2	Yes	Yes
HexDTet	6	2	No	No
HeptF	7	35	No	Yes
HeptW	7	15	No	Yes
OctCu	8	17	Yes	Yes
OctB	8	10	Yes	Yes

Table 5.2: Design considerations of the variable tilt concepts

5.5.1 Qualitative Comparison

The qualitative grading for the variable tilt concepts is shown in table 5.3. The reasoning behind the grading is given next.

Concept	Flying stability	Design complexity	Downscaling ability	Upscaling ability	Redundancy	Costs
Quad4Hor	-	+++	+	- - -	+	-
HexC	++	+++	-	++	- - -	+++
HexCD	++	+++	+	++	- - -	+++
CoHexC	++	+++	-	+++	+++	- - -
HexDTet	- -	++	- -	- -	- - -	+++
HeptF	+++	- - -	- - -	-	-	+
HeptW	+++	+	- -	- -	-	++
OctCu	+	- -	- -	- -	+	- -
OctB	+++	-	-	+ +	+	- -

Table 5.3: Qualitative criteria for fixed tilt concepts.

Flying Stability

The flying stability is generally very high for fixed tilt fully actuated UAVs. The lateral translational actuation can be used to reject position disturbances very fast compared to an underactuated UAV, which first has to tilt in order to reject these disturbances. This actuation is also faster than variable tilt designs, because these designs need to change the rotor tilt to reject the disturbances, which is much slower than the fixed tilt designs which only need to change rotor speed. Another property that increases flying stability is omnidirectionallity. Omnidirectional UAVs can fly stable at any orientation, so when an outside wrench is applied, the UAV should be able to remain on the trajectory in its current orientation. If the UAV is not omnidirectional, it will need to return to the desired orientation and stray from the trajectory.

The use of bi-directional rotors is disadvantageous for the flying stability due to the singularities that occur when bi-directional rotors change rotation direction, as discussed in chapter 2.3.1.

Another negative impact on the flying stability results from airflow interference between rotors, as discussed in chapter 2.6. If the airflow interference between rotors is high, there will be a high amount of coupling between the thrust produced by the rotors. If this coupling is not taken into account in the control of the UAV, the flying stability will reduce significantly. Considering the thrust coupling due to airflow interference in the control involves very complex aerodynamics and is not advisable. A better approach is to make sure during the design of the UAV that the distance between the rotors is large enough to assure there is negligibly little airflow interference between rotors. The airflow interference between the coaxial rotors of CoHexC does not influence the flying stability, because the interference is constant, as mentioned in chapter 3.2.4. This also applies for Quad4Hor.

Lastly the susceptibility to side wind disturbance is considered. Concepts with high body drag coefficient will have a reduced flying stability, since they are more susceptible to wind disturbance. High body drag can result from a large frame and out-of-plane rotor configuration.

The Quad4Hor and HexDTet are not omnidirectional, so these concepts have lower flying stability than the other concepts. Based on stability tests done for the HexTet [10] it can be concluded that this design is very unstable, mainly due to the limited horizontal actuation, as well as the high body drag coefficient. Wind disturbance rejection experiments showed that the Quad4Hor performs marginally better flying stability than an underactuated quadrotor [37]. However, compared to the omnidirectional UAVs the flying stability is limited. From the omnidirectional concepts, the HeptF and HeptW are the only designs with on-directional rotors. That is why these concepts have the highest flying stability. OctB also scores high, since this concept has overcome the issue of esc-singularity by using a selective mapping algorithm. This algorithm is proven by performing a peg-in-hole operation, which requires high flying stability. The OctCu suffers from a very high drag coefficient due to the large frame, which reduces the flying stability

Design Complexity

The design complexity consists of optimization complexity and manufacturing complexity. The manufacturing complexity depends heavily on the frame of the UAV. For a number of concepts, a commercially available frame can be slightly adapted to be used as a frame, which heavily reduces the manufacturing complexity. The concepts that require a custom frame and thus have high manufacturing complexity are: HexDTet, HeptF, OctCu and OctB, although HexDTet could be manufactured with a heavily adapted hexarotor frame.

Regarding the optimization complexity, the HeptF scores the lowest, as there is no symmetry in the design. All seven rotors require five parameters (x,y and z position and two orientation angles), so there are 42 parameters. HeptW and OctCu do have symmetry in the position of the rotors: all rotor positions are defined by a single variable. however, the orientation still requires two parameters per rotor, making the total amount of parameters 15 for HeptW and 17 for OctCu, which is still very high compared to the other concepts. For OctB, the amount of rotors is reduced by defining symmetric rotor pairs with equal orientation, resulting in ten variables. For the remaining concept the amount of variables is sufficiently low to consider optimization of these concepts similarly complex.

Downscaling Ability

The downscaling ability of UAVs is limited by the increase in airflow interference between rotors, which is undesirable for the flying stability. Generally UAVs with less rotors suffer less from airflow interference when scaling down. However, if the rotors are not spread out evenly, two closely placed rotors can still interfere. Furthermore the if the rotors are orientated to face each other, airflow interference on smaller scale is more likely. Next to airflow interference, which only results in reduced flying stability, rotor interference is a hard limit to the downscaling ability.

The HeptF has many rotors that are facing each other and will interfere when scaling down. The same applies for the Heptarotor wrench optimized, however the distance between the rotor is much more uniform, increasing the downscale ability slightly. The OctCu and OctB both have many rotors. However both designs have their rotors spaced uniformly. The rotor orientation of the OctCu makes it a bit more prone to airflow interference than the OctB. HexCD suffers less from airflow interference at small scale than HexC and CoHexC due to the outward dihedral angle, which redirects the rotor airflow away from the other rotors. For the Quad4Hor the horizontal rotors have to be placed between the frame arms, which is not possible at very small scale.

Upscaling Ability

Since there is a maximum to the thrust that can be achieved using brushless motors, the upscaling of UAVs is limited by the total rotor thrust that can be achieved. If the UAV has a high amount of rotors, this thrust is generally larger. If the UAV has a frame that requires a lot of material in order to assure sufficient stiffness, the mass will become very high and the thrust required to fly will increase as well. Another consideration is the practical usability at large scale. If the UAV is very high, for example, it will become impractical to use.

The Quad4Hor is worst on upscaling ability due to the limited amount of rotors. The OctCu does have a high amount of rotors. However, it has a very large cage around it, which is impractically at large scale. This impracticality applies to a lesser extend to the HexTet. The HeptW and HeptF have one-directional rotors with opposite orientation, so the thrust used for flying is limited, which limits the upscaling ability, although the optimization to minimized frame mass of HeptF is advantageous for the upscalability. The HexC and HexCD give a good trade-off between the amount of available thrust and the frame mass. However, at very large size, the thrust produced by six rotors will be insufficient. The OctB does produce enough thrust, but upscaling is limited by the frame stiffness of the center beam, which will have to be very thick to be stiff enough for the large sized rotors. The concept that can be scaled up the best is the CoHexC: the frame can be stiffened easily and the amount of rotors is very high, so the available thrust is sufficient.

Redundancy

The redundancy follows directly from the amount of rotors and the amount of DoFs, which is six. HexC, HexCD and HexDTet have no redundancy, the HeptF and HeptW have a redundancy of one, Quad4Hor, OctCu and OctB have a redundancy of two and the concept with by far the highest redundancy is the CoHexC, which has a redundancy of six.

Costs

The most important criteria for the costs is the amount of rotors, which is why CoHexC is most expensive. From the eight rotor concepts, Quad4Hor is the cheapest due to the commercial available frame. For the same reason, the HeptW is the cheapest seven rotor concept. From the six rotor concepts, HexDTet has a custom frame, which results in slightly higher costs. However, the one-directional rotors reduce the costs of the HexDTet relative to the other six rotor concepts.

5.5.2 Static Comparison

The statics comparison, as defined in chapter 4.2.1, is presented here. The maximum uncoupled wrench in all directions, as well as the thrust efficiency η_F, of the fixed tilt concepts is shown in table 5.4. The three concepts with the highest performance for each criteria are highlighted.

	Maximum uncoupled wrench						
Concept	Longitudinal [N]	Lateral [N]	Vertical [N]	x-Rotation [Nm]	y-Rotation [Nm]	z-Rotation [Nm]	η_F [-]
Quad4Hor	2.83	**2.83**	4.00	2.06	2.06	0.08	0.50
HexC	2.31	2.00	4.90	**2.48**	**2.87**	**3.36**	**0.82**
HexCD	2.26	1.95	4.84	2.46	2.84	3.29	0.81
CoHexC	**4.62**	**4.00**	**9.80**	**4.90**	**5.66**	**6.93**	**0.82**
HexDTet	0.10	0.09	**5.80**	0.22	0.24	0.06	**0.97**
HeptF	1.66	1.14	1.50	0.46	0.49	0.80	0.21
HeptW	1.49	1.17	1.69	1.21	1.29	1.17	0.24
OctCu	**4.54**	**4.54**	4.54	**3.37**	**3.37**	**4.62**	0.57
OctB	**5.44**	2.24	**5.44**	1.30	1.56	0.93	0.68

Table 5.4: Static comparison of the fixed tilt concepts

To better compare the concepts, the ranking of the concepts is shown in table 5.5, where the ordering from low to high represents the best to the worst performing concept.

Concept	Maximum uncoupled wrench						η_F
	Longitudinal	Lateral	Vertical	x-Rotation	y-Rotation	z-Rotation	
Quad4Hor	4	**3**	7	5	5	8	7
HexC	5	5	4	**3**	**3**	**3**	**3**
HexCD	6	6	5	4	4	4	4
CoHexC	**2**	**2**	**1**	**1**	**1**	**1**	**2**
HexDTet	9	9	**2**	9	9	9	**1**
HeptF	7	8	9	8	8	7	9
HeptW	8	7	8	7	7	5	8
OctCu	**3**	**1**	6	**2**	**2**	**2**	6
OctB	**1**	4	**3**	6	6	6	5

Table 5.5: Graded static performance of the fixed tilt concepts

Forces

A strong relation between the amount of rotors and the achievable force is observed. The concepts with a high amount of rotors produce the highest forces. This relation is best shown by the difference between the CoHexC and the HexC, which have a similar rotor configuration. Because the CoHexC has twice as many rotors, its force is about twice as high in all directions. If more rotors are added to the coaxial pair, the thrust will increase even more. The disadvantages of adding rotors, additional mass and airflow interference, are not taken into account in the static comparison.

Furthermore a trade-off between horizontal and vertical force is observed: as the rotor tilts the vertical component of the thrust will decrease and the horizontal component will increase. Two exception to this observed trade-off between horizontal and vertical force, as well as the observed relation between the amount of rotors and the achievable force, are the HeptF and HeptW. These concepts are both omnidirectional with one-directional rotors, which is only possible if some rotors are orientated in opposite direction. Due to this only a limited amount of rotors contribute to the force in a direction and the force that is achieved is limited.

HexC and HexCD can achieve very similar force, as a result of the similar design. However, HexC, with $\alpha = 35.3°$, can achieve higher horizontal forces than HexCD, with $\alpha = 35°$ and $\beta = 10°$. This observation is inconsistent with the mentioned relation between tilt angle and horizontal force. The reason for this is that, in order to obtain uncoupled horizontal force, HexCD has rotors that do not produce full rotor thrust to prevent coupling with the torques. This reduced thrust contributes to a reduce in horizontal force. Since HexCD does not exhibit this coupling, it can be assumed that the coupling is a result of the added dihedral angle. The difference in vertical force does comply with the proposed relation between horizontal and vertical force.

For the Omnidirectional concepts the orientation of the UAV should not matter for the performance, so the Force in all directions should be similar. This is the case for the Heptarotor max. wrench, HeptF and OctCu. Based on the forces it can be concluded that this UAV does not have a preferred orientation. The OctB has been optimized to produce twice as much force in longitudinal and vertical direction than the lateral direction, since this direction is assumed less important by the designer. The HexC, HexCD and CoHexC can achieve a lot higher force in vertical direction than horizontal. This means that these UAVs do have a clear preferred orientation, although they are omnidirectional.

Torque

Similar to the forces, the Torque increases when the amount of rotors increases. Due to the high amount of rotors the coaxial hexagon canted performs the best for all torques. Like the forces, the torques of this concepts are twice as high as the HexC. Based on the difference between HexC and HexCD the effects of cant and dihedral tilting of the rotors is observed. Although the torque in all directions is very similar, it can be observed that the difference in x- and y-rotation is less than the difference in z-rotation. This complies with the statement in chapter 3.2.3 that cant angle contributes to the yaw, where dihedral angle does not.

The tilting of the rotors has a clear influence on the torque: the x- and y-torque decreases due to the reduced thrust in vertical direction, while for concepts with high cant angle: HexC, HexCD, CoHexC and OctCu, a clear increase in z-torque is observed, as mentioned. If there is no canting at all, the z-torque torque will depend only on the drag torque from the rotors, as observed for Quad4Hor and HexDTet. The latter has the lowest z-torque, since the drag torque contribution is reduced due to the tilting of the rotors.

For HeptF and HeptW, the torque in all directions is low as a result of the one-directional rotors: only a few rotors can contribute to the uncoupled torques in a direction. For OctB the torques are also very low. This results from the small arm as a result of the slender design, as well as the high dihedral angle of the rotors.

Thrust Efficiency

The thrust efficiency gives an indication of how much vertical thrust is lost when the horizontal direction is actuated. The highest thrust efficiency is achieved by the HexDTet, because this concept has very little rotor tilting. This also results in very low horizontal force. The OctCu has very low thrust efficiency, however the horizontal force is very high: The thrust is used efficiently, however not for vertical force. Based on only the thrust efficiency, no conclusion can be made on the amount of thrust that is actually lost and the amount of thrust that is repurposed into horizontal force. For the HeptF and HeptW the amount of 'lost' thrust is very high, because both vertical and horizontal force is low.

In general it can be seen that omnidirectional concepts suffer from low thrust efficiency. This can be contributed to the fact that the force in all directions needs to be high, which reduces the vertical thrust.

5.5.3 Dynamic Comparison

As mentioned the dynamic comparison will be done based on the UAV dimension, Inertia and rotors specified in the articles of the concepts. In this section these specifications are first presented and compared based on the thrust-to-weight ratio , as defined in chapter 4.2.2. With the specifications the dynamic comparison is done. The results from the dynamic comparison are compared to the results from the static comparison in section 5.5.2. The inconsistencies between the results are considered and the importance of going through the extra effort of finding the inertia of the concept is emphasized.

The specifications required for the dynamic comparison are given in table 5.6 of each concept as presented by the respective reference. It can be observed that not all relevant specifications have been given in the references. However, the specifications required for determining the translational acceleration; total mass and rotor thrust, can be deduced for all concepts, except HexDTet and CoHexC.

The rotor thrust of the CoHexC is based on the maximum payload, which is defined in the article to be 5 kg. This results in rotors with a thrust of 7.3 N for the considered design with α =35.3°. For the HexDTet, no specifications could be found. Since there is no similar concept that could be used, this concept cannot be compared dynamically. The Quad4Hor has an external battery which is not included in the total mass of this UAV. The mass of a battery [38] with the specifications given in the reference of Quad4Hor has been added to the mass.

A breakdown of the rotor mass of the concepts, consisting of the mass of the rotor and the propeller, has been given in appendix B.

Concept	Length [m]	Inertia [kgm^2]	Total mass [kg]	Rotor mass [kg]	Thrust [N]	$(T/w)_{rotor}$ [-]	$(T/w)_{tot}$ [-]
Quad4Hor	0.31	-	2.44	-	36.3/9.81*	-	12.43
HexC	0.60	eq. 5.1a	1.50	-	6.0	-	2.45
HexCD	0.80	eq. 5.1b	2.48	0.14	12.0	8.49	2.96
CoHexC	1.00	-	3.12	-	7.3	-	2.86
HexDTet	-	-	-	-	-	-	-
HeptF	0.94	eq. 5.2c	1.90	0.12	13.0	23.77	10.52
HeptW	0.80	eq. 5.2d	1.30	-	12.9	-	7.08
OctCu	0.45	-	0.89	0.06	6.7	12.20	6.17
OctB	0.80	-	2.60	0.13	9.7	7.72	3.04

Table 5.6: Dynamic specifications of the fixed tilt concepts. *Vertical rotors/horizontal rotors

The rotational acceleration have only been given for the HexC, HexCD, HeptF and HeptW. The

inertia specified in these references are:

$$I_{HexC} = \begin{bmatrix} 0.02 & 0 & 0 \\ 0 & 0.02 & 0 \\ 0 & 0 & 0.05 \end{bmatrix}, \qquad I_{HexCD} = \begin{bmatrix} 0.12 & 0 & 0 \\ 0 & 0.11 & 0 \\ 0 & 0 & 0.19 \end{bmatrix} \tag{5.1}$$

$$I_{HeptF} = \begin{bmatrix} 0.35 & 0.07 & -0.05 \\ 0.07 & 0.16 & 0.01 \\ -0.05 & 0.01 & 0.41 \end{bmatrix}, \qquad I_{HeptW} = \begin{bmatrix} 0.03 & 0 & 0 \\ 0 & 0.03 & 0 \\ 0 & 0 & 0.03 \end{bmatrix} \tag{5.2}$$

The inertia of HexC and HeptW is significantly lower than that of HexCD and HeptF. For the HexC this can be explained, since the mass and length, which is squared, are very low. For HeptW, the length is equal to the length of HexCD and although the mass is much lower, it does not fully explain the large difference in inertia. Furthermore, the inertia around the z-axis is equal to the inertia around the x- and y-axis, which is peculiar for an in-plane rotor configuration. HeptF has very high inertia, as a result of the high length. Furthermore, this inertia has high off-diagonal terms, as result of the nonsymmetric rotor configuration.

Thrust-to-Weight Ratio

The thrust-to-weight ratio of the rotor, $(T/w)_{rotor}$, and for the total UAV, $(T/w)_{tot}$, are shown in table 5.6. There is a large difference in $(T/w)_{rotor}$ between the different rotors, in accordance with the findings in appendix D. By far the highest $(T/w)_{rotor}$ is achieved by HeptF, which has one-directional rotors, while the other concepts have bi-directional rotors. This confirms the loss of energy efficiency of bi-directional rotors discussed in chapter 2.3.1. From the bi-directional rotors, the OctB performs the worst. For this concept a very inefficient stacked propeller setup has been used.

For $(T/w)_{tot}$ the HeptF performs best as well. This can partly be contributed to the high $(T/w)_{rotor}$, but also to the fact that the rotor configuration has been optimized to minimal frame mass. This combination yields a very high $(T/w)_{tot}$. The HexC, HexCD, CoHexC and OctB have very low $(T/w)_{tot}$ compared to the other concepts. Based on the references it is considered that the prototypes of these concepts are mere proof of concept and not optimized designs.

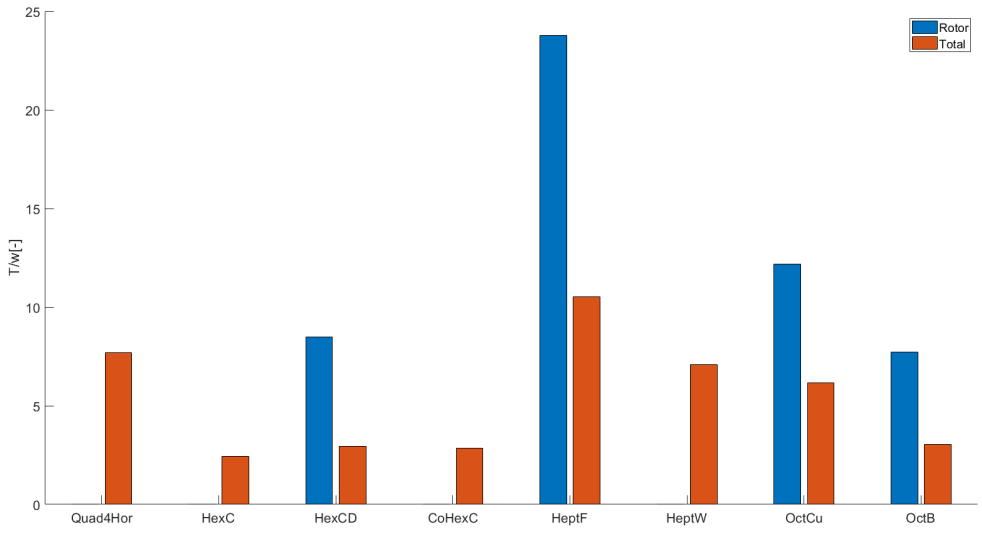

Figure 5.1: Thrust-to-weight ratio for fixed tilt concepts

The accelerations in all directions, as well as the flying thrust, are shown in table 5.7. The results are based on the specifications from table 5.6. The three best results are highlighted.

Concept	Maximum uncoupled acceleration						λ_f
	Longitudinal [m/s^2]	Lateral [m/s^2]	Vertical [m/s^2]	x-Rotation [s^{-2}]	y-Rotation [s^{-2}]	z-Rotation [s^{-2}]	[N]
Quad4Hor	11.4	11.4	**59.5**	-	-	-	36.1
HexC	9.2	8.0	19.6	**204.3**	**235.9**	**125.2**	**22.8**
HexCD	10.9	9.4	23.4	**97.3**	**126.6**	**78.7**	31.6
CoHexC	14.4	**12.4**	**30.5**	-	-	-	37.5
HexDTet	-	-	-	-	-	-	-
HeptF	**24.5**	16.8	22.1	35.4	93.7	53.4	39.1
HeptW	14.7	11.6	16.3	**213.2**	**221.2**	**196.4**	**25.0**
OctCu	**33.2**	**33.2**	**33.4**	-	-	-	**15.1**
OctB	**20.3**	8.4	20.3	-	-	-	37.5

Table 5.7: Dynamic comparison of the fixed tilt concepts

The concepts have been compared in table 5.8, where the ordering represents the best to the worst performing concept.

Concept	Maximum uncoupled acceleration						λ_f
	Longitudinal	Lateral	Vertical	x-Rotation	y-Rotation	z-Rotation	
Quad4Hor	5	4	**1**	-	-	-	5
HexC	8	8	7	**2**	**1**	**2**	**2**
HexCD	6	6	**3**	**3**	**3**	**3**	4
CoHexC	7	5	4	-	-	-	7
HexDTet	-	-	-	-	-	-	-
HeptF	**2**	**2**	5	4	4	4	8
HeptW	4	**3**	8	**1**	**2**	**1**	**3**
OctCu	**1**	**1**	**2**	-	-	-	**1**
OctB	**3**	7	6	-	-	-	6

Table 5.8: Graded dynamic performance of the fixed tilt concepts

Translational Acceleration

In section 5.5.2, it was observed that the static performance generally improves as the amount of rotors increases. This is not the case for the dynamic comparison, since an increase in rotors results in an increase in mass. This is best illustrated with the difference in performance between the CoHexC and the HexC. The only difference between these concepts is that the CoHexC has coaxial rotor pairs instead of single rotors. In the static comparison, the coaxial rotors produce twice as much thrust as the single rotor, which results in a wrench that is twice as great. Based on this, the CoHexC outperforms the HexC in all directions. However, when the mass of the rotors, frame, batteries, etcetera are taken into account in the dynamic comparison, the superiority of the CoHexC vanishes and concepts perform similar. If the concept choice would be made based on the static performance, the coaxial hexagon would always be chosen, while the dynamical performance, which is much more important for UAVs, is significantly worse. This is why the extra step to the dynamical comparison is not a waste of time.

The highest longitudinal and lateral acceleration is achieved by the OctCu. This concept produces high omnidirectional wrench and has a high $(T/w)_{tot}$. What does strike is that the accelerations obtained for the OctCu are actually higher than the accelerations according to the reference, which uses a different coordinate frame, in which the principle translation directions are not actually the optimal directions. The OctB, which produces the highest longitudinal force, is surpassed by two concepts based on the longitudinal accelerations due to the low $(T/w)_{tot}$.

Apart from these results, a difference worth mentioning is the performance of the HeptF. This concept comes to its right in the dynamic comparison, because it was optimized for minimized mass. Based on the static comparison, this concept would be discarded, while the actual dynamic performance is rather good. However, instead of minimizing the frame, a better practice would be to optimize the accelerations, since the inertia of this concept is still very high, despite the low mass. This concept does show the importance of a good frame design, as reflected by the high $(T/w)_{tot}$.

Rotational Acceleration

HeptF produces the lowest rotational accelerations of the four concepts for which the inertia is given, due to the high inertia and very low possible torque. The HeptW, which also has very low torque, produces very high accelerations due to the very low inertia. The HexC and HexCD perform very similar based on the static torques, while the acceleration of the HexC is double that of HexCD. It can be concluded that the positive effect of the reduced length of the HexC has on the inertia, outweighs the negative effect it has on the torque. This makes sense because the length is squared in the inertia.

For the concepts for which the inertia is not given, an estimation of the rotational acceleration has been made: the Quad4Hor has an inertia that is similar to a standard quadrotor, because the horizontal rotors have low mass and are placed close to the CoM. This limits their contribution to the inertia. Since the standard quadrotor has excellent rotational acceleration, it can be assumed that these concepts also have high rotational acceleration.

The CoHexC has a great inertia due to the large amount of rotors. If its size is equal to HexC, it is expected that the inertia of CoHexC is about twice as great as the inertia of the HexC. However, the torque is also about twice as high, so the rotational acceleration should be about equal. Based on the difference in translational acceleration, which is higher for CoHexC, it is predicted that the rotational acceleration of the CoHexC will be higher than HexC's rotational acceleration.

The remaining concepts all have an out-of-plane rotor configuration. This configuration yields similar inertia in all directions, while the in-plane configuration has a higher z-inertia compared to the x- and y-inertia. Due to the similar inertia, the x and y rotational accelerations are relatively low and the z rotational acceleration is relatively high for out-of-plane concepts. This does not apply for the HexDTet, since this concept barely produces z-torque. The OctCu has a symmetric configuration, which yields the same inertia in all directions. Along with the torque that is almost equal in all directions, this results in very similar rotational accelerations in all directions. For the OctB, the x-inertia (around the beam) is very low, while this torque is rather high, so the acceleration in this direction is high.

Flying Thrust

In general, the required flying thrust increases as the mass increases, because the thrust required to accelerate increases. The concept with the lowest mass, theOctCu, performs the best, as it has the lowest flying thrust . The HeptF, however, has a very high flying thrust, despite its low mass. The reason for this is that the rotors produce opposing thrust, so in order to achieve the desired acceleration, some rotor thrust will be canceled out. This also applies, to a lesser extend, to the HeptW.

Based on the results it can be concluded that the flying thrust not only depends on the mass, but also on efficiency of the thrust. This is also shown by the HexC, which has average mass, but very high horizontal acceleration. This means that a small portion of the total available thrust is required for the required horizontal acceleration. For the HexCD a much higher portion of the available thrust is required to achieve this horizontal acceleration and consequently the flying thrust is higher. The low performance of the other concepts can be explained by either the high mass or the low horizontal acceleration.

The thrust efficiency is compared to the flying thrust based on how well they describe the flying efficiency of the UAV. The thrust efficiency mainly emphasizes the thrust that is lost due to the horizontal actuation and does not indicate how efficient this 'lost' thrust is used for horizontal actuation. The flying thrust does give an indication of how efficient the horizontal actuation is, which gives a much better insight in the efficiency of the thrust distribution. However, the flying thrust does depend heavily on the mass of the UAV.

5.5.4 Conclusion

The framework for optimization of fixed tilt concepts has been presented here. It consisted of qualitative and quantitative criteria, which can be used to find the optimal concept for any application. It has been shown that all concepts have different advantages and disadvantages based on the qualitative criteria. Furthermore, it has been shown that the performance of the UAV based on the dynamic comparison can be very different from the static performance. For that reason, it is important to consider the dynamics of the UAV to determine its performance. A number of relations between concepts can be seen based on the static and dynamic comparison:

- Concepts with a high number of rotors have high redundancy, but also high cost and generally a more complex design. Furthermore, the upscaling ability increases but the downscaling ability

decreases. The static performance increases as long as the added rotors do not counteract the other rotors. The dynamic performance increases much less, because the mass of the rotors is taken into account. The flying thrust requires more thrust because the UAV mass is generally higher.

- Using bi-directional rotors rather than one-directional rotors has a positive effect on the static and dynamic performance, although the design complexity and costs are higher and the rotor thrust-to-weight ratio is lower. Furthermore, 'ESC-induced singularity' may result in reduced flying stability.
- Omnidirectional concepts generally have high horizontal actuation, resulting in a very low thrust efficiency. The flying stability is very high because every disturbance can be rejected.

5.6 Variable Tilt Concepts

In this section, the framework for the variable tilt concepts from chapter 3.3 is presented in a similar fashion as the framework for the fixed tilt concepts was given. The design considerations for the variable tilt concepts are given in table 5.9.

Concept	Number of rotors	Number of tilt actuators	Design variables	Bi-directional rotors	Omnidirectional
Tri1Hor	4	1	1	Yes*	No
QuadvC	4	4	1	No	Yes
QuadvD	4	4	1	No	No
QuadvCD	4	8	1	No	Yes
QuadvCDc	4	2	1	No	No
HexvC	6	6	1	No	Yes
HexvCc	6	1	6	No	No
PentvD	5	3	6	No	No

Table 5.9: Design considerations of the variable tilt concepts (*only the horizontal rotor is bi-directional)

5.6.1 Qualitative Comparison

The qualitative comparison of the variable tilt concepts is given in table 5.10. These results are discussed next.

Concept	Flying stability	Design complexity	Downscaling ability	Upscaling ability	Redundancy	Costs
Tri1Hor	- -	+	-	- - -	- - -	+++
QuadvC	-	+	++	- -	-	++
QuadvD	-	+	++	- -	-	++
QuadvCD	+	-	- -	- -	++	-
QuadvCDc	+	- - -	- - -	- - -	- - -	++
HexvC	++	+	+	++	+++	- - -
HexvCc	++	- - -	- - -	+	- -	- -
PentvD	- - -	- -	+	- - -	-	- -

Table 5.10: Qualitative criteria variable tilt concepts

Flying Stability

As mentioned in section 5.3, the flying stability of variable tilt concepts is generally low due to the slow response to disturbance. However, when the tilting actuator is not actively used like the HexvCc, the flying stability is as high as a fixed tilt UAV. Although the HexvC does require the tilting actuator for omnidirectional flight, it can also fly fully actuated without active tilting the rotor, yielding a similar flying stability to HexvCc. The Tri1Hor uses only one tilting actuator to counteract yaw, so the reduction in stability of the tilting rotor is limited. However, this concept cannot directly reject disturbance in y-direction

due to the limited actuation. Furthermore, there is airflow interference between the horizontal rotor and the tail rotor. These negative influences results in a very low flying stability. The other concepts do depend on the tilt actuator for full actuation and have low flying stability. The QuadvCD and QuadvCDc score higher than other concepts because these concepts can orientate each rotor in the same direction, making it possible to reject disturbances in all directions faster than other concepts. The PentvD performs worse than the other concepts because it is more susceptible to wind disturbances due to the high body drag of the ducts.

Contrary to the fixed tilt concepts, airflow interference barely influences the performance of variable tilt concepts. The only concepts that may suffer from airflow interference are the HexC, when the tilt angle of the rotors is very high, and the Tri1Hor. For the HexC, the influence of the airflow interference can be neglected, since it occurs rarely.

Design Complexity

The manufacturing complexity of the variable tilt rotors is high. The concepts with coupled rotor tilting, QuadvCDc and HexvCc, have the highest manufacturing complexity, since the tilting-mechanism is very complex. The PentvD also has high manufacturing complexity due to the high manufacturing complexity of the ducts with coaxial rotors. Of the remaining concepts, the QuadvCD is the most complex, because the rotor is rotated around two axes, which is more complex to manufacture than a one tilt axis.

The optimization complexity of all variable tilt concepts is low, since the orientation is variable and does not need to be optimized.

Downscaling Ability

The downscaling ability is limited by the amount of space required by the rotors and tilt actuators. The QuadvCDc and HexvCc require a lot of space for their tilting mechanisms. Furthermore, the mechanisms are very difficult to manufacture on small scale. This makes the downscaling of these concepts very difficult. The QuadvCD also requires a lot of space for the two tilting actuators on each arm. From the concepts with one tilting angle, the HexvC has limited downscaling ability, because the amount of rotors and tilt actuators is the highest and the airflow interference between rotor increases when downscaling. The PentvD has limited downscaling ability, because the ducts require a lot of space. Although the Tri1Hor has a limited amount of actuators, downscaling will increase the airflow interference even more.

Upscaling Ability

The main limitation for upscaling is the maximum thrust a brushless motor can produce and the maximum torque a tilt actuator can produce. The required tilt actuator torque increases when the rotor increases in size. Due to the limited rotor thrust and tilt actuator thrust, the concepts with only three or four rotors have limited upscaling ability. The PentvD has five rotors, but the thrust is mainly produced by the two coaxial rotors, which means that the limit of rotor thrust is reached even earlier than the three or four rotor concepts. The HexvC and HexvCc both have six rotors that contribute equally to the vertical thrust, so these concepts can be scaled up better. The coupled tilting for the QuadvCD and HexvCc have high torque requirements for the tilting actuators, since they have to tilt all rotors. This limits the upscaling ability of these coupled concepts.

Redundancy

The redundancy of variable tilt concepts is generally very high, since each tilt actuators contributes to the amount of actuators just like a rotor. However, the tilt actuator does not contribute to the fail-safety similar to a rotor, since they do not produce thrust. For safety, a high amount of rotors is favoured over a high amount of tilt actuators. This disability is not taken into account in the redundancy.
The Tri1Hor and QuadvCDc have no redundancy, the HexvCc has a redundancy of one, the QuadvC, QuadvD and PentvD have a redundancy of two and the QuadvCD and HexvC have a redundancy of six. The HexvC has two more rotors than the QuadvCD, making it the most fail-safe.

Costs

The costs of variable tilt concept are governed by the actuators. The rotors are more expensive than the tilting actuators, since the motors of the rotors have higher requirements. Apart from the actuator, the costs are determined by the complexity of the frame.
The Tri1Hor has the lowest costs due to the low amount of rotors, tilt actuators and the standard frame.

The QuadvC and QuadvD have little higher costs, since the amount of actuators is higher. QuadvCDc also has less actuators, but the frame is more complex, resulting in similar costs. The same applies for the HexvCc compared to the HexvC, although the difference in the amount of actuators is higher. The PentvD has an expensive custom frame. The QuadvCD and HexvC have the same amount of actuators, but the QuadvCD has less rotors so less costs.

5.6.2 Static Comparison

The variable tilt concepts can actively rotate their rotors to obtain the maximum wrench in any direction. For that reason, the attainable force is very high for the amount of rotors. If servo motors are used for actuating the tilt of the rotors, the tilt angle is limited. This is not the case when brushless motors are used. In appendix C, an overview of the tilt actuators used for the concepts is presented. To make the comparison between concepts with servo motors and brushless motors unbiased, it is assumed that all tilt actuators can rotate $360°$, as discussed in chapter 2.5. The overview of the tilt actuators shows that the difference in mass between servo and brushless motors, which is relevant for the dynamic comparison, is limited.

Despite the assumption of full rotation of the tilt actuators, the tilt angle of the rotors is still limited by the frame for some concepts. The maximum inward dihedral angle depends on the propeller size and the vertical distance between the propeller and the frame. It is assumed that the rotor can tilt $45°$ inward, before the propeller collides with the frame. The maximum outward rotation of the rotor is $225°$, before it collides with the frame. In cant direction, the rotor will never hit the frame, so the rotor can rotate $360°$. The QuadvCDc has coupled rotor tilt, so there is always a rotor with an inward dihedral angle that will collide with the frame if the rotation angle is too high. For that reason, the maximum tilt angle of this concept is $45°$. The HexvCc has a limited canting angle due to the canting mechanism that does not allow for large canting. The maximum canting angle is also assumed to be $45°$. These limitation to the tilting angles are taken into account in the static and dynamic comparison.

The static comparison, consisting of the maximum uncoupled wrench and thrust efficiency, as discussed in chapter 4.2.1 of the variable tilt concepts are shown in table 5.11. The limited tilt angles mentioned above are taken into account in this comparison. The three best scoring concepts are highlighted.

	Maximum uncoupled wrench						
Concept	Longitudinal [N]	Lateral [N]	Vertical [N]	x-Rotation [Nm]	y-Rotation [Nm]	z-Rotation [Nm]	η_F [-]
Tri1Hor	1.00	0	3.00	0.58	1.00	0.02	0.76
QuadvC	2.83	2.83	4.00	**2.83**	**2.83**	**4.00**	1.00
QuadvD	2.00	2.00	4.00	0.05	**2.83**	0.00	1.00
QuadvCD	**4.00**	**4.00**	4.00	**2.83**	**2.83**	**4.00**	1.00
QuadvCDc	**3.39**	**3.39**	4.00	1.41	1.41	0.04	1.00
HexvC	**4.00**	**3.46**	**6.00**	**4.00**	**3.46**	**6.00**	1.00
HexvCc	1.41	1.22	**6.00**	2.00	1.73	2.16	1.00
PentvD	2.00	1.73	**5.00**	1.73	2.00	0.02	1.00

Table 5.11: Static comparison of the variable tilt concepts.

The results have been graded in table 5.12, where the grades represent the ordering of the performance from best to the worst.

	Maximum uncoupled wrench						
Concept	Longitudinal	Lateral	Vertical	x-Rotation	y-Rotation	z-Rotation	η_F
Tri1Hor	8	8	8	7	8	6	8
QuadvC	4	4	4	**2**	**2**	**2**	**1**
QuadvD	5	5	4	8	**2**	8	**1**
QuadvCD	**1**	**1**	4	**2**	**2**	**2**	**1**
QuadvCDc	**3**	**3**	4	6	7	5	**1**
HexvC	**1**	**2**	**1**	**1**	**1**	**1**	**1**
HexvCc	7	7	**1**	4	6	4	**1**
PentvD	5	6	**3**	5	5	6	**1**

Table 5.12: Graded static performance of the variable tilt concepts

Forces

Because the rotors can be actively tilted, the force in any direction can be optimized by tilting the rotors in that direction. The QuadvCD can orientate all rotors in any desired direction, yielding maximum force in all directions. The QuadvCDc should be able to achieve the same, but due to the coupling between the rotor tilting, the maximum tilt angle of all rotors is limited. The other concepts have only one variable angle, so it is impossible to achieve maximum force in all directions for these concepts. The QuadvD has slightly lower horizontal force than QuadcC, due to the limited tilting angle. The Tri1Hor produces very low force, because only a limited amount of rotors produce thrust in a desired direction due to the amount of tilting actuators. Furthermore, it should be stressed that the direction of the maximum vertical force is variable, due to the lateral actuation of the tilting rotor, as discussed in chapter 3.3.1.

Torque

For obtaining torque, the ability to actively tilt the rotors is exploited a lot less than it is for the forces. The reason for this is that for the maximum x- and y-torque, the rotors are always orientated vertical, since canting transforms the torque in these directions into z-torque and a dihedral angle depletes the torque, as discussed in section 5.5.2. Despite this, the variable tilt is still advantageous for the fact that the rotors can be tilted $180°$, enabling it to produce negative thrust. The x- and y-torque are effectively doubled compared to the concept with rotors that can only produce thrust in one direction. This can be seen by comparing the HexvC to the HexvCc: as the HexvCc cannot rotate the rotors fully, negative thrust cannot be achieved. This yields a x- and y-torque that is half that of the HexvC. The same applies to the QuadvCDc compared to the other quadrotor concepts.

The QuadvD has very low torque performance: the x- and z-torque are extremely low. The reason for this is that the rotation direction of the rotors is not alternating. According to the reference, this is required for translation without disturbance from rotor drag. However, it makes x-torque without drag torque disturbance impossible. Furthermore, z-torque, which is already low since there is no canting actuation, is even lower because it cannot be achieved using the drag torque. The claim that the non-alternating rotation direction is required for translational force is checked by using the same concept with alternating rotation direction, which showed that the UAV is able to produce uncoupled horizontal force, with only a very small reduction in horizontal force compared to the non-alternating rotation direction. The alternating configuration yields an x-torque that is equal to the y-torque and a z-torque that results from the drag torque. However, since this is a comparison between the concepts defined by the references, the non-alternating rotors are used in the comparison. It should be noted that it is possible to increase the performance of the concept by using rotors with alternating rotation direction.

The QuadvCDc cannot cant the rotors without creating horizontal force, so this concept also depends on the drag torque for z-torque. The PentvD only has two rotors that produce drag torque, so the yawing is even lower. This also applies for the Tri1Hor.

Thrust Efficiency

It is clear that variable tilt concepts can achieve maximum vertical force by orientating all rotors vertically, yielding a thrust efficiency of one. One exception to this is the Tri1Hor, which has a fixed horizontal rotor that does not contribute to the vertical force. Since the vertical force is maximum for all other concepts, the thrust efficiency is not a useful criteria for comparing these concepts. Fortunately, a different measure of the flying efficiency is proposed in the dynamic comparison, presented next.

5.6.3 Dynamic Comparison

The dynamic comparison of the variable tilt concepts, defined in chapter 4.2.2, is presented in this section. The required specifications for the dynamic comparison are shown in table 5.13. The mass of the motor and propeller can be found in appendix B. For the QuadvCDc, no specifications are given and for the HexvCc the rotor thrust is not given, so these concepts cannot be compared dynamically. The QuadvC and QuadvD are both based on a QuadvC designed by Oosedo [39], which makes that the QuadvC and QuadvD are almost exactly equal, so assuming equal specifications is allowed.

Concept	Length [m]	Inertia [kgm^2]	Total mass [kg]	Rotor mass [kg]	Thrust [N]	$(T/w)_{rotor}$ [-]	$(T/w)_{tot}$ [-]
Tri1Hor	0.70	-	2.31	0.13/0.09*	13.8/8.6*	12.7/9.6*	1.83
QuadvC	0.45	-	1.40	0.08	11.1	12.8	3.2
QuadvD	0.45	-	1.40	0.08	11.1	12.8	3.2
QuadvCD	0.58	eq. 5.3	3.06	0.17	21.6	12.9	2.9
QuadvCDc	-	-	-	-	-	-	-
HexvC	0.45	-	3.20	0.09	9.5	11.1	1.8
HexvCc	0.63	-	2.40	0.15	-	-	-
PentvD	0.45	-	1.00	0.08/0.06**	9.8/4.6**	13.3/8.1**	3.4

Table 5.13: Specifications of the variable tilt rotors (*vertical rotor/horizontal rotor, **coaxial rotors/tilting rotors)

The only inertia specified in the references is:

$$I_{QuadvCD} = \begin{bmatrix} 0.05 & 0 & 0 \\ 0 & 0.05 & 0 \\ 0 & 0 & 0.08 \end{bmatrix} \tag{5.3}$$

Thrust-to-Weight Ratio

$(T/w)_{rotor}$ and $(T/w)_{tot}$ have been plotted in figure 5.2. Contrary to the fixed tilt concepts, the $(T/w)_{rotor}$ of the concepts is very similar. Two exceptions are the Tri1Hor horizontal rotor, which is a custom rotor mounted on a boom, and the PentvD tilting rotor, which is integrated in a duct resulting in a high rotor mass.

The $(T/w)_{tot}$ is less similar for all concepts. The Quad1H and HexvC have very low $(T/w)_{tot}$. The added mass from the extra tilt actuators of QuadvCD does not influence the $(T/w)_{tot}$ much compared to QuadvC. The highest $(T/w)_{tot}$ is achieved by PentvD, which is surprising because it consists of a number of ducts, that add mass to the UAV.

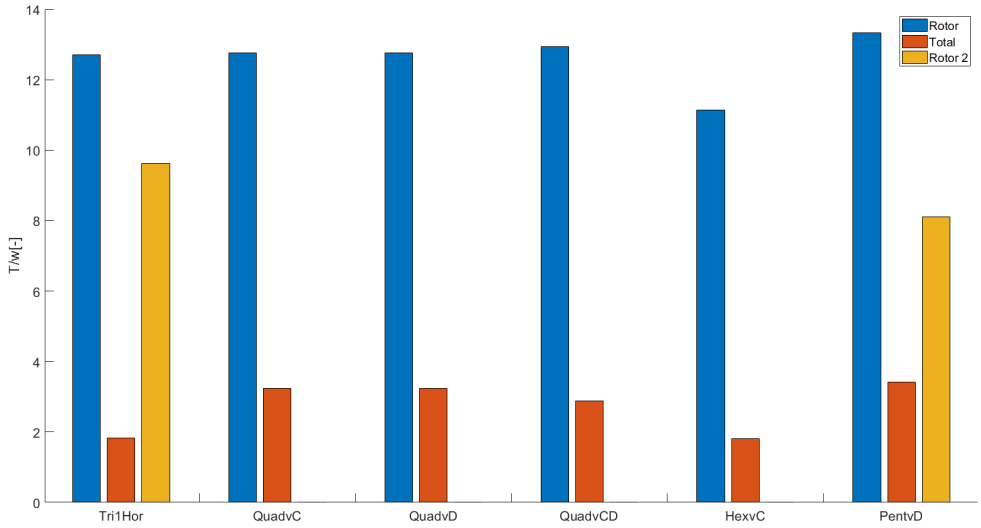

Figure 5.2: Rotor thrust-to-weight ratio and total thrust to mass ratio for variable tilt concepts (for Tri1Hor, rotor 2 is the horizontal rotor and for PentvD, rotor 2 is the variable tilt rotor)

The dynamic performance of each concept is shown in table 5.14. Note that the rotational acceleration is missing for most concepts, since the inertia of these concepts is unknown. However, a qualitative estimation of the rotational acceleration of these concepts has been discussed.

Concept	Maximum uncoupled acceleration						λ_f
	Longitudinal [N]	Lateral [N]	Vertical [N]	x-Rotation [Nm]	x-Rotation [Nm]	z-Rotation [Nm]	[-]
Tri1Hor	3.7	0.8	17.9	-	-	-	34.2*
QuadvC	**22.4**	**22.4**	**31.7**	-	-	-	**15.4**
QuadvD	15.9	15.9	**31.7**	-	-	-	**15.4**
QuadvCD	**28.2**	**28.2**	**28.2**	**247.5**	**251.7**	**209.6**	33.7
QuadvCDc	-	-	-	-	-	-	-
HexvC	11.9	10.3	17.8	-	-	-	36.4
HexvCc	-	-	-	-	-	-	
PentvD	**19.6**	**17.0**	**49.0**	-	-	-	**12.0**

Table 5.14: Dynamic comparison of the variable tilt concepts (*virtual flying thrust)

The dynamic performance of the UAVs has been graded based on performance compared to the other concepts in table 5.15.

Concept	Maximum uncoupled acceleration						λ_f
	Longitudinal	Lateral	Vertical	x-Rotation	x-Rotation	z-Rotation	
Tri1Hor	6	6	5	-	-	-	5*
QuadvC	**2**	**2**	**2**	-	-	-	**2**
QuadvD	4	4	**2**	-	-	-	**3**
QuadvCD	**1**	**1**	4	**1**	**1**	**1**	4
QuadvCDc	-	-	-	-	-	-	-
HexvC	5	5	6	-	-	-	6
HexvCc	-	-	-	-	-	-	-
PentvD	**3**	**3**	**1**	-	-	-	**1**

Table 5.15: Graded dynamic performance for variable tilt concepts (*virtual flying thrust)

Translational Accelerations

Since the concepts have very similar $(T/w)_{tot}$, there is little difference between the force and translational acceleration for these concepts relatively. The QuadvCD achieves the highest horizontal acceleration, because the force in this direction is high. The PentvD has the highest $(T/w)_{tot}$ and thus performs the best in vertical direction. The HexvC, which produces the highest force in longitudinal and vertical direction, achieves very low translational accelerations due to the low $(T/w)_{tot}$ and high amount of rotors.

By comparing the QuadvCD with the QuadvC and QuadvD it can be concluded that for the acceleration it is worthwhile to add an extra tilt actuator. The added mass from the added rotor is excessively compensated by the added actuation. It should be noted that the UAV will not be able to fly with this acceleration, because there is no actuation in z-direction in this configuration. However, when a very high instant acceleration is required, this acceleration can be achieved for a small time before the UAV falls down.

The PentvD performs a lot better dynamically than statically relative to other concepts, due to the high $(T/w)_{tot}$. Despite this, the horizontal accelerations are still very low, due to the low horizontal wrench of these concepts. The vertical acceleration is very high because the wrench in this direction was already rather high.

Rotational Accelerations

A quantitative comparison based on the rotational acceleration is impossible, since the inertia of only one concept is given. However, a few general considerations can be made based on the wrench of the concepts. This is because the torque of the quadrotor concepts are equal to that of a standard quadrotor and the main difference in inertia is the addition of the tilting actuators. If more tilting actuators are added, the inertia will increase more. This would mean that the QuadvCDc, which has only two tilt actuators placed close to the CoM, performs the best of the Quadrotor concepts. However, this concept has a coupling mechanism which adds a lot of inertia. For the hexarotor concepts the same applies: the HexvCc has only one tilt actuator but a large tilting mechanism. The Tri1Hor has low inertia since the amount of rotors is low. This will result in high rotational accelerations compared to the torque. For

the PentvD the inertia is also very low, since the main rotors are placed at the CoM.

Flying Thrust

It can be seen that, contrary to the thrust efficiency, the flying thrust does give different results for the different variable tilt concepts. However, similar to the fixed tilt concepts, it can be observed that the concept with the lowest mass yields the best flying efficiency. Since the thrust of the variable tilt rotors can be orientated in the exact desired direction, the flying efficiency depends only very little on the design of the concepts.

5.6.4 Conclusion

The framework for optimization of variable tilt concepts has been presented here. Similar to the fixed tilt concepts, it has been shown that all concepts have different advantages and disadvantages based on the qualitative and quantitative criteria. Similar to the fixed tilt concept comparison, the importance of considering the dynamics of the UAV to determine its performance is shown, although the difference in dynamics is not very high due to the similarities in design between the concepts. A number of relations between concepts can be seen for these criteria:

- An increase in tilt actuators yields an increase in redundancy, costs and flying stability. However, tilt actuators do not produce thrust, so this redundancy gives an unrealistic measure of the flyability if actuators fail. Furthermore, the down- and upscaling is reduced. The static and dynamic performance increases, because the thrust can be redirected in almost any direction, at the costs of only a small increase in mass.
- Coupled rotation decreases the required amount of tilt actuators. However, the static and dynamic performance reduces, because the tilting angle of the rotors is limited. Furthermore, the required tilting mechanism drastically increases the design complexity and limits the up- and downscaling ability.
- Concepts with variable cant perform better than concepts with variable dihedral, because the dihedral angle is limited and does not contribute to z-torque. A variable dihedral concept is only advised if the application specifically requires it.

Chapter 6

Application of Fully Actuated UAVs: Crop Spraying

The first application of fully actuated UAVs that is considered, is agricultural application. There are various possibilities for the application of UAVs in agriculture. One of these applications, as proposed by the company Drone4Agro [40], is the crop spraying. Crop spraying consists of: pesticide, fungicide and herbicide spraying, liquid fertilizer spraying and biological spraying. In this chapter, the use of a UAV for this application is investigated and a horizontally actuated UAV is designed using the framework presented in chapter 5.

First, the currently available spraying methods are discussed in section 6.1, to determine how these methods could be improved by using UAVs and whether this actually provides a better spraying alternative. Next, the currently available crop spraying UAVs are considered in section 6.2. In section 6.3, the requirements for a crop spraying UAV are declared. Before the concept is chosen, some preliminary design considerations are discussed in section 6.4. Based on the requirements and design considerations, a concept is chosen in section 6.5, with the framework as a guideline. After the concept is chosen, the atomization of the pesticide is considered in section 6.6. After that, the rotor configuration is optimized, to meet the requirements in section 6.7. This yields a number of optimized concepts for different situations, which are shown and compared in section 6.8. Based on this comparison, the best design has been chosen in section 6.9. In section 6.10 a conclusion of this chapter is given.

6.1 Traditional Crop Spraying Methods

There are a number of crop spraying methods available. A number of these methods is discussed in this section, to determine how a UAV could outperform these conventional methods. The considered methods are shown in figure 6.1.

(a) Plane [41]

(b) Tractor with boom [42]

(c) Chemigation [43]

(d) Knapsack [44]

Figure 6.1: Traditional crop spraying

These methods have been compared to using a UAV based on five general criteria:

- Spraying speed: the amount of land that can be sprayed in a certain amount of time.

- Spraying precision: the precision at which the pesticide is sprayed. It should be sprayed uniformly and only on the places where it is required.
- Applicability: the types of land that can be sprayed. For example, a tractor is only applicable on flat land with space for the tractor to ride.
- Costs: the costs of the spraying method, without considering labour costs.
- Labour intensity: the amount of human effort required for the crop spraying.

These criteria have been graded similar to the qualitative comparison between concepts in chapter 4.1, where - - is very poor and ++ is excellent. The results are shown in table 6.1.

Method	Spraying speed	Spraying precision	Applicability	Costs	Labour intensity
Plane	++	- -	++	- -	+
Tractor	+	-	- -	- -	+
Chemigation	-	-	+	++	++
Knapsack	- -	++	+	++	- -
UAV	+	+	++	+	++

Table 6.1: Comparison between different spraying methods

It can be seen that each spraying method has very clear advantages and disadvantages. The UAV provides a solution that combines the advantages of a number of the methods: high spraying speed as well as high spraying precision, while being less costly than a plane or a tractor. Furthermore, using a UAV provides the possibility of fully autonomous operation, which reduces the labour intensity and, just like a plane, a UAV is applicable to any terrain, since it will fly over it. These advantages validate the possibility of using UAVs for crop spraying over other methods.

6.2 Currently Available Crop Spraying UAVs

The advantages of UAVs over other crop spraying methods have already been already considered some time ago. One of the earliest rotary wing UAVs used for crop spraying is called the Yamaha RMAX [45], which resembles a helicopter and was designed specifically for crop spraying. Miller [46] performed an experiment to determine the effectiveness of this spraying method. Results showed that overall it performed reliably. An overview of recent application of UAVs in agriculture in Asia is given by He [47]. He showed that the use of UAVs is already quite large in China and Japan. He states: *"Up to 2016, China has more than 200 UAV manufacturers and over 169 types of agricultural unmanned aerial vehicles for chemical application in Chinese market, having already conducted the work of the control of pest and disease in the fields of paddy, wheat, corn, cotton and sugarcane and in the orchard."* and: *"As of the year of 2012, the working area covered by Japanese agricultural UAV was 963,000 hm^2/a and accounted for $50\% - 60\%$ of cultivated area."* A number of UAVs that are commercially available have been compared, to establish the minimum requirements of the UAV that is designed. This is shown in table 6.2.

Company	Model	Span [m]	Tank size [L]	Flying time [min]	Flying speed [m/s]
Joyance[48]	JT15L-608 Pro	2.7	15	10-15	12
TT Aviation[49]	M8A PRO	1.6	20	15	15
SprayingUAV[50]	15kg	2.7	15	10-25	15

Table 6.2: Existing crop spraying UAVs

All these concepts have parallel rotors placed in-plane around the vertical axis and are thus underactuated. These UAVs show that full actuation is not required for this application, because the UAVs are allowed to tilt in all directions. However, horizontal actuation does have a number of advantages when spraying crops:

- The spraying precision increases: when an underactuated UAV needs to reject disturbances, like side wind drag, it will need to tilt its entire body, resulting in a constantly changing spraying direction, since the spraying nozzles are connected directly to the UAV. This is why disturbance rejection without tilting is advantageous for the spraying precision,
- The upscaling ability increases: to ensure well pesticide distribution over the land, the UAV needs to fly relatively close to the ground. If the width of the UAV is large, rolling of the UAV will result in collision with the ground. For this reason, a UAV with large width will require lateral actuation to be able to reject disturbance without rotation and collision.

Based on these arguments, the UAV will be designed such that it can actuate the horizontal direction.

6.3 Requirements

There are a number of very specific requirements for this application, most of which are proposed by Drone4Agro. These requirements are:

- The width of the UAV needs to be 9 m, such that a large section of land can be sprayed at once.
- The UAV will need to carry 100 L of pesticide, which is stored in a tank on the UAV. The tank capacity is very high compared to other crop spraying UAVs in table 6.2. As a result, the great width enables the UAV to spray a large amount of pesticide at once. To maintain a spraying cycle of approximately 10-20 minutes, a large pesticide storage tank is required.
- The distance between the rotors should be high enough to be able to neglect the airflow interference between the rotors, as mentioned in chapter 2.6. Airflow interference between rotors is unbeneficial for the control complexity and flying stability of the UAV.
- In order to distribute the pesticide, it needs to be atomized by the UAV. This atomizing of pesticide by a UAV is conventionally done by a nozzle, as discussed by Huang et al. [51]. An aspect that is not considered, is that the airflow from the rotors can be used for the atomization. Since the airflow from the rotors is used for the atomization, it is important that the rotor configuration is such, that the pesticide is sufficiently atomized and divided evenly over the land by the airflow from the rotors.

Next to these requirements, the criteria from the framework in chapter 5 are considered. For each criteria the relevance and importance for this application is discussed. The qualitative criteria are:

- **Flying stability**: this is important. If the UAV cannot follow the trajectory closely, the pesticide will not be placed at the correct location. Furthermore, orientation error will result in the pesticide being sprayed in the wrong direction.
- **Design complexity**: the UAV will be exposed to a lot of debris. This is why having as little moving parts as possible is desirable. Because the UAV will be optimized for this application, low optimization complexity is desired as well.
- **Downscaling**: as mentioned, the UAV will need to have a large width, so downscaling is not relevant.
- **Upscaling**: the upscaling ability is very important, because the UAV will have a large width. To carry the 100 L pesticide tank, the required payload is also very high.
- **Redundancy**: the high amounts of debris in the working environment advocates rotor failure. For safety reasons it is very important that the UAV can still land safely after rotor failure.
- **Cost**: because this UAV will be a replacement of very expensive alternatives, the cost requirements are not very high. Obviously, a cheap alternative is favoured over an expensive UAV. However, this should not be at the cost of other criteria.

Instead of the quantitative criteria, only the relevant actuation directions are given:

- **Longitudinal actuation**: this actuation is not necessary, because underactuated forward flight by rotation around the y-axis is allowed. The reason for this is that spraying direction does not change by y-rotation and there is no minimum required length, so ground collision during y-rotation is not an issue. However if for some reason y-rotation is not allowed, the longitudinal direction does need to be actuated.
- **Lateral actuation**: this is required for counteracting side-winds without y-rotation. As mentioned this rotation is not possible due to the large width. The lateral acceleration should be high, such that wind disturbance can be rejected as fast as possible.
- **Vertical actuation**: this actuation is required for the UAV to ascend. Due to the high payload, the force in this direction needs to be high. Furthermore, higher maximum vertical acceleration results in lower thrust required for hovering. For that reason, the acceleration in this direction should be high.
- **y-rotation**: this rotation is required for forward flight. Fast y-rotation results in faster disturbance rejection in longitudinal direction. This rotation is not required if the longitudinal direction is actuated.

6.4 Preliminary Design Consideration

There are a number of considerations that can to be done before a UAV concept is chosen. These considerations are discussed below.

6.4.1 Rotor Type

For the rotor, there are a number of considerations: motor type, motor size and propeller design. For this UAV, these considerations have already been done by Drone4Agro. It resulted in a brushless motor with a 1.80 m diameter propeller, which has a maximum thrust of around 736 N. The rotors are designed such that they can operate the UAV at an optimal energy consumption, producing 238 N. The rotors are one-directional, since bi-directional thrust is not necessary for this application. The mass of the brushless motor is 4.1 kg and the mass of the carbon fiber propellers is estimated at 2.6 kg, resulting in a total rotor mass of 6.7 kg.

6.4.2 Power Source

For the power source there are alternatives: fossil fuel and batteries. Since electric motors are used, fossil fuel will first have to be transformed into electricity, while batteries can be used directly. For this reason almost all UAVs with electric motors use batteries. However, a new trend that is emerging, especially for large UAVs, is the use of so-called range extenders. A range extender is a combustion engine generator that transforms fossil fuel (diesel or gas) into electric power. A range extender is a good alternative to batteries since it has a much higher energy density. Matt McRoberts, developer of the GE-30 Range Extender, claimed: *"For the purposes of UAV operators, gasoline also has more than fifty times the energy density of the best batteries you can buy"*[52]. A range extender often serves as a back-up power source when the batteries are depleted to extend the range of the UAV, hence the name. For crop spraying, a range extender will not be used, because the range of the UAV is not only limited by the power source, but also by the amount of pesticide that can be stored. Furthermore, the UAV will fly over a field, so it will always be relatively close to the take-off place. This makes that the operation time does not need to be very high. Lastly, the fumes generated by a range extender may be hazardous for some crops.

6.4.3 Pesticide Storage

Based on the expected amount of pesticide that can be sprayed by the UAV and the required operation time of 15 to 20 minutes, Drone4Agro determined that the tank capacity should be between 80 and 100 liter. The problem of a tank filled with liquid placed on a UAV is the sloshing of the content of the tank, which will cause very large disturbances for the UAV. For that reason, it is very important to minimize this sloshing. Huang et al. [51] proposed an alternative tank design with baffles to reduce liquid movement in the tank for UAVs . The use of baffles in tanks to reduce sloshing has been investigated intensively for a number of applications. Kandasamy et al. [53] investigated the use of baffles in circular tanks and found that an oblique baffle configuration are very effective at reducing sloshing as a result of longitudinal and lateral loads, as well as pitching of the tank. Based on this report the best fuel tank design with baffles is a circular tank with oblique baffles.Another promising anti sloshing method designed especially for crop spraying UAVs, is a given by a patent by Wang [54].The tank is surrounded by fluorine rubber pads or inflation and deflation air cushions, in a frame around the tank that can be inflated or deflated to actively reduce sloshing. Unfortunately, the patent does not include specifics of the working method and proof that this method works. At least it is worth mentioning that the reduction of sloshing in crop spraying UAVs is being investigated. Alternative to a solid tank, a pressurized fuel bladder can be used to store the spraying fluids. If the bladder is kept in vacuum, the sloshing should be reduced drastically. Unfortunately, no study to this has been found and more investigation to it is required.

6.5 Concept Choice

In this section, the best concept for this application is determined based on the requirements given in section 6.3. For making this choice the framework is used. Using the framework, one first requires a choice between fixed or variable tilt rotors. After that, a concept is given that is proposed specifically for the requirement called the V-shape. This concept has been compared to the framework, to determine if this is the most suitable concept for this application and if there is a way to improve it. Lastly, limitations to the rotor orientation to ensure pesticide distribution are considered.

Before the concepts can be compared, a choice is made whether to use fixed tilt or variable tilt rotors. As mentioned in chapter 5.3, variable tilt concepts are preferred when high accelerations in all directions is required. For this application, it would be beneficial to be able to switch between very efficient flight with all rotors facing upward, while being able to withstand wind disturbances by tilting the rotors. Furthermore, the high redundancy of variable tilt concepts is advantageous for this application.

However, there is a practical disadvantage to variable tilt rotors that makes their use undesired for this application. This disadvantage results from the high amount of debris the UAV will be covered in during operation. This debris is extremely dangerous for any exposed moving part. Since the variable tilt rotor has many moving parts, due to the tilting of the rotors, the UAV is very susceptible to failure. This alone is reason enough to choose for the more reliable option, which is fixed tilt concepts. Another argument for using fixed tilt concepts is that the costs are slightly lower. However, the lower thrust efficiency will result in higher power consumption and thus higher operation costs, so this advantage is debatable.

6.5.1 Proposed Concept

Drone4Agro proposed a fixed tilt UAV especially for this application, based on the requirements. The rotors are symmetrically placed in a V-shape, with three rotors on each side at a distance l_i from the vertex of the V-shape. The reason for choosing a V-shape is that it can reach a very high width, when the V-shape angle θ (see figure 6.2a) is sufficiently large. To maximize the width, the angle should be $90°$, which would make the V-shape a line. However, this solution is unfeasible because it provides no pitch torque, witch is required for forward flight. Actuation in lateral direction (y-direction) is added to the concept by tilting the rotors with an angle β around their axis parallel to the x-axis. Note that the maximum tilt angle is limited by the frame. The rotors can be separated into three pairs that are mirrored, with respect to the x-axis. The two mirrored rotors have opposite l_i and β_i, so for rotor 2 $l_2 = -l_1$ and $\beta_2 = -\beta_1$.

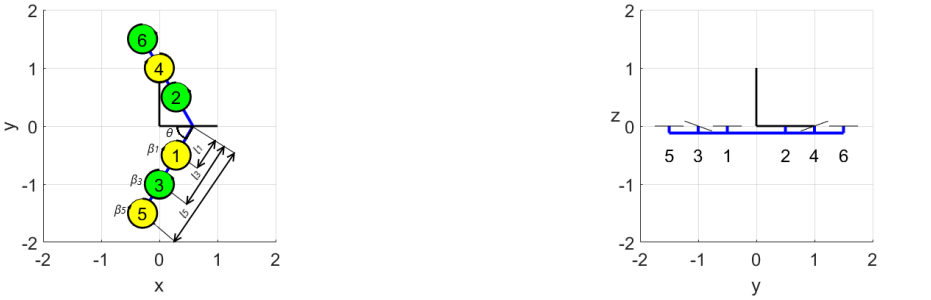

(a) Rotor configuration, top view

(b) Rotor configuration, front view

Figure 6.2: V-shape five DoFs rotor configuration

The mapping matrix of rotor i of this concept is given by:

$$\vec{M}_i = \begin{bmatrix} 0 \\ \sin(\beta_i) \\ \cos(\beta_i) \\ -l_i \cos(\beta_i) \sin(\theta) \\ \gamma\sigma_i \sin(\beta_i) + l'_i \cos(\beta_i) \cos(\theta) \\ \gamma\sigma_i \cos(\beta_i) - l'_i \sin(\beta_i) \cos(\theta) \end{bmatrix} \tag{6.1}$$

Where the variables l_i, β_i and θ are defined in figure 6.2a. By declaring the distance between rotor 1 and 3 ($l_3 - l_1$) and rotor 3 and 5 ($l_5 - l_3$) to be equal, the CoM (based on the rotors) will always be at the origin of $\mathbb{F}_\mathbb{W}$, in line with rotor 3 and 4. As mentioned in chapter 2.1, having the CoM and $\mathcal{F}_\mathcal{W}$ coincide is very desired. This position of the origin does make the definition of the mapping matrix a bit complex, since the x-position of the rotors is not defined by the $l_i \sin(\theta)$, but by $l'_i \sin(\theta)$ (where l'_i is the distance between rotor 3 and rotor i). It would be $l_i \sin(\theta)$ when the origin would be at the front of the UAV. The total mapping matrix is:

$$\mathbf{M} = \left[\vec{M}_{\{1,\ldots,6\}}\right] \tag{6.2}$$

6.5.2 Comparison of Proposed Concept with the Framework

This concept has been compared to the concepts in the framework, to determine if it is in fact the best suited concept for this application. For that reason it has been graded based on the comparison

criteria from chapter 5. The qualitative criteria are shown in table 6.3. The design cannot be compared quantitatively, because the design is only conceptual; the values of the design variables have not been determined yet.

Concept	Flying stability	Design complexity	Downscaling	Upscaling	Redundancy	Costs
Hexarotor V-shape	- -	+	+	++	-	++

Table 6.3: Qualitative criteria for the V-shape concept

The next step is to compare the fixed tilt concept based on the criteria that are important for this application.

As a first criterion, the payload the concepts can carry is considered. The payload is given in table 6.4 for the maximum one-directional thrust of 736 N (maximum payload), as well as the power efficient hovering thrust of 238 N (efficient payload), as discussed in section 6.4.1. Here the empty mass of the UAV is approximated as the mass of the rotors (6.7 kg). The payload needs to be very high as the UAV needs to carry a 100 L pesticide tank, as well as batteries and a frame. It can be seen that the only concept capable of carrying the full pesticide tank efficiently is the CoHexC. Although the other concepts are not able to fly efficiently, it can be seen that the maximum thrust is sufficient for carrying the full tank for most concepts. It is considered acceptable if the UAV is able to carry at least half the pesticide tank with the efficient payload, such that the majority of the spraying cycle can be done with a thrust around the efficient thrust. Based on this criterion and considering that a part of the empty mass of the UAV is not yet taken into account, Quad4Hor, HeptF, HeptW and OctCu are considered unfit for this application.

Concept	Maximum payload [N]	Efficient payload [N]
Quad4Hor	2417	426
HexC	3211	772
HexCD	3371	824
CoHexC	6422	1544
HexDTet	3870	985
HeptF	643	-103
HeptW	785	-57
OctCu	2806	552
OctB	3477	769

Table 6.4: Maximum payload of the considered concepts

Based on the required width, some more concepts that are impractically large at this scale are disregarded. This applies to HexDTet, HexC, HexCD and CoHexC. Due to the symmetry, these concepts will require the length of the UAV to be equal to the width. Since a very large width is required, the length, which does not contribute to the spraying surface, will have to be very high as well. This does not apply to the OctB and the V-shape, which can scale the width independently of the length, resulting in a much lower frame mass for these concepts.

The pesticides will be atomized using the airflow from the rotor. For even distribution of pesticide the position of the sprayers, and thus the position of the rotors, will have to be distributed over the entire width of the UAV. This requirement eliminates the OctB, as this concept only has rotors at its edge. Using this concept would require an alternative method for pesticide atomization, which adds design complexity, power consumption and mass to the UAV.

The V-shape can be designed such that the vertical force is sufficient, the length is limited and rotors are evenly distributed for crop spraying. There are other concepts in the framework that could be used for crop spraying, although based on these requirements the V-shape is considered the best applicable concept.

From the framework it can be seen that canting the rotors around the axis of the arm of the rotor can yield high wrench. In the current design the rotors from the V-shape are tilted parallel to the x-axis. However, canting the rotors will increase the amount of DoFs to six. Furthermore, the cant angle is not limited by the frame. This alternative rotor orientation will be considered in the optimization.

6.6 Pesticide Atomization

As mentioned, the pesticide will be atomized by the airflow from the rotors. The pesticide nozzles are placed directly under the rotors, such that the airflow is optimally utilized in the atomizing of the pesticide and the pesticide is divided equally over the entire width of the UAV. Due to the tilting of the rotors, the direction of the airflow, and thus the spraying direction of the pesticide, is altered. For certain rotor configurations, the distribution becomes inconsistent and some places may not be reached by the spray at all.

To investigate the influence of the rotor configuration on the spraying density, an estimate of the spraying pattern of the UAV with nozzles placed under the rotors is investigated. First, the spraying angle of the nozzles is considered. The spraying angle of nozzles is investigated by Zhou et al. [55], who found that a spraying angle of up to 120° can be achieved. However, when the nozzles are placed in the airflow from the rotors, the spraying angle reduces. Because an extensive study on the airflow of the rotor is beyond the scope of this research, it is estimated that the spraying angle is around $90\circ$. When the rotors are tilted, the spray will be directed sideways, which results in a reduction in spraying angle due to gravity. This reduction is estimated by reducing the upper limit of the spraying direction by 0.2β. The resulting pesticide distribution has been illustrated in figure 6.3.

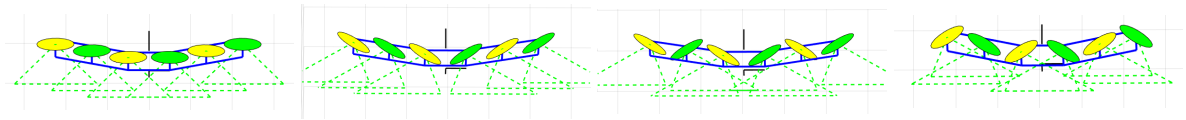

(a) $\vec{\beta} = \{0 \quad 0 \quad 0\}$ (b) $\vec{\beta} = \{\beta \quad \beta \quad \beta\}$ (c) $\vec{\beta} = \{\beta \quad -\beta \quad \beta\}$ (d) $\vec{\beta} = \{-\beta \quad \beta \quad -\beta\}$

Figure 6.3: Spraying estimation for different rotor orientations

It can be observed in figure 6.3a that without rotor tilting, the pesticide is sprayed very consistently over the entire width of the UAV. When a tilt angle of β=30° is added for all rotors, as shown in figure 6.3b), the spraying consistency remains relatively high. However, since all rotors produce an airflow away from the center, there is a rather large area in the centre of the UAV that may not be covered by the spray. This problem can be solved by placing an extra nozzle in the center, but this nozzle will need to atomize the spray without rotor airflow, which is very undesirable. When the rotors are tilted in the other (negative) direction, there will be a lack of spray at the ends of the UAV, instead of in the centre. Furthermore, the spray density will be very high in the center of the UAV, which makes this tilting method even worse for spraying. For alternating rotor tilting, it can be seen that there is a large difference in spraying density for a different order of alternation. For the order of alternation shown in figure 6.3c, the distribution of pesticide is very even. However, it is questionable whether the centre of the UAV, which should be sprayed by rotor 3 and 4, will be sprayed in reality, since it is barely reached for this estimated case. For the other alternating configuration, shown in figure 6.3d, the spraying seems to be distributed equally as well, but the full coverage over the width of the UAV is also questionable. Furthermore it can be seen that the airflows from rotor 1 and 2 are colliding. This may result in undesired aerodynamic effects.

It is possible to take the spraying density into account during the optimization, but this would require a better estimation of the spraying surface, which is beyond the scope of the report. To maximize the chance that the UAV is able to reach the entire width, the rotors are constrained to be alternating like figure 6.3c, since this is considered to provide the highest change of full coverage. To check the effect this constraint to the tilt angles has on the attainable acceleration, the optimization has also been done with unconstrained angles. When the difference between the constrained and unconstrained tilt results is very high, an alternative method for pesticide atomization could be considered.

6.7 Optimization

The optimization of this UAV will be done with the MATLAB build-in non-linear optimization function: *fmincon* [56]. This optimized design will have to fulfill the requirements. The UAV performance is governed by two criteria: flying- efficiency and precision. Flying thrust is the ability to fly with minimal power consumption, and when the maximum z-acceleration is higher than the gravitational acceleration, it will be able to hover using less than maximum thrust, which increases flying thrust. Flying precision is the ability to follow the given trajectory. In order to do this, wind loads need to be rejected fast. This is achieved with high lateral acceleration. For this reason, the best performance is achieved by maximizing the sum of the y- and z-acceleration. The other requirements that are influenced by the rotor placement are taken into account with constraints. The optimization problem is defined in this section. It consists

of the definition of the rotor configuration, design simplifications, the objective function, boundary conditions, constraints and optimization options.

6.7.1 Rotor Configuration

Before the optimization is considered, the orientation and position of the rotors is given, in accordance with the the rotor numbering in figure 6.2a and the mapping matrix (equation 6.1):

$$u = \begin{bmatrix} 0 & 0 & 0 & 0 & 0 & 0 \\ \sin(\beta_1) & -\sin(\beta_1) & \sin(\beta_3) & -\sin(\beta_3) & \sin(\beta_5) & -\sin(\beta_5) \\ \cos(\beta_1) & -\cos(\beta_1) & \cos(\beta_3) & -\cos(\beta_3) & \cos(\beta_5) & -\cos(\beta_5) \end{bmatrix} \tag{6.3}$$

$$r = \begin{bmatrix} (l_3 - l_1)\cos(\theta) & (l_3 - l_1)\cos(\theta) & 0 & 0 & -(l_3 - l_1)\cos(\theta) & -(l_3 - l_1)\cos(\theta) \\ -l_1 \sin(\theta) & l_1 \sin(\theta) & -l_3 \sin(\theta) & l_3 \sin(\theta) & -(2l_3 - l_1)\sin(\theta) & (2l_3 - l_1)\sin(\theta) \\ 0 & 0 & 0 & 0 & 0 & 0 \end{bmatrix} \tag{6.4}$$

where $l_5 = 2l_3 - l_1$, such that the distance between l_5 and l_3 is equal to the distance between l_1 and l_3 and the CoM will always remain at the origin of $\mathcal{F}_{\mathcal{W}}$. As mentioned, a second optimization is done with the rotor canted among the frame axis instead of the x-axis. The solution is similar to the HexC from chapter 3.2.2 and results in six DoFs. The only difference with the five DoFs design is the definition of the orientation vector:

$$u = \begin{bmatrix} \sin(\alpha_1)\sin(\theta) & \sin(\alpha_1)\sin(\theta) & \sin(\alpha_3)\sin(\theta) & \sin(\alpha_3)\sin(\theta) & \sin(\alpha_5)\sin(\theta) & \sin(\alpha_5)\sin(\theta) \\ \sin(\alpha_1)\cos(\theta) & -\sin(\alpha_1)\cos(\theta) & \sin(\alpha_3)\cos(\theta) & -\sin(\alpha_3)\cos(\theta) & \sin(\alpha_5)\cos(\theta) & -\sin(\alpha_5)\cos(\theta) \\ \cos(\alpha_1) & \cos(\alpha_1) & \cos(\alpha_3) & \cos(\alpha_3) & \cos(\alpha_5) & \cos(\alpha_5) \end{bmatrix} \tag{6.5}$$

Optimization of the rotor configuration with this orientation vector showed that it is nearly impossible to reject all drag torque from the rotors, when they are canted this way. The optimization yields a solution with very small canting angles, resulting in very low horizontal acceleration relative to the five DoF solution. For this reason, and because x-actuation is not a necessity, this solution is disregarded and not considered further.

6.7.2 Design Simplifications

A number of simplifications to the UAV design can be done to speed up the optimization of the rotor configuration. These simplifications should have a minimal effect on this configuration.

The inertia of the pesticide tank, batteries, wiring, etcetera are not considered in the rotational inertia. The reason for this is that the position and dimensions of these parts is not determined. By assuming that these parts are either placed close to the CoM, like the tank and batteries, or have insignificant mass, like the wiring, it is considered allowed to neglect these parts for the rotational inertia. The inertia of the frame is included. However, the required cross-section of the frame is estimated based on simple beam deflection theory. In order to obtain the exact required cross section of the frame, the position of the rotors is required, which will be a result of the optimization. It is possible to include the optimization of the frame in the optimization, but this increases the optimization time and will not influence the results enough to make it worthwhile.

The frame of the UAV is simplified to two rods where the rotors are placed on. The rods are made from carbon fiber. This frame allows very limited tilt angles without frame collision. An alternative frame has been proposed that allows these angles. However, this frame adds a lot of complexity to the optimization, so the simple frame is used for the optimization, neglecting the limited tilt angle. This approximation is considered valid, because the acceleration in y- and z-direction suffer from added mass equally, so a change in mass would not change the optimal tilt angles. However, the increased mass does increase the vertical force required for hovering. For that reason, the mass of the rods is doubled for the optimization, to approximate the mass of the new frame even closer. If this approximation of the adapted frame is insufficient, it can also be compensated by adjusting the capacity of the pesticide tank.

6.7.3 Objective Function

The objective of this optimization is to find the rotor configuration for which the vertical and lateral acceleration is maximized. This optimization will result in a trade-off between these two accelerations. This

trade-off is managed with a weighing factor x, which gives more importance to one of the accelerations. This results in the objective function given by:

$$f(l_1, l_3, \theta, \beta_1, \beta_3, \beta_5, \vec{\lambda_y}) = x\vec{A_z}\vec{\lambda}_{max} + (1-x)\vec{A_y}\vec{\lambda_y} \tag{6.6}$$

where $\vec{\lambda}_{max}$ is the thrust vector with the maximum thrust (736 N) of the six rotors. This thrust yields the maximum acceleration in z-direction for this concept for all the rotor configurations within the boundary conditions and constraints of the optimization. Similarly to the vertical direction, $\vec{A_y}$ is the second row of the acceleration matrix, which maps to the lateral acceleration. The thrust vector $\vec{\lambda_y}$ consists of the thrust of the six rotors for which the lateral acceleration is maximized. Unlike to the thrust for vertical acceleration, the thrust required for maximum uncoupled lateral acceleration does depend on the rotor configuration. For that reason, the λ_y of each rotor required for maximum lateral acceleration is included in the optimization. x is the weighing factor between the vertical and lateral acceleration. When $x = 0.5$, both directions are equally important. The parameters l_1, l_3, θ, β_1, β_3 and β_5 are the design variables, as defined in figure 6.2.

6.7.4 Boundary Conditions

The boundary conditions of the design variables are given by:

$$0.1 \text{ m} \leq l_1 \leq 5 \text{ m}, \quad 0.2 \text{ m} \leq l_3 \leq 7 \text{ m}, \tag{6.7}$$

$$0.001 \leq \theta \leq 0.499\pi, \tag{6.8}$$

$$0 \leq \beta_1 \leq \frac{\pi}{2}, \quad -\frac{\pi}{2} \leq \beta_3 \leq 0, \quad 0 \leq \beta_5 \leq \frac{\pi}{2}, \tag{6.9}$$

$$0 \leq \lambda_{y,\{1,\dots,6\}} \leq \lambda_{max} \tag{6.10}$$

The boundary conditions of l_1 and l_3, given by equation 6.7, are not significant: due to the constraints on these variables, which are stated in section 6.7.5, these variables will not reach the boundaries. The V-shape angle θ can vary between zero and $\frac{\pi}{2}$. However, at these boundaries, the design will be a line instead of a V-shape, which eliminates either the x- or y-rotation actuation. This situation is undesirable and could lead to errors in the optimization So the boundary, given by equation 6.8, is defined to just exclude these extreme values. For the tilt angle β, the boundaries given by equation 6.9, are such that the rotors will have the desired tilting direction alternation for spraying coverage, as defined in section 6.6. Note that, for comparison, the optimization has also been done without the constraints on the rotor tilt direction. In this optimization, the boundary of each tilt angle is given by: $-\frac{\pi}{2} \leq \beta_i \leq \frac{\pi}{2}$. The thrust for maximum uncoupled lateral acceleration is limited to the maximum thrust λ_{max} (735 N), by equation 6.10. Since one-directional rotors are used, the minimum thrust is zero.

6.7.5 Constraints

There are a number of constraints to assure the solution found actually fulfills the requirements. These constraints are separated into non-equality constraints, which need to be below zero, and equality constraints, which need to be exactly zero. The non-equality constraints are:

$$g - \frac{m_{tot}}{m_{tot} - \frac{1}{2}m_{tank}}\vec{A_z}\vec{\lambda}_h \leq 0 \tag{6.11}$$

$$1.5g - \vec{A_z}\vec{\lambda}_{max} \leq 0 \tag{6.12}$$

$$-|\vec{A_y}\vec{\lambda_y}| \leq 0 \tag{6.13}$$

$$\alpha_{y,min} - |\vec{A}_{r,y}\vec{\lambda}_{r,y}| \leq 0 \tag{6.14}$$

$$d_{aero} + R - d \leq 0 \tag{6.15}$$

The first constrain, equation 6.11, is required to ensure the UAV is able to fly with the power efficient rotor thrust of 238 N. Here g is the gravitational constant (9.81 m/s^2) and $\vec{\lambda_h}$ is thrust vector where all rotors produce the efficient rotor thrust. Since the pesticide tank will deplete during flight, the power efficient flight is demanded of the UAV with the half full tank, so the mass used to determine $\vec{A_z}$ reduced by $\frac{1}{2}m_{tank}$. As a result, the UAV will always require hovering thrust that is close to the optimal thrust.

Next to efficient flight, the UAV must be able to ascend with a full tank. This is demanded with equation 6.12. To make sure the ascending can be done sufficiently fast, the maximum vertical acceleration needs to be at least 1.5 g. The lateral acceleration is required to be higher than zero with equation 6.13.

To ensure the y-rotation acceleration is sufficient, which is required to fly forward, equation 6.14 is used, where $\alpha_{y,min}$ is the minimum y-rotation, which is estimated at $\frac{1}{2}\pi$ s^{-2}, $\vec{A}_{r,y}$ is the y-rotation row of the acceleration mapping matrix (5th row) and $\lambda_{r,y}$ is the required thrust for uncoupled y-rotation, which has been estimated as rotor 1 and 2 producing λ_{max} and all other rotors producing no thrust.

To make sure the distance between the rotors is sufficiently large to be able to neglect the airflow interference, equation 6.15 is used, where d is the distance between the rotors and the airflow from the other rotors, as given in chapter 2.6, R is the radius of the propeller (0.9 m). Since there no data available for d_{aero} of the rotors used and determining this distance is beyond the scope of this report, the distance is estimated, corresponding to the experiments by Parks [6], which resulted in a $d_{aero} \approx R$, to be similar to the rotor diameter at 1.1 m, to make absolutely sure there is no airflow interference.

The equality constraints are:

$$w_{req} - 2l_5 \sin(\theta) = 0 \tag{6.16}$$

$$\mathbf{A_y}' \vec{\lambda_y} = \vec{0} \tag{6.17}$$

$$\mathbf{A_z}' \vec{\lambda}_{max} = \vec{0} \tag{6.18}$$

Equation 6.16 is used to make sure the width of the UAV is equal to the required width w_{req} of nine meter. This width is defined as the distance between the crop spraying nozzles, which are placed under the rotors. That is why any added width from the frame is not considered. Equation 6.17 makes sure that the accelerations in all directions, except for the y- and z-directions, are zero when the UAV is accelerating in y-direction. As such, the UAV does produce rotational acceleration during lateral acceleration. Here $\mathbf{A_y}'$ is the acceleration matrix without the y- and z-acceleration (row 2 and 3). Equation 6.18 is used to make sure all accelerations except for the z-acceleration are zero when the UAV is ascending, where $\mathbf{A_z}'$ is the acceleration matrix without the z-acceleration row.

6.7.6 Optimization Options

There are a number of options defined for *fmincon* to improve the optimization. A number of these options have been adjusted to improve the performance of this optimization. All other options are left at the standard value. The adjusted options are:

Iterations : Due to the nonlinearity of the optimization function and the amount of constraints, the amount of iteration before convergence is generally high. That is why the maximum amount of iterations is increased to 10^6.

Function toleration : When the difference in results between the old iteration and the new iteration is lower than the function tolerance, an optimal is found. Since the manufacturing tolerance of the rotor configuration is rather high, it is not necessary to demand unfeasibly high precision for the design variables. That is why the function tolerance is increased to 10^{-3}.

Multistart : Due to the amount of constraints and boundary conditions and the nonlinearity of the problem, there are a lot of local optima: solutions that are better than all solutions surrounding it. The optimization algorithm will accept these local optima as the optimal solution, because all solutions around this solution are inferior. There are multiple ways to make sure the optimization yields the best solution overall, the global optimum. A very robust method is multistart, which simply repeats the optimization from different starting points (initial values of the variables) and presents the best local optima found as the global optimum. When the optimization is repeated often enough, the probability that the global optimum will be found approaches 1. For this optimization, a hundred multistarts are used. To make sure the optimization does not take forever, a maximum allowed optimization time has been added. Due to this limitation not every optimization reaches a hundred multistarts. However, in all cases at least fifty multistarts are reached, which is considered plenty to find the global optimum.

6.8 Results and Comparison

The optimization has been done a number of times for $0 \leq x \leq 1$. The optimal design variables for the different x, along with the result of the objective function, given by equation 6.6, and the relevant maximum acceleration are shown in table 6.5. The hovering acceleration is the acceleration given in equation 6.11. The solutions are given for two cases: solution with alternating rotor tilting angles, constrained by equation 6.9, denoted with c, and solutions without the constrained rotor tilt alternation, denoted with u.

Based on a number of simulations, the upper and lower limit of x for which the solution is relevant has been determined. The lower limit is given as $x = 0.3$, because for this solution the hovering acceleration is equal to g. Any solution with $x < 0.3$ result in the same solution. The upper limit of x is given

by $x = 0.8$, because for this x the tilt angles are almost equal to zero. Higher values of x will result in smaller tilt angles, yielding a negligibly small lateral acceleration. For this reason all solutions for $x < 0.3$ and $x > 0.8$ have not been shown.

									Maximum uncoupled acceleration			
		l_1	l_3	θ	β_1	β_3	β_5	Obj. fun.	Lateral	Vertical	Hovering	y-rotation
x	Case	[m]	[m]	[rad]	[rad]	[rad]	[rad]	[m/s^2]	[m/s^2]	[m/s^2]	[m/s^2]	[s^{-2}]
0.3	c	2.82	4.94	0.69	0.38	-0.54	0.42	9.08	3.57	21.95	9.81	12.07
	u	1.87	4.03	0.81	-0.54	-0.42	0.55	10.73	6.00	21.77	9.81	16.94
0.4	c	1.33	3.55	0.89	0.26	-0.59	0.32	11.25	3.39	23.04	10.43	23.46
	u	1.87	4.04	0.81	-0.54	-0.42	0.55	12.31	6.00	21.77	9.81	16.89
0.5	c	1.20	3.29	0.99	0.05	-0.36	0.15	13.33	1.87	24.80	11.27	30.64
	u	1.22	3.28	1.00	-0.22	-0.30	0.25	13.71	2.81	24.60	11.18	30.71
0.6	c	1.51	3.55	0.94	0.19	-0.24	0.24	15.55	1.88	24.67	11.18	26.18
	u	1.21	3.26	1.01	-0.21	-0.26	0.24	15.89	2.58	24.77	11.26	31.72
0.7	c	1.16	3.18	1.05	0.07	-0.16	0.14	18.07	1.10	25.34	11.53	35.04
	u	1.17	3.19	1.04	-0.10	-0.19	0.14	18.19	1.71	25.25	11.49	34.33
0.8	c	1.15	3.15	1.06	0.02	-0.09	0.10	20.52	0.65	25.49	11.61	36.18
	u	1.15	3.16	1.06	0.10	0.08	-0.08	20.57	1.01	25.46	11.59	35.79

Table 6.5: Results for constrained and unconstrained rotor tilt optimization with different x

Constrained Rotor Tilt

The results of the constrained optimization show that the maximum tilting angle is reached for $x = 0.3$, since the hovering acceleration is equal to g here. When x increases and the weighing of the lateral acceleration decreases, the rotor tilt angles decrease, resulting in an increase of vertical acceleration and decrease of lateral acceleration. The objective function increases as well when x increases. The reason for this is that the vertical acceleration is always much higher than the horizontal acceleration, thus increasing weight of the vertical acceleration increases the objective function.

Apart from a decrease in tilt angle, it can be observed that the length of the V-shape, given by l_1 and l_3, increases as the tilt angle increases. This decrease can be contributed to the airflow interference between rotors, constrained by equation 6.15. When the rotor tilt angle increases, the airflow of the rotors will interfere with the rotor next to it, which forces the rotors to be placed further away. θ will decrease as a result of the increase of l_1 and l_3, due to the constrained total width, given in equation 6.16.

The y-rotation acceleration is much higher than the required y-rotation acceleration of $\frac{1}{2}\pi$ s^{-2} for all concepts, so this requirement does not influence the rotor configuration. What can be seen, is that the pitch does decrease as the tilt angle increases.

Unconstrained Rotor Tilt

For each x, the unconstrained optimizations yield a rotor configuration with the tilt direction of β_1 and β_3 opposite to β_5. The reason for this comes from the constraint on rotation during y-translation (equation 6.17). To explain this, image a solution with all rotors tilted in the same direction. In this case, maximum lateral acceleration is achieved when all rotors on one side of the UAV (rotor 1, 3 and 5) produce maximum thrust. However, this results in an unwanted x-rotation acceleration. To counteract this rotation, a rotor from the other side of the UAV needs to produce thrust. This rotor will also produce lateral force in the undesired direction, reducing the lateral acceleration. This undesired opposite y-actuation can be prevented by changing the tilt direction of the rotor used to counteract the rotation, such that it contribute positively to the lateral acceleration. Since this rotor will need to counteract the thrust from two rotors, the torque it produces has to be as high as possible. The highest x-rotation is achieved by the rotor with the highest y-distance from the CoM, which is rotor 5. For that reason, the tilt angle of this rotor (β_5) is opposite to the other rotors in the rotor configuration with unconstrained tilt angles. Whether β_1 and β_3 are positive or β_5 is positive does not influence the obtainable accelerations due to the mirrored rotor configuration.

It can be observed that for $x = 0.4$, the hovering acceleration is equal to g, indicating that the maximum tilt angle is reached. As a result, the solution for $x = 0.3$ is equal to the solution for $x = 0.4$.

Constrained Rotor Tilt versus Unconstrained Rotor Tilt

It is observed that the objective function for unconstrained solutions is always higher than the constrained solution. The reason for this is that a higher lateral acceleration can be obtained for non-alternating rotor tilt. This is a result of the higher torque of rotor 5 compared to rotor 3, as was just

explained. The vertical acceleration is only a little lower.

The maximum tilt angle for unconstrained rotor tilt is observed for $x = 0.4$, while the constraint maximum rotor tilt angle is obtained for $x = 0.3$. The reason for this is that it is more beneficial to increase the tilt angle for the unconstrained solution, because the vertical acceleration that can be obtained is much higher. This is why the tilt angle is also high when the weight of the vertical acceleration is low, resulting in a maximum tilt angle for higher x than for the constrained rotor tilt.

6.8.1 Wind Drag

To determine the ability of the UAV to withstand side wind disturbance, the maximum wind speed the optimized UAVs can reject with the lateral actuation has been determined. The wind speed is given by:

$$\nu_{max} = \sqrt{\frac{2F_w}{\rho C_D A_c}} \tag{6.19}$$

Where ν is the maximum wind speed the UAV is able to withstand, F_w the maximum wind drag force, ρ the density of the air ($1.20 kg/m^3$), C_D the drag coefficient of the UAV, and A_c is the cross-sectional area of the UAV in the direction of the wind. For the drag coefficient an estimated guess needs to be made.

For the circular frame the drag coefficient of a cylinder can be used. According to Franzluebbers [57], at a low Reynolds number, this is around 0.7 if the angle between the air and the cylinder is $0°$ ($C_{D,0°}$), 1.1 if it is $45°$($C_{D,45°}$) and 0.9 if it is $90°$($C_{D,90°}$). For the worst case wind direction, the $45°$ drag coefficient is used. The cross-sectional area of the frame at an angle of $45°$ is $l_5 cos(45°) D_1$, where D_1 is the outer diameter of the frame bar. It is assumed that the drag from the other bar of the frame is negligibly small, because it is in the lee of the other frame bar. This yields a cross-sectional area A_{frame} of 0.30 m^2.

The drag coefficient of the rotating propellers is very difficult to determine. The drag coefficient of the propellers and the pesticide tank is 0.7, assuming they are cylinders as well. For the propellers, the cross sectional area is estimated at 0.18 m, so for six propellers A_{props} is 1.08 m^2. For the tank the volume is 100 L and the height is assumed to be 0.4 m, resulting in a cross-sectional area A_{tank} of 0.11 m^2.

In order to reject the wind drag, the UAV must be able to accelerate opposite to the direction of F_w. To achieve this, the required lateral force to counteract F_w is estimated as $2F_w$. This yields a wind speed given by:

$$\nu_{max} = \sqrt{\frac{F_y}{\rho(C_{D,0}(A_{tank} + A_{props}) + C_{D,45} A_{frame}}} \approx \sqrt{\frac{F_y}{1.40}} \tag{6.20}$$

The resulting maximum operation wind speed for the different concepts are shown in table 6.6. The maximum allowed wind speeds are very high. At the obtained maximum wind speeds spraying crops is not possible, since the pesticide drift will be too high. Based on this, even the lateral actuation for $x = 0.8$ is higher than required. However, high lateral acceleration is still desirable because it results in faster response to wind disturbance.

x	Case	F_y[N]	ν_{max}[m/s^2]
0.3	c	646	21.27
	u	1063	27.29
0.4	c	594	20.4
	u	1063	27.29
0.5	c	325	15.08
	u	488	18.5
0.6	c	328	15.17
	u	448	17.71
0.7	c	191	11.56
	u	295	14.38
0.8	c	112	12.51
	u	175	8.85

Table 6.6: Wind speed rejection for different x

6.9 Design Choice

This optimization yields a large number of possible solutions. Each of these solutions fulfills the requirements of the application and could therefore be chosen. To choose which solution should be used for the design of the UAV, a trade-off between vertical and lateral acceleration needs to be made, which depends on the wind speed, which is variable. For that reason a design with manually adjustable rotor tilt angles is proposed. This design will consist of an adapted frame that allows the rotors to be tilted to any angle, as is done for the hexarotor with variable cant and dihedral by Rajappa [58]. The rotor position, which cannot be altered without redesigning the frame, will be equal to the position for $x = 0.4$ with unconstrained tilt angles: l_1 = 1.88 m, l_3 = 4.03 m and θ = 0.81 rad. With this rotor position, almost all optimized rotor orientations can be obtained without airflow interference. In order to be able to quickly change the rotor orientation to a different solution, a locking mechanism that locks the rotors at the different optimal tilt angles should be designed. Alternatively tilt actuators could be used for changing the rotor configuration, although tilt actuators are undesired, as mentioned in section 6.5. In order to be able to tilt the rotors freely, an adapted frame has been proposed.

6.9.1 Adapted Frame

As mentioned, an adapted frame is required if the rotors are manually tilted, to prevent the propellers from hitting the frame. For small tilt angles, the rotors can be placed on a small vertical rod to prevent this. At large tilt angles, this solution will not be viable, since the vertical rod will cause problems like buckling, resonating, etcetera. This can be seen for the unconstrained rotor configuration for $x = 0.3$ in figure 6.4a. For that reason, all concepts except $x = 0.8$ will require an adapted frame. The optimal frame has not been investigated in depth, but a viable option has been proposed in figure 6.4b. When the diameter of the frame is kept equal to the simple frame, the frame mass increases from 11 kg to 40 kg. However, the stiffness of this new frame is much higher, so a smaller diameter could be used to reduce the frame mass. As mentioned before, the difference in mass does not influence the rotor configuration. A higher mass will either result in a higher required hovering thrust or a decrease in payload. Since the required pesticide payload is between 80 L and 100 L, the latter option is viable.

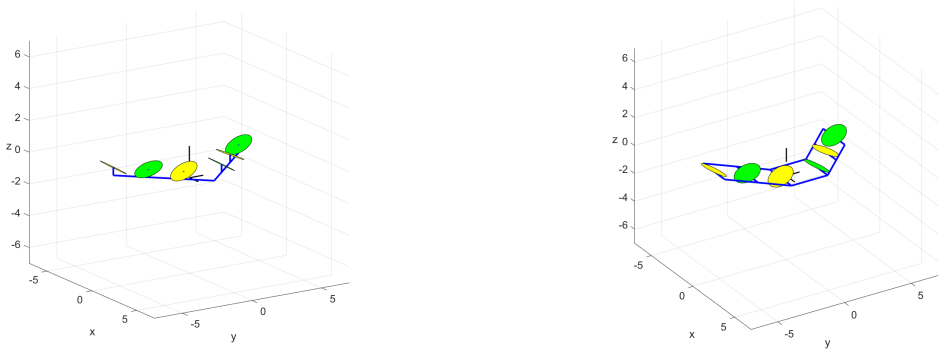

(a) Old frame

(b) New frame

Figure 6.4: Optimized UAV with different frames

It should be noted that the adapted frame allows the rotors to be manually tilted to any angle, while the simple frame only allows the very limited tilt angles. With the adapted frame, all optimized configurations can be achieved. For that reason, using the adapted frame is favoured over the simple frame, despite the added mass.

6.10 Conclusion

In this chapter the framework has been used to design a UAV for crop spraying. Due to the specific requirement, a very specific design by Drone4Agro: the V-shape, has been designed for this exact application. The rotor configuration of this concept has been optimized for both lateral acceleration for wind disturbance rejection and vertical acceleration for efficient hovering. The relative importance of these two accelerations is determined with a weighing factor. The optimization has been done for two cases: enforced alternating rotor tilting and unconstrained rotor tilting, yielding two sets of optimized designs for different weighing factors. An estimation of the maximum wind speed that can be rejected is given for all designs. To enable optimized rotor configuration, a redesign of the frame has been

proposed. With this frame all possible rotor combinations can be obtained, such that the tilt angle can be adjusted manually to the current situation.

Chapter 7

Application of Fully Actuated UAVs: Human Interaction

A new application of UAVs that is enabled by the introduction of fully actuated UAVs, is a UAV that can interact with humans. Human interaction (HI) enables the UAVs to work safely alongside humans. Being able to detect and properly respond to applied forces will be fundamental to provide safety when humans and UAVs share the same space. In this chapter, the rotor configuration of a UAV will be optimized for HI using the framework from chapter 5. This application is completely different from crop spraying UAV in chapter 6, to proof that the framework and can be applied to UAV design for a wide array of applications.

The optimization procedure will be similar to that of the crop spraying UAV. In section 7.1, previous work on HI is discussed. After this, the requirements for HI are specified in section 7.2. In section 7.3, a concept is chosen, based on these requirements, by applying the framework of chapter 5. The chosen concept is then optimized in section 7.4. The results from these optimization are presented in section 7.5 and compared in chapter 7.6. A conclusion has been given in section 7.8.

7.1 Previous Work

HI is possible with a conventional quadrotor UAV, as shown by Augugliaro [59] and Rajappa [58]. They showed that externally applied wrench can be rejected within limited time. However, the underactuated nature of this UAV makes it impossible to maintain stable flight when an external wrench is applied, since the orientation of this UAV plays a crucial role in its position control. When the orientation is externally changed, the coupling between rotation and translation will cause the UAV to translate. For HI, this can result in very unsafe situations. Furthermore, rejecting forces or stopping by first changing the pitch or roll of the entire UAV, is a rather slow process. In case an emergency stop is required to prevent collision, this method will not suffice. For these reasons save HI will require full actuation in order to perform safely.

These shortcomings of underactuated UAVs were acknowledged by Rajappa [60], who used the hexarotor with canted and dihedral rotors discussed in chapter 3.2.3 for HI. It was shown using simulation, that fully actuated UAVs outperform underactuated UAVs due to these shortcomings of the underactuated UAV.

7.2 Requirements

A number of requirements the UAV will need to have to fulfill for safe HI have been defined:

- The UAV needs to be omnidirectional to respond to all possible applied wrench and to be able to hover in any orientation.
- In order to minimize stopping time, the translational acceleration in all directions must be as high as possible.
- As the UAV needs to fly among humans, it needs enough redundancy to be able to safely land when a rotor fails
- During flight, the propellers must not come in contact with humans. To prevent this, a cage structure can be used, similar to the octorotor cube discussed in chapter 3.8a.

- Since the UAV will have to manoeuvre in confined and crowded area, its size should be limited to fit into a sphere of radius 0.25 m.
- The distance between the rotors should be high enough to be able to neglect the airflow interference between the rotors, as discussed in chapter 2.6, because airflow interference between rotors is unbeneficial for the control complexity and flying stability of the UAV.

7.3 Concept Choice

To determine the best concept for HI, the framework from chapter 5 is used. Before the framework can be used, the choice between fixed and variable tilt rotors needs to be made. Both these UAV types are able to be omnidirectional, but the variable tilt rotors are outperformed by the fixed tilt rotors, based on the disturbance rejection speed, because adjusting direction by changing rotor tilt angle is much slower than by changing rotor speed. Since fast response to disturbance is the most important requirement, fixed tilt rotors will be used.

With this choice made, the framework can be considered. Since the UAV requires to be omnidirectional, the concepts from the framework that are unable of omnidirectional flight, Quad4Hor and HexDTet, can already be disregarded. Next, the available wrench and acceleration are considered. The UAV will require high accelerations in all directions to be able to response to external wrench fast. The HeptW and HeptF suffer from very low wrench, due to the limitations of using one-directional for omnidirectional wrench and are thus disregarded. The Octorotor Beam is unfit, because it has very low lateral translational acceleration. The coaxial hexagon has the highest wrench, but the accelerations are not very high due to the high mass.

The remaining concepts are: the hexarotor canted, hexarotor canted/dihedral and the Octorotor Cube. Instead of choosing one of these concepts and optimizing the rotor configuration constrained by the parameters defined for the concepts (e.g. planar rotor positions), the rotor configuration is optimized independently of these parameters to ensure the best solution for HI is obtained, as defined by section 7.2. A number of design considerations of the concepts from the framework are considered for this optimization:

- **Symmetry**: the concepts show that there are a number of advantages to exploiting symmetry in the UAV design. For this reason, the rotors are defined in symmetric pairs, that with the position of the rotors mirrored with respect to the CoM, have equal orientation and opposite rotation direction. This results in zero torque if all rotors producing the same thrust. Furthermore, symmetric rotor pairs reduce the amount of optimization parameters, which reduces the optimization complexity and time.
- **Rotor placement**: the rotors will be placed on the edge of a sphere. It has been shown in these concepts that the highest torque in all direction is achieved, when all rotors are placed at the maximum distance from the CoM. With this constraint to the rotor position, the amount of optimization parameters reduces further.
- **Bi-directional rotors**: based on the HeptF and HeptW, it is concluded that using one-directional rotors for omnidirectional UAVs reduced the attainable wrench. For this reason, bi-directional rotors have been used.
- **Amount of rotors**: Since concepts with different rotors have different advantages, the optimization will be done multiple times for different amounts of rotors. Due to the required symmetry, the amount of rotors needs to be even. Furthermore, the minimal amount of rotors is six, since this is the minimum required amount of rotors for six DoFs actuation. The maximum amount of rotors is limited by the size of the UAV, because all rotors will have to be fitted on the sphere and due to the amount of optimization complexity that is allowed, since the amount of parameters increases when the amount of rotors increases. The optimization has been done for six, eight and ten rotors.

7.3.1 Rotor Choice

The choice of the rotor has been made, based on the amount of rotors that have to be fitted inside a 0.25 m sphere. The maximum propeller diameter of 6” is defined, such that ten rotors can be fitted inside the 0.25 m sphere with sufficient space to prevent airflow interference. A motor for this propeller diameter has been chosen based on the thrust to weight ratio. The rotor characteristics are shown in table 7.1. To obtain the desired bi-directional thrust, two stacked propellers are used.

Motor type [-]	Motor mass [kg]	Propeller diameter [in]	Propeller mass [kg]	λ_{max} [N]
KDE2304XF-2350[61]	0.033	6”	0.0048 (2x)[62]	9.71

Table 7.1: Specifications of the rotor used for the HI UAV

7.4 Optimization

In this section, the strategy for optimizing the rotor configuration of the UAV for omnidirectional wrench is presented. Similar to the pesticide spraying UAV in chapter 6, the build-in MATLAB function *fmincon* is used for the optimization. This optimization strategy consists of the definition of the rotor configuration, design simplifications, the objective function, boundary conditions, constraints and optimization options.

7.4.1 Rotor Configuration

As discussed, the position and orientation of all rotors will be optimized. Since symmetric rotor pairs are used and the rotors are placed on a sphere, each rotor pair can be described with only four parameters. The orientation of rotor i is defined according to the definition given in chapter 2.2:

$$u_i = \begin{bmatrix} \sin(\beta_i) \\ \cos(\beta_i)\sin(\alpha_i) \\ \cos(\alpha_i)\cos(\beta_i) \end{bmatrix} \tag{7.1}$$

Since the rotors are placed on a sphere, the position of rotor i can be defined in a similar way:

$$r_i = R \begin{bmatrix} \sin(\theta_i) \\ \cos(\theta_1)\sin(\phi_i) \\ \cos(\phi_i)\cos(\theta_i) \end{bmatrix} \tag{7.2}$$

where R is the radius of the sphere the rotors are placed on (0.25 m), ϕ_i the angle between the positive z-axis and the positive x-axis in F_W and θ_i is the angle between the positive z-axis and the positive y-axis in F_W. These angles specify the position of the rotor on the sphere. The definitions of θ_i and ϕ_i are the same as the definitions for α and β, because this resulted in a more simplified definition of $\mathcal{A}$ for the optimization in MATLAB. This definition for the rotor position is considered more difficult to interpret physically than, for example, the spherical angle definition.

7.4.2 Design Simplifications

A number of other simplifications have been made to speed up the optimization, without influencing the optimal rotor configuration. These simplifications are:

- For the mass and inertia of the frame, only the rotors are considered. The reason for this is that a lot of extra considerations are required to determine the mass and inertia of the frame. The rotational inertia of the rotors, which are considered as mass points, is given by equation 2.12. To validate neglecting the frame and battery in the mass, an additional optimization has been done with double rotor mass, as shown in chapter 7.5. Based on these results, it is concluded that this assumption does not influence the rotor configuration.
- For the inertia, only the diagonal terms are taken into account, because the off-diagonal terms are negligibly low compared to the diagonal terms and neglecting these terms reduces the size of the acceleration matrix and thus the optimization function considerably.
- The drag coefficient γ of the rotor is set to zero to reduce the size of the mapping matrix. This assumption is allowed, because the rotor drag torque is already rejected due to the symmetric pairs with opposing rotation direction.

7.4.3 Objective Function

The UAV requires high omnidirectional accelerations. In theory, the UAV could be maximized for all accelerations or wrench just like the crop spraying UAV is optimized for y- and z-acceleration. However, for a UAV with n rotors, every acceleration direction requires a set of n rotor thrusts that produce this optimal acceleration. To optimize all accelerations $6n$ extra parameters are added. This high amount of parameters cannot be handled by the *fmincon* solver.

Fortunately, there is a method to optimize the acceleration in all directions without requiring any thrust: dynamic manoeuvrability, as considered in chapter 2.5.1. This is a scalar measure of the volume spanned by the attainable accelerations in all directions. The use of this measure was already considered for the concept comparison in chapter 4.2. However, it was not used the comparison, since the measure is limited to bi-directional rotors and does not give insight in acceleration in specific directions. Since this optimization requires high acceleration in all directions and will have bi-directional rotors, the dynamic manoeuvrability can be applied here. The optimization will be done for a number of different optimization functions: kinematic manoeuvrability, dynamic manoeuvrability, decoupled dynamic manoeuvrability and constrained dynamic manoeuvrability.

Optimization of Kinematic and Dynamic Manoeuvrability

The optimization is done for both kinematic manouvrability w_K and dynamic manoeuvrability w_D, to determine whether accounting for the inertia of the UAV actually results in rotor configuration with a higher omnidirectional acceleration. The only difference between the two optimization procedures is that w_K is based on the mapping matrix, where w_D requires the acceleration mapping matrix. The objective function for w_D is given by:

$$f(\vec{\theta}, \vec{\phi}, \vec{\alpha}, \vec{\beta}) = -w_D \tag{7.3}$$

Where $\vec{\phi}, \vec{\theta}, \vec{\alpha}, \vec{\beta}$ are vectors of length $\frac{1}{2}n$ consisting of the angles, specified in section 7.4.1. These define the configuration of n rotors and w_D is the dynamic manoeuvrability. As defined in chapter 2.5.1, w_D is given by:

$$w_D = \sqrt{\det \mathbf{A}\mathbf{A}^T} \tag{7.4}$$

It can be observed that the rotor thrust $\vec{\lambda}$ is not specified in this function: w_D spans the volume of the acceleration matrix for a unit thrust. To be able to take the actual thrust produced by the rotor into account, the mass of the rotors has been scaled down to m_r' by the ratio between the unit thrust and the actual thrust: $m_r' = m_r/\lambda_{max}$. Since the mass of rest of the UAV is not considered, the thrust-to-weight ratio of the UAV remains equal when both the thrust and the mass of the rotor are scaled equally. For six rotors, $\mathbf{A}$ is square and w_D reduces to:

$$w_D = |\mathbf{A}| \tag{7.5}$$

This drastically increases the optimization speed, since the matrix multiplication $\mathbf{A}\mathbf{A}^T$ results in a very long objective function. The objective function for w_K is identical to equation 7.3, with the exception that w_K is optimized, which is given by:

$$w_K = \sqrt{\det \mathbf{M}\mathbf{M}^T} \tag{7.6}$$

Again, the function can be rewritten for six rotors:

$$w_K = |\mathbf{M}| \tag{7.7}$$

Optimization of Decoupled Dynamic Manoeuvrability

Since the simplification of w_D, given in equation 7.5, can only be done for six rotors, the eight and ten rotor objective function will have to be optimized with the definition of w_D given by equation 7.4. As a result, the symbolic objective function, which is required for optimization with *fmincon*, will become too long for MATLAB to process. To be able to find an optimal solution, either a different optimization program or the use of a different objective function is required. The latter option is chosen. The optimization is split into two optimizations: an optimization of the translational dynamic manoeuvrability $w_{D,t}$ followed by an optimization of the rotational dynamic manoeuvrability ($w_{D,r}$). The decoupling of the dynamic manoeuvrability into translation and rotation is explained in chapter 2.5.2. First, the orientation angles ($\vec{\alpha}$ and $\vec{\beta}$) will be determined by optimizing $w_{D,t}$, since the translational part of the $\mathbf{A}$ only depends on the orientation of the rotors. The first objective function is given by:

$$f_1(\vec{\theta}, \vec{\phi}, \vec{\alpha}, \vec{\beta}) = -w_{D,t} = -\sqrt{\det \mathbf{A_t}\mathbf{A_t}^T} \tag{7.8}$$

After the optimal orientation is found, the orientation angles are substituted in $\mathbf{A}$. The position of the rotors ($\vec{\phi}$ and $\vec{\theta}$) is then determined by optimizing $w_{D,r}$. This second objective function is given by:

$$f_2(\vec{\theta},\vec{\phi}) = -w_{D,r} = -\sqrt{\det \mathbf{A_r}\mathbf{A_r}^T} \tag{7.9}$$

Due to the rotor symmetry, the CoM will always be at the origin of the body fixed frame, so w_D can be written as: $w_D = w_{D,t}w_{D,r}$. To determine the influence of the decoupling of the objective function on the results, the uncoupled optimization is compared to the coupled optimization with equation 7.5 for the six rotor UAV, since this UAV can be optimized with both methods. This comparison can be found in section 7.5.

Optimization of Dynamic Manoeuvrability and Thrust Efficiency

Apart from achieving high omnidirectional acceleration, it is desired that the UAV is able to fly efficiently, meaning that the thrust required to fly is low. To take the flying efficiently into account, the thrust efficiency (η_F) is considered in the optimization. This measure is described in chapter 4.2.1. To optimize the UAV for high manoeuvrability and high thrust efficiency, the two objectives, a weighing factor x is applied, similar to the objective function of the crop spraying UAV. To use this weighing factor, the order of magnitude of the two objectives must be equal. To achieve thi, w_D is scaled by the ratio between w_D and the maximum possible w_D, $w_{D,max}$. This results in the following objective function:

$$f(\vec{\theta},\vec{\phi},\vec{\alpha},\vec{\beta}) = -\left(x\frac{w_D}{w_{D,max}} + (1-x)\eta_F\right) \tag{7.10}$$

The thrust efficiency η_F is the ratio between the vertical force and the total rotor thrust. Since the orientation of the UAV is not defined, the vertical force is given as the resultant force produced when all rotors produce maximum thrust:

$$\eta_F = \frac{||\mathbf{M_t}\vec{\lambda}_{max}||}{n\lambda_{max}} \tag{7.11}$$

where λ_{max} = 1 N. For six rotors, $w_{D,max}$ is given by the result from the optimization of equation 7.5. For more than six rotors, the decoupled translational and rotational optimization is required. The thrust efficiency is considered in the first optimization:

$$f(\vec{\theta},\vec{\phi},\vec{\alpha},\vec{\beta}) = -\left(x\frac{w_{D,t}}{w_{D,t,max}} + (1-x)\eta_F\right) \tag{7.12}$$

Where $w_{D,t,max}$ is the maximum $w_{D,t}$ obtained from equation 7.8. In the optimization of $w_{D,r}$, η_F is not taken into account because the η_F depends only on the rotor orientation.

A number of optimizations with different x has shown that this method for considering the thrust efficiency in the optimization is ineffective: for high x, w_D will be equal to $w_{D,max}$, and for low x, the rotors are nearly parallel, resulting in a η_F of almost 1 and a very low w_D. The reason for this undesired behaviour is that the scaling w_D results in a very unstable optimization. For some x, the desired trade-off between η_F and w_D is found, but finding this x is difficult. Finding a desired η_F is even more difficult. An alternative method to obtain high η_F, as well as high w_D, is to include a minimum required η_F in the constraints. The optimization will yield the highest possible w_D for the required η_F. This method provides much more control over η_F than the previous. For that reason the optimization will be done for constrained η_F instead of optimizing η_F.

7.4.4 Boundary Conditions

Since all parameters are angles, all boundary conditions are between $-\frac{\pi}{2}$ and $\frac{\pi}{2}$. Although these boundaries only span the upper half of the sphere of attainable orientations, it is considered enough to cover the entire sphere. The rotor position will cover the entire sphere because each rotor has a symmetric pair, so if rotor 1 can be placed on the entire upper half of the sphere of attainable positions, rotor 2 will automatically be placed on the lower half of the sphere. This way, all rotor positions are covered by only half the circle. For the rotor orientation, the lower half of the sphere can be omitted since the rotor is bi-directional, so it does not matter if the rotor is placed facing upward or downward. Taking the entire circle as a boundary condition is also possible, but this unnecessarily increases the search space of the optimization and thus the optimization time.

7.4.5 Constraints

There are a number of constraints to make sure the optimization solution actually fulfills the requirements. These constraints consist only of non-equality constraints, which need to be below zero. The constraints are:

$$2g - \mathbf{A_z}\vec{\lambda}_{max} \leq 0 \tag{7.13}$$

$$d_{aero} + R - d \leq 0 \tag{7.14}$$

The first constraint, given by equation 7.13, is used to make sure the UAV is able to ascend with sufficient acceleration. The direction of this acceleration when all rotors produce λ_{max} is not necessarily in vertical direction. However, since the UAV will be omnidirectional, it should be able to ascend in any orientation. The second constraint, give by equation 7.14, is used to make sure the distance between the rotors and the airflow is high enough to be able to neglect airflow interference. Here d is the distance between the airflow and the rotors as defined in chapter 2.6. Like the rotors used by Parks [6], it is assumed that the minimal distance d_{aero} is equal to R, which is 0.07 m.

As mentioned, a separate optimization is done with a constrained thrust efficiency. For this optimization an extra constraint is given by:

$$\eta_{F,min} - \eta_F \leq 0 \tag{7.15}$$

where $\eta_{F,min}$ is the minimum required thrust efficiency.

7.4.6 Optimization Options

There are a number of optimization options that are adjusted to improve the optimization speed or precision. These options are equal to the options for the crop spraying UAV, discussed in chapter 6.7.6.

7.5 Results

In this section, the results of the different optimizations are presented. The results have been categorized by the amount of rotors. The optimization has been done a number of times for a number of different cases. These cases are given in table 7.2. The different solutions will be referred to by the amount of rotors followed by the case, e.g. 6.1 is case 1 for six rotors.

Number of rotors	Case	Objective function
6	6.1	w_K, equation 7.7
	6.2	w_D, equation 7.5
	6.3	w_D double rotor mass, equation 7.5
	6.4	$w_{D,t}$ and $w_{D,r}$, equation. 7.8 and 7.9
	6.5	w_D and η_F, equation 7.5 and 7.15 with $\eta_{F,min} = 0.8$
8	8.1	$w_{D,t}$ and $w_{D,r}$, equation 7.8 and 7.9
	8.2	$w_{D,t}$, $w_{D,r}$ and η_F, equation 7.8, 7.9 and 7.15 with $\eta_{F,min} = 0.8$
10	10.1	$w_{D,t}$ and $w_{D,r}$, equation. 7.8 and 7.9
	10.2	$w_{D,t}$, $w_{D,r}$ and η_F, equation 7.8, 7.9 and 7.15 with $\eta_{F,min} = 0.8$

Table 7.2: Optimizations done for the different amounts of rotors

The results consist of the four design parameters $\vec{\theta}$, $\vec{\psi}$, $\vec{\alpha}$ and $\vec{\beta}$ describing the rotor configuration of the first rotor of each symmetric pair, as defined in section 7.4.1.

7.5.1 Optimizations with Six Rotors

The design parameters of the optimized design with six rotors is given in table 7.3.

Case	θ			ϕ			α			β		
6.1	0.00	0.00	-1.57	-0.74	0.83	0.14	0.28	-0.74	0.83	1.57	0.00	0.00
6.2	-1.17	1.17	1.17	0.28	1.33	-0.76	-1.23	-0.24	0.81	-0.45	0.45	-0.45
6.3	-1.17	1.17	1.17	0.33	1.38	-0.72	-1.24	-0.20	0.85	-0.45	0.45	-0.45
6.4	1.30	-0.20	-0.18	-0.36	-1.09	0.51	0.51	-0.36	-1.09	-0.17	1.30	-0.20
6.5	0.81	-1.57	-0.81	-1.55	1.31	-1.55	-0.37	0.67	-0.37	-0.52	0.00	0.52

Table 7.3: Optimized parameters for six rotor UAV

7.5.2 Optimizations with Eight Rotors

The design parameters of the optimized design with eight rotors is given in table 7.4.

Case	θ				ϕ				α				β			
8.1	0.45	-0.99	-0.68	0.23	-0.67	0.84	-1.19	0.63	0.05	1.50	0.20	-1.11	-1.0	0.48	0.22	0.64
8.2	-0.23	0.72	0.95	-0.11	-1.23	-1.34	1.39	1.25	0.39	-0.39	0.56	-0.56	0.52	-0.52	-0.34	0.34

Table 7.4: Optimized parameters for eight rotor UAV

7.5.3 Optimizations with Ten Rotors

The design parameters of the optimized design with ten rotors is given in table 7.5.

Case	θ					ϕ					α					β				
10.1	0.94	-0.83	0.23	-0.82	0.08	0.97	-0.17	0.52	1.30	-0.82	1.43	0.87	-0.94	-0.08	0.17	-0.69	0.41	-0.33	0.17	-1.41
10.2	1.13	0.65	-0.21	0.53	1.27	-1.57	1.29	-1.35	-1.25	0.45	-0.31	0.58	-0.14	0.5	-0.64	0.57	-0.29	-0.63	0.42	-0.08

Table 7.5: Optimized parameters for ten rotor UAV

7.5.4 UAV Orientation in World Inertial Frame

Since the wrench and acceleration in all directions are optimized, the orientation of the UAV is not defined in the optimization. In order to determine the maximum wrench and acceleration, the vertical, longitudinal and lateral directions need to be specified in $\mathcal{F}_{\mathcal{W}}$.

First, the vertical direction of the UAV is orientated to coincide with the z-direction in $\mathcal{F}_{\mathcal{W}}$. The vertical direction is defined as the direction of the maximum force. To determine this direction, The maximum resultant force F_{max} in the current orientation is determined, by optimizing (using *fmincon*) the norm of the three translational directions of the mapping matrix:

$$f(\vec{\lambda}) = F_{max} = ||\mathbf{M_t}\vec{\lambda}|| \tag{7.16}$$

where λ is the vector of the rotor thrust for which the resultant force is the highest. The direction of F_{max} can be expressed by two angles, α_h and β_h, which are defined the same as the orientation. By defining $\vec{F}_{max}$ as the three components of the resultant force in $\mathcal{F}_{\mathcal{W}}$, the direction of F_{max} can be determined:

$$\vec{F}_{max} = \begin{bmatrix} F_{max,x} \\ F_{max,y} \\ F_{max,z} \end{bmatrix} = F_{max} \begin{bmatrix} \sin(\beta_h) \\ \cos(\beta_h)\sin(\alpha_h) \\ \cos(\alpha_h)\cos(\beta_h) \end{bmatrix} \tag{7.17}$$

The angles α_h and β_h are be given by:

$$\beta_h = \sin^{-1}\left(\frac{F_{max,x}}{r_h}\right) \tag{7.18}$$

$$\alpha_h = \cos^{-1}\left(\frac{F_{max,z}}{r_h\cos(\beta_h)}\right) \tag{7.19}$$

With these angles, the UAV can be rotated using the rotation matrix. The rotation matrix around the x-axis is used to rotate α and the rotation matrix around the y-axis is used for β:

$$R_x = \begin{bmatrix} 1 & 0 & 0 \\ 0 & \cos(\alpha_h) & \sin(\alpha_h) \\ 0 & -\sin(\alpha_h) & \cos(\alpha_h) \end{bmatrix} \tag{7.20}$$

$$R_y = \begin{bmatrix} \cos(\beta_h) & 0 & -\sin(\beta_h) \\ 0 & 1 & 0 \\ \sin(\beta_h) & 0 & \cos(\beta_h) \end{bmatrix} \tag{7.21}$$

$$\tag{7.22}$$

The new rotor position (r') and orientation (u') are given by:

$$r' = R_y R_x r \tag{7.23}$$
$$u' = R_y R_x u \tag{7.24}$$

The rotation of the vertical force to the z-axis is illustrated in figure 7.1b. Now that the vertical direction corresponds to the direction of the maximum force, the UAV needs to be rotated around the z-axis, such that the maximum horizontal force, the longitudinal force F_l, is directed in the x-direction in $\mathcal{F}_\mathcal{W}$. This is rotation is explained in chapter 4.2.1. This rotation is illustrated in figure 7.1c. It should be noted that a constraint could be added to the optimization, that makes sure the resultant force is in the vertical direction. However, this constraint heavily reduced the convergence rate, which reduces optimization speed.

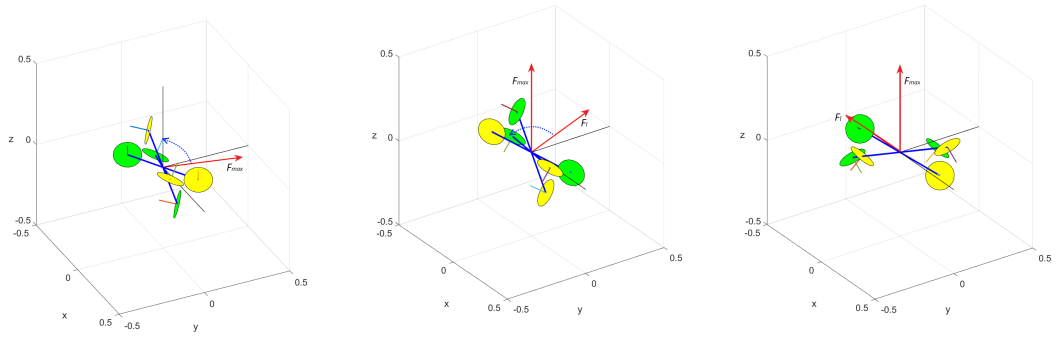

(a) Vertical force before rotation

(b) Vertical force rotated to z-direction

(c) Longitudinal force rotated to x-direction

Figure 7.1: Reorientation of case 6.2 in $\mathcal{F}_\mathcal{W}$. First the maximum force is rotated to the z-direction and then the maximum horizontal force is rotated to the x-direction

The rotor configuration of the other cases, rotated in $\mathcal{F}_\mathcal{W}$, are shown in appendix F. The rotated rotor configuration of case 6.4 and case 6.1 in $\mathcal{F}_\mathcal{W}$ are identical, as well as case 6.3 and case 6.2, as explained in section 7.6.

7.6 Comparison of Optimization Solutions

In this section, the designed UAVs have been compared. First the manoeuvrability, which was used to optimize the UAVs, is discussed, to determine how well the optimizations performed. After that, the static and dynamic performance, as defined in section 4.2, are used to compare the different optimization solutions and compare these solutions with the concepts of the framework.

7.6.1 Manoeuvrability

The manoeuvrability for the optimized concept is shown in table 7.6. Note that the rotor mass is normalized to the thrust, identical to the optimization ($m_r' = m_r/\lambda_{max}$). The best performing solution has been highlighted. The results have been compared next.

Case	$w_{K,t}$ [-]	$w_{K,r}$ [10^{-2} m^{-3}]	w_K [10^{-1} m^{-3}]	$w_{D,t}$ [10^{5} kg^{-3}]	$w_{D,r}$ [10^{7} kg^{-3}m^{-3}]	w_D [10^{12} kg^{-6}m^{-3}]
6.1	2.83	4.42	1.25	**1.55**	3.35	5.19
6.2	2.59	2.97	0.77	1.42	**5.05**	**7.16**
6.3	2.59	2.97	0.77	1.42	**5.05**	**7.16**
6.4	2.83	4.42	1.25	**1.55**	3.35	5.20
6.5	2.11	3.95	0.83	1.16	4.11	4.75
8.1	4.35	6.85	2.98	1.00	2.19	2.20
8.2	3.26	6.01	1.96	0.75	2.44	1.84
10.1	**6.08**	**9.46**	**5.60**	0.72	1.55	1.12
10.2	4.55	7.58	3.45	0.54	1.43	0.77

Table 7.6: Results of the optimization for six rotors

Six Rotors

It is observed that the results for the kinematic optimization (case 6.1) are nearly identical to the results for separated dynamic optimization (case 6.4). The reason for this is that for case 6.4, the orientation of the rotors depends only on $w_{D,t}$. Since the translational accelerations are proportional to the forces (by the total mass), the optimal orientation for maximum $w_{D,t}$ and $w_{K,t}$ are equal. Although case 6.1 optimizes w_K, not $w_{K,t}$, the orientations are still equal because the highest achievable $w_{K,r}$ can be achieved for any orientation, by placing the rotors such that they are only canted, since the dihedral angle does not contribute to the torque, as discussed in chapter 5.5.2. When optimizing $w_{D,r}$ in case 6.4, the orientation is already defined and the optimal rotor position will result from the orientation. The inertia does not influence the results in this case. As such $w_{D,r}$ and w_K also yield the same rotor position.

Judging by the difference between case 6.2 and case 6.3, it can be concluded that doubling the rotor mass does not influence the rotor configuration. This validates the assumption of the total mass done in section 7.4.2. When w_D is optimized (case 6.2 and 6.3), the rotor orientation will not only depend on $w_{D,t}$, but on $w_{D,r}$ as well. Also, the influence of the inertia is visible in the optimization. This results in a 'stretched out' design with very low inertia around one axis. This solution resembles the OctB in chapter 3.2.9, although this is just coincidental, because that concept was optimized for wrench with a weighing factor. It can be seen that this rotor configuration results in a slight decrease in $w_{D,t}$, but a large increase in $w_{D,r}$, compared to the decoupled optimization (case 6.4). The increase in $w_{D,r}$ is much higher than the decrease in $w_{D,t}$, w_D, which is the sum of $w_{D,t}$ and $w_{D,r}$, and this is higher than in case 6.4. An advantage of decoupling of case 4 is that this optimization will yield the optimal $w_{D,t}$, instead of w_D, which could be beneficial for this application.

When η_F is taken into account in the optimization of w_D (case 6.5), the solution resembles the HexC from the framework (chapter 3.2.2). w_D decreases compared to case 2, where only w_D is optimized. Increase in η_F yields a decrease in $w_{D,t}$, because the forces are more concentrated in one direction, as well as a decrease in $w_{D,r}$, as a result of the constraint rotor orientation due to the required η_F. Compared to case 6.4, $w_{D,r}$ does increase, due to the low inertia around the x- and y-axis, as a result of the rotor configuration in the xy-plane. Although a planar configuration is advantageous for $w_{D,r}$ in case 6.5, it is apparantly not optimal for the rotor orientation in case 6.4.

Eight Rotors

For the eight rotor optimization based on the separated $w_{D,t}$ and $w_{D,r}$ in case 8.1, the solution resembles the OctCu from the framework (see chapter 3.2.8), for which the rotor position was fixed to the vertices of a cube. The w_K is a lot higher than in the six rotor results, because eight rotors always produce more thrust than six rotors. The six rotor concepts all perform better than the eight rotor concept for $w_{D,t}$, $w_{D,r}$ and thus w_D. This is unexpected, because each added rotor adds a lot more thrust than mass. A number of reasons can be given for this reduction. First of all, the amount of rotors might be too high to prevent airflow interference in most configurations, resulting in a very limited solution space for the optimal configuration. Although this may be the case, based on the rotor configuration it is expected that the attainable accelerations should still be higher for the eight rotor configuration. Another possible explanation for the low w_D is that the manoeuvrability is not a general measure for comparing designs with different amount of rotors. To investigate this possibility, the maximum accelerations of all concepts have been compared in section 7.6.4.

When η_F is taken into account in the optimization for eight rotors, with separated $w_{D,t}$ and $w_{D,r}$ (case 8.2), the same trend as was observed for six rotors applies: $w_{D,t}$ decreases and $w_{D,r}$ increases. The w_D is still lower than the solution without constrained η_F.

Ten Rotors

For the solution with ten rotors, based on the separated $w_{D,t}$ and $w_{D,r}$ (case 10.1), w_K increases, while w_D decreases compared to case 8.1. This result is similar to what was observed when comparing eight rotors to six rotors. It can be seen that the rate at which the results change, based on the amount of rotors, is nearly linear, when comparing case 6.4, 8.1 and 10.1. In case 10.1, the possibility that the amount of rotors is too high to find enough solutions without airflow interference, is more plausible than for case 8.1.

When η_F is taken into account for the ten rotor, in case 10.2, $w_{D,t}$ and w_D decrease, just like it does for case 6.5 and 8.2. However, $w_{D,r}$ decreases as well in this case, albeit only slightly. The reason for this is that in this case the amount of rotors is so high that the amount of possible solutions without

airflow interference is very limited. The best solution for $w_{D,r}$ of these limited solutions is coincidentally higher for case 10.1 than 10.2.

7.6.2 Volume of Accelerations

The translational and rotational dynamic manoeuvrability, which are a measure of the volume of attainable accelerations, can be visualized with the brute force method. This can be done by plotting the translational and rotational acceleration for all possible thrust combinations, yielding a volume of attainable coupled accelerations. These volumes are plotted in appendix G for all cases.

When comparing the optimizations for separated $w_{D,t}$ and $w_{D,r}$, without constrained η_F, in case 6.1, 6.4, 8.1 and 10.1, it can be observed that the shape of the volume of attainable translational and rotational accelerations transform from a cube into a sphere, as the amount of rotors increases. The reason for this is that the amount of possible thrust combinations increases when the amount of rotors increases, which results in more directions in which the maximum force can be achieved. A similar increasing spherical shape is observed for the rotational acceleration. A spherical volume is desirable for omnidirectional UAVs, as the UAV will be able to achieve the same acceleration in all directions.

For the optimization of w_D, in case 6.2, it can clearly be seen why w_D is so high: the rotational acceleration in one direction is very high. As mentioned, this high acceleration is a result of the low inertia in this direction. Due to this high acceleration, the volume of rotational acceleration and $w_{D,r}$ is high. The volume of translational acceleration is similar to case 6.1 and 6.4, albeit slightly smaller according to $w_{D,t}$.

For the optimizations with η_F constrained, in case 6.5, 8.3 and 10.2, the volume of translational acceleration is very stretched due to the high vertical force required for η_F. Similar to the other optimizations, the volume becomes increasingly ellipsoidal when the amount of rotors increases. The rotational volume on the other hand is very flat due to the high z-inertia compared to the x- and y-inertia. Again, the volume becomes more round as the amount of rotors increases.

In appendix G.2, an approximation of the volume spanned by the translational acceleration is given, based on the results of the brute force method for case 6.1, 6.4 and 8.1. These volumes differ greatly from the $w_{D,t}$, obtained from table 7.6. This results in the conclusion that either the brute force method or $w_{D,t}$ does not yield the correct volume spanned by the attainable acceleration. This observation should be investigated further in future work.

7.6.3 Static Comparison

In this section, the concepts are compared based on the quantitative criteria defined in chapter 4.2. The static comparison is shown in table 7.7. Contrary to the static comparison of the framework in chapter 5, the actual scale and λ_{max} for the rotor which is used, have been used for this comparison. To compare these concepts with the framework, a scaled comparison with the framework is given in section 7.6.5.

	Maximum wrench						
Case	Longitudinal [N]	Lateral [N]	Vertical [N]	x-rotation [Nm]	y-rotation [Nm]	z-rotation [Nm]	η_F [-]
6.1/6.4	31.71	27.46	33.64	6.17	6.35	7.83	0.58
6.2/6.3	32.70	22.75	36.00	6.62	4.31	5.64	0.62
6.5	24.32	19.25	46.61	6.88	5.11	6.61	**0.80**
8.1	44.85	44.85	44.85	8.15	10.54	8.24	0.58
8.2	32.96	32.95	62.14	8.37	10.91	7.11	**0.80**
10.1	**53.70**	**47.59**	55.17	**11.30**	10.79	9.92	0.57
10.2	37.72	35.86	**77.68**	10.41	**12.07**	**9.97**	**0.80**

Table 7.7: Static comparison for HI UAVs

Force

Based on the static comparison, it is clear why the ten rotor optimization, case 10.1, yields the highest w_K: the horizontal forces are highest in all directions and the vertical force is only surpassed by case 10.2, which has a higher vertical force due to the required η_F.

It can be observed that for case 8.1 and 10.1, where $w_{D,t}$ is optimized separately, the forces in all directions are very similar. For case 6.2 and 6.3, there is a larger difference between the forces in

the different direction. The optimizations with constrained η_F, have high vertical force to achieve the required η_F, which results in a low horizontal force. The optimizations for decoupled w_D, case 8.2 and 10.2, have very similar forces in longitudinal and lateral directions, while for the optimization for w_D, case 6.5, this is not the case.

Torque

The results for the maximum torque are rather inconsistent with the results for $w_{K,r}$. For example, case 10.1, which has the highest $w_{K,r}$, has lower y- and z-torque than case 10.2. The reason for these inconsistencies is twofold: the $w_{D,r}$ does not consider the uncoupled, but the total volume of torques. The torques considered in the static comparison are not necessary the maximum uncoupled torques, because the orientation of the UAV is based on the translations.

Thrust Efficiency

It can be seen, that for the optimization constraint by η_F, case 6.5, 8.2 and 10.2, the thrust efficiency is 0.80, as required by the constraint. The results show that this is a good method to optimize the manoeuvrability, as well as the thrust efficiency. It is clear that the increase in vertical force results in a reduction in horizontal force. Notably, for all optimizations with optimal $w_{D,t}$ (case 6.1, 6.4, 8.1 and 10.1), η_F is around 0.58. Apparently, this η_F yields the best trade-off between horizontal and vertical acceleration for maximal $w_{D,t}$.

7.6.4 Dynamic Comparison

The dynamic comparison, defined in chapter 4.2.2, is shown in table 7.8. The accelerations of all optimized configurations are very high compared to the concepts comparison from chapter 5, because only the rotor mass is considered for the mass and inertia of these solutions. For that reason, the results cannot be compared to the the concepts from the framework.

The dynamic comparison between solutions with different amounts of rotors is not biased, because the mass of the frame and battery also increases when the amount of rotors increases. However, if it is assumed that the added frame mass is equal per rotor and the frame is a simple beam, as shown in figure 7.1, it can be assumed that the mass and inertia of the frame of a rotor is proportional to the mass and inertia of the rotor, since the direction of the inertia is equal. When the frame mass could be added to the rotor mass, it will result in a lower $(T/w)_{rotor}$. This influences the accelerations of all concepts equally, as shown in chapter 5.5.3. Note that the proportional contribution of the frame to the mass is higher than the contribution to the inertia, due to the reduced distance to the CoM. When the influence of the heavier battery required for more rotors is neglected, it can be assumed that the relative accelerations are unaffected by neglecting the mass and inertia of the frame and battery.

	Maximum acceleration						
Case	Longitudinal [m/s^2]	Lateral [m/s^2]	Vertical [m/s^2]	x-rotation [s^{-2}]	y-rotation [s^{-2}]	z-rotation [s^{-2}]	λ_f [N]
6.1/6.4	124.1	107.4	131.6	579.4	596.6	**735.1**	4.3
6.2/6.3	128.0	89.0	140.9	535.6	879.9	468.5	**3.2**
6.5	95.2	75.3	**182.3**	634.7	**1019.7**	416.8	3.1
8.1	**131.6**	**131.6**	131.6	574.0	742.2	580.3	5.8
8.2	96.7	96.7	**182.3**	**1105.8**	708.1	361.6	4.2
10.1	126.1	111.7	129.5	612.2	591.2	595.3	5.7
10.2	88.5	84.2	**182.3**	728.9	776.3	365.9	5.2

Table 7.8: Dynamic comparison for HI UAVs

Translational Acceleration

Based on the dynamic comparison, case 8.1 achieves the highest longitudinal and lateral acceleration, while the vertical acceleration is only surpassed by the optimizations with constrained η_F. These solutions all achieve the same vertical acceleration, because the η_F and $(T/m)_{tot}$ are equal. Case 8.1 does have a higher translational acceleration in all directions compared to all other concepts, while $w_{D,t}$ is lower than the six rotor solutions, as discussed in section 7.6.1. The only remaining conclusion is that comparing a six rotor concept to a eight rotor concept yields inconsistencies. For case 10.1 the same applies: compared to case 6.1 and 6.4, the translational accelerations are similar (if not higher), while

the $w_{D,t}$ of 10.1 is more than a factor two lower than 6.1 and 6.4.

For the ten rotor solutions, the translational accelerations are lower than for eight rotors. It could appear that the problem of too much airflow interference has actually occurred here. Also, the amount of solutions is too small to find one that actually performs better than the eight rotors solution.

It is observed that the uncoupled translational accelerations presented here, are equal to the translational accelerations found with the brute force method in appendix G.2. Apparently, the maximum force is already uncoupled. This can also be seen from the plotted volumes of the translational accelerations in appendix G, as the maximum accelerations in the three principle directions are found at their respective axes.

Rotational Accelerations

When comparing the results for six rotors, it can be seen that case 2 and 3, which have the highest $w_{D,r}$, do not have very high rotational accelerations. The reason for that is that the direction of the rotation is dictated by the vertical and lateral acceleration direction, so the maximum rotational acceleration is not around this axis. The uncoupled rotational accelerations resulting from the brute force method shown in appendix G.2, do give rotational accelerations that agree with this high $w_{D,r}$. It can be seen by the volume (appendix G), that the maximum rotational acceleration in this direction is coupled, which is why it is not shown in table 7.8. For the other concepts, the uncoupled rotational acceleration is also lower than the coupled rotational acceleration. However, the difference is much smaller. For eight and ten rotors, spherical shape of the acceleration volume results in coupled rotational acceleration, that are almost equal to the uncoupled rotational acceleration.

As mentioned in section 7.6.2, the solutions with constrained η_F achieve high x- and y-rotation acceleration, due to the low inertia in these directions. The cases optimized for $w_{D,t}$ achieve equal rotational accelerations in all directions, due to fact that the rotors are orientated in all directions for maximized $w_{D,t}$ and the position is such that the dihedral angle is limited. This results in equal torque and inertia in all directions.

Flying Thrust

It is expected that λ_f increases as the amount of rotors increases, due to the increased mass. However, this is not the case when comparing 8.1 and 10.1. The reason for this is that case 8.1 needs to produce thrust in opposite direction, in order to reach the desired horizontal acceleration, as well as the required vertical acceleration. It is more energy efficient to fly faster than 5 m/s without opposite thrust. Since a minimal required horizontal acceleration is defined, the λ_f for this higher acceleration is given. Although this is also the case for 10.1, this concept can achieve the required vertical acceleration with lower horizontal acceleration. For the six rotor concepts, the same trend can be seen, where case 6.2 and 6.4 require a lower horizontal force to achieve the vertical force than in case 6.1 and 6.4.

It can be seen that constraining η_F reduces λ_f. This partly can be contributed to the reduced thrust required for hovering, but it also results from the ability to achieve the required combination of vertical and horizontal acceleration without producing opposite, which the other concepts lack.

Due to the required opposite thrust to obtain the required combination of horizontal acceleration, it can be concluded that the performance of the concepts in this measure depends on the required horizontal acceleration. What can be concluded is that the constrained η_F can fly more energy efficient at low acceleration.

7.6.5 Comparison to Framework

In table 7.9, the solutions for the different cases have been compared statically to the omnidirectional concepts of the framework in chapter 5.5.2. Despite being omnidirectional, the HeptF and HeptW have not been included, because is was already established that these concepts are outperformed statically by the other omnidirectional concepts in all directions, due to the one-directional rotors.

Case/Concept	Maximum wrench						η_F
	Longitudinal [N]	Lateral [N]	Vertical [N]	x-rotation [Nm]	y-rotation [Nm]	z-rotation [Nm]	[-]
6.1/6.4	3.27	2.83	3.46	2.47	2.77	3.40	0.58
6.2/6.3	3.37	2.34	3.71	1.90	1.81	2.51	0.62
6.5	2.50	1.98	4.80	2.87	2.18	2.73	0.80
8.1	4.62	4.62	4.62	3.38	4.54	3.38	0.58
8.2	3.39	3.39	6.40	3.52	4.54	3.02	0.80
10.1	**5.53**	**4.90**	5.68	4.66	4.30	4.17	0.57
10.2	3.88	3.69	8.00	4.36	5.15	4.06	0.80
HexC	2.31	2.00	4.90	2.48	2.87	3.36	**0.82**
HexCD	2.26	1.95	4.84	2.46	2.84	3.29	0.81
CoHexC	4.62	4.00	**9.80**	**4.90**	**5.66**	**6.93**	0.82
OctCu	4.54	4.54	4.53	3.37	3.37	4.62	0.57
OctB	**5.44**	2.24	5.44	1.30	1.56	0.93	0.68

Table 7.9: Static comparison between HI UAVs and framework concepts

The mentioned ,resemblance between case 6.5 and HexC is also apparent in the static performance, which is almost equal. The same applies for case 8.1 and the OctCu. Although case 6.2 and 6.3 resemble OctB, the two extra rotors of OctB result in a much better static performance compared to case 6.2 and 6.3.

The CoHexC outperforms all optimized concepts based on the vertical force and the torques, as a result of the high amount of rotors. However, when comparing the concepts with the same amount of rotors, a few observations can be made.

For the six rotor concepts, HexC and HexD, the horizontal force is much lower than in case 6.1, while the torques are similar. This means that this case is more omnidirectional than the HexC and HexD.

For the eight rotor concept OctCu, the results are similar to case 8.1, as explained. The OctB performs best only in longitudinal direction. The thrust efficiency of these concepts is very low compared to case 8.2.

Since there are no ten rotor concepts, the ten rotor optimization is compared to the CoHexC, which has two more rotors and should outperform both case 10.1 and 10.2. This is not the case for the horizontal forces, because case 10.1 outperforms the CoHexC here. It can be said that case 10.2 resembles CoHexC based on the horizontal force relative to the vertical force, the thrust efficiency and the in-plane configuration, although CoHexC performs better due to the higher amount of rotors. Furthermore, case 10.2 does not have airflow interference between the rotor, which CoHexC does, but this is not considered in the static comparison.

7.7 Design Choice

In section 7.6, the possible concepts presented in section 7.5 have been compared extensively. Despite this, making a decisive choice for one concept is difficult. The six rotor solutions achieved the highest w_D, as well as a high coupled and uncoupled acceleration. The highest w_D is achieved by case 6.2 and 6.3, but this solution does not produce high acceleration in all directions and is thus not favored. Case 6.1 and 6.4 do yield high accelerations in all directions and case 6.5 provides a good trade-off between efficient flight and high accelerations. However, none of these concepts is chosen, due to the lack of redundancy, which not only results in dangerous situations if a rotor fails, but also lower accelerations in some orientations.

Based on the translational accelerations, the best concept would be case 8.1, since it can achieve the highest translational acceleration that is about equal in all directions, as can be seen by the spherical acceleration volume. Like case 6.5, case 8.2 provides a trade-off between efficient flying and high omnidirectional acceleration. The eight rotor concepts provide sufficient redundancy for safe HI.

When the amount of rotors is increased to ten rotors, it is observed that the achievable accelerations decrease due to the limited amount of possible rotor configurations, which results from the required distance between rotors and the airflow from other rotors. Due to this, the ten rotor solutions are inferior to the solutions with less rotors and are thus disregarded.

This means that the eight rotor optimizations result in the best UAV design for this application. From the two solutions, case 8.2 is chosen, because the ability to fly more efficiently is favoured over the higher maximum translational acceleration.

7.8 Conclusion

In this chapter, an omnidirectional UAV that is able of physical contact with humans has been designed from scratch, by optimizing the rotor configuration in a confined area. The optimization is based on the kinematic and dynamic manoeuvrability. Before doing this optimization, the framework from chapter 5 has been used to determine which design considerations can be applied to the optimization of the UAV. This resulted in bi-directional symmetric rotor pairs. This optimization has been done for a number of different objective functions to optimize either the kinematic performance, dynamic performance, decouple translational and rotational dynamic performance and dynamic performance with constrained thrust efficiency.

Although the physical interpretation is questionable, it can be concluded that the dynamic manoeuvrability provides a good measure for optimization of omnidirectional UAVs with bi-directional rotors. By uncoupling the translation and rotations, the design will be optimized for the translational manoeuvrability, although the total manoeuvrability will be reduced. By constraining the minimum thrust efficiency, a trade-off between efficient flight and high accelerations is achieved. It has been concluded that for the application of human interacting, the best solution is a UAV with eight rotors, that is optimized based on the decoupled dynamic manoeuvrability with a constrained minimum thrust efficiency.

Chapter 8

Conclusion and Recommendations

In this chapter, the conclusion of the report is given in section 8.1 and the recommendations for further work have been given in section 8.2.

8.1 Conclusion

In this report, a general framework for comparing fully actuated UAVs has been made. This framework serves as a starting point for optimizing the rotor configuration of a UAV for any application. To demonstrate the usefulness of this framework, it has been used for the optimization of a UAV for two applications that require full actuation.

First of all, a large number of available concepts have been described. In this description, the main characteristics of the UAVs are briefly discussed and the rotor configuration is shown, along with the mapping matrix that can be used to determine the static performance of the UAV.

It has been shown that a rather accurate quantitative comparison between concepts can be made, without extended knowledge of its design: the kinematic comparison. This comparison only requires the rotor positions and orientation. By scaling the position of the rotors to fit inside a unit sphere and having a uniform maximum rotor thrust, a very general comparison of the possible exerted wrench of a UAV can be made. However, the wrench does not provide an accurate measure of the flying ability of the UAV, because a UAV needs to accelerate in order to fly. For this reason the dynamics of the UAVs are considered.

It has been shown that the main difficulty in determining the dynamic performance of a UAV, is determining the mass and inertia, because this depends on the entire UAV design. It is very difficult to make a general dynamic comparison between different concepts, independents of the scale, because this requires a complete redesign of the concepts to adjust the mass to this new scale. Instead, the design that presents the concept that is specified in the reference has been used.

By comparing the dynamic performance to the static performance of the concepts relative to the others, it has been shown that the extra effort of determining the mass and inertia of a concept is a necessary step in comparing UAV performance, because inconsistencies are observed in the results for the kinematic and dynamic performance. Furthermore, it has been shown that design considerations like the rotor choice greatly influence the dynamic performance of the UAV.

To prove the usability of the framework, it has been applied to design UAVs for two applications. The first application is a crop spraying UAV. This application requires horizontal actuation, because it allows very limited roll due to the large width of the UAV, the fact that it flies close to the surface and the required spraying distribution. In order to be able to reject side-wind disturbances, the UAV needs to be able to actuate this (lateral) direction.

The framework has been used to find the best suited concept for this application. Mainly due to the high required width, the V-shape concept, which was developed especially for this application, was chosen. This concept was then optimized to be able to fly efficiently, withstand side-wind by lateral actuation and fulfill all requirements, using MATLAB's *fmincon* optimization function. A number of designs have been proposed, with different trade-off between lateral acceleration for side-wind disturbance and vertical acceleration for the ability to hover with minimal thrust requirement. To adjust the lateral actuation to the wind speed, a design with manually tiltable rotors has been propesed.

The second application that has been considered, is a UAV used for human interaction. This UAV needs to be omnidirectional in order to react to human interference. This application is completely different from the first application and, as such, it proofs that the framework can be applied for all wide range of applications. Instead of choosing a concept from the framework, a completely new design has been made, based on the characteristics of the best performing UAVs from the framework. The position and orientation of a number symmetric rotor pairs placed in a sphere have been optimized using *fmincon*. In order to maximize the omnidirectional acceleration, the manoeuvrability, a scalar measure of the volume spanned by the maximum accelerations of the UAV, has been optimized. A number of designs has been made based on different variations of the manoeuvrability, as well as based on a minimum required thrust efficiency, for six, eight and ten rotor designs.

The optimization showed that the kinematic and dynamic manoeuvrability provide a good method for optimizing a UAV for omnidirectional flight. The decoupling of translation and rotation yielded a better translational performance. However, the total manoeuvrability is reduced. When the amount of rotors increases, the kinematic manoeuvrability increases. For the dynamic performance, an inconsistency between the maximum accelerations and the dynamic manoeuvrability is observed, which might indicate that the dynamic manoeuvrability does not give a good insight in the difference in dynamic performance between a different number of rotors. When the amount of rotors increases further from eight to ten, it can be seen that fitting all the rotors in the limited sized sphere without airflow interference between rotors is difficult, resulting in a less than optimal solution.

8.2 Recommendations

In this section the recommendations for further work are given. These recommendations have been itemized per chapter.

Preliminary Calculations (Chapter 2)

For the preliminary calculations, the recommendations are:

- **Manoeuvrability**: The application of the dynamic manoeuvrability can be increased, if it is applicable to one directional rotors. Investigating the possibility of this is recommended for further work. Furthermore the physical interpretation of the manoeuvrability and the observed inconsistency for different amounts of rotors needs to be investigated further.

Criteria for Comparing Fully Actuated UAVs (Chapter 4)

For the comparison criteria, the recommendations are:

- **Flying efficiency**: Two measures for the flying efficiency have been proposed in this chapter: thrust efficiency and flying thrust. However, both criteria have limitations for describing the flying efficiency. For that reason, another measure could be proposed, that properly describes the flying efficiency of the concepts.

Comparison of Fully Actuated UAVs (Chapter 5)

For the concept comparison, the recommendations are:

- **Rotational Inertia**: The rotational dynamic performance of the UAVs is lacking for many concepts, because the articles did not provide the rotational inertia. As a result, the dynamic comparison is incomplete, which reduces the usability of the framework if rotational acceleration is required. In order to improve the frame, it is important to complete these missing inertia, either by a different reference, or by defining a better approximation of the inertia than the approximation based on the rotors as point masses.
- **Concepts**: Although the framework already consists of quite a few fully actuated concepts, there may still be concepts that have not been represented in the framework. Furthermore future work will yield new concepts. That is why more concepts could be added to the framework to keep it relevant.

Application of Fully Actuated UAVs: Crop Spraying (Chapter 6)

For the crop spraying UAV, the recommendations are:

- **Spraying distribution**: Although an estimation of the spraying distribution is made, it should be investigated much more before a good estimation of the actual spraying distribution can be done. If a proper description of the development of the spray from the rotor is presented, guaranteeing good spraying distribution can be taken into account in the optimization.
- **Wind disturbance**: An estimation of the wind speed that can be rejected by the UAV is given. However, this estimate is very imprecise. To make a well considered decision which design to use, it is important to have a better estimate of the wind speed at which the UAV can operate.
- **Scaling effects**: There are a number of challenges that occur when UAVs are scaled up to this very large size, that have not been considered in the design. Examples are: nonlinear propeller performance, ground effects and frame stiffness. These scaling effects should be considered if the design is worked out in detail.
- **Prototype**: In order to validate the performance of this UAV, a prototype should be made. However, this requires a lot more work to optimize the frame, power source, etcetera and also a control algorithm needs to be designed.

Application of Fully Actuated UAVs: Human Interaction (Chapter 7)

For the human interacting UAV, the recommendations are:

- **Rotor choice**: The rotor choice of this concept has been estimated, based on the rotors from the concepts from the framework. To fully optimize the performance of this UAV, the rotor choice could be optimized further. For the chosen rotor the aerodynamic interference distance should be determined as well.
- **Optimization limitations** As mentioned, the MATLAB *fmincon* solver was unable to handle the large amount of parameter in the dynamic manoeuvrability. When the total dynamic manoeuvrability of a UAV with more than six rotors needs to be optimized, it is recommended to either use a different optimization software or find another way to describe the determinant of the acceleration matrix that requires less computing power.
- **Inertia**: In this optimization, a simplified inertia is used, where only the mass of the rotors is considered by point masses. Although it has been proven that doubling the rotor mass does not influence the optimal design, it is expected that adding a frame, battery, etcetera does influence the optimal result slightly. By taking this into account, a better optimal will be found.
- **Prototype**: Just like the crop spraying UAV, the design should be validated with a prototype. Again, there are many considerations that should be done before an actual prototype can be made.

Bibliography

[1] Kenzo Nonami, Farid Kendoul, Satoshi Suzuki, Wei Wang, and Daisuke Nakazawa. Autonomous flying robots. pages 219–250, 01 2010.

[2] D. Mellinger, Q. Lindsey, M. Shomin, and V. Kumar. Design, modeling, estimation and control for aerial grasping and manipulation. In *2011 IEEE/RSJ International Conference on Intelligent Robots and Systems*, pages 2668–2673, Sept 2011.

[3] F. Augugliaro, A. Mirjan, F. Gramazio, M. Kohler, and R. D'Andrea. Building tensile structures with flying machines. In *2013 IEEE/RSJ International Conference on Intelligent Robots and Systems*, pages 3487–3492, Nov 2013.

[4] K. Alexis, C. Huerzeler, and R. Siegwart. Hybrid modeling and control of a coaxial unmanned rotorcraft interacting with its environment through contact. In *2013 IEEE International Conference on Robotics and Automation*, pages 5417–5424, May 2013.

[5] A. Albers, S. Trautmann, T. Howard, Trong Anh Nguyen, M. Frietsch, and C. Sauter. Semi-autonomous flying robot for physical interaction with environment. In *2010 IEEE Conference on Robotics, Automation and Mechatronics*, pages 441–446, June 2010.

[6] S. Park, J. Lee, J. Ahn, M. Kim, J. Her, G. H. Yang, and D. Lee. Odar: Aerial manipulation platform enabling omni-directional wrench generation. *IEEE/ASME Transactions on Mechatronics*, pages 1–1, 2018.

[7] Florentin von Frankenberg and Scott Nokleby. Disturbance rejection in multi-rotor unmanned aerial vehicles using a novel rotor geometry. In *Proceedings of the 4^th International Conference of Control, Dynamic Systems, and Robotics*, pages 130–1–130–10, 08 2017.

[8] Emissary drones. What is pitch, roll and yaw ? `https://emissarydrones.com/what-is-roll-pitch-and-yaw`, September 2017. Accessed: 4-11-2018.

[9] G. Jiang, R. Voyles, K. Sebesta, and H. Greiner. Estimation and optimization of fully-actuated multirotor platform with nonparallel actuation mechanism. In *2017 IEEE/RSJ International Conference on Intelligent Robots and Systems (IROS)*, pages 6843–6848, Sept 2017.

[10] M. Tognon and A. Franchi. Omnidirectional aerial vehicles with unidirectional thrusters: Theory, optimal design, and control. *IEEE Robotics and Automation Letters*, 3(3):2277–2282, July 2018.

[11] T. Yoshikawa. Manipulability of robotic mechanisms. 4:3–9, 06 1985.

[12] T. Yoshikawa. Dynamic manipulability of robot manipulators. In *Proceedings. 1985 IEEE International Conference on Robotics and Automation*, volume 2, pages 1033–1038, March 1985.

[13] K. Kiso, T. Ibuki, M. Yasuda, and M. Sampei. Structural optimization of hexrotors based on dynamic manipulability and the maximum translational acceleration. In *2015 IEEE Conference on Control Applications (CCA)*, pages 774–779, Sept 2015.

[14] Nicolas Staub, Davide Bicego, Quentin Sablé, Victor Arellano-Quintana, Subodh Mishra, and Antonio Franchi. Towards a flying assistant paradigm: the othex. In *2018 IEEE Int. Conf. on Robotics and Automation*, Brisbane, Australia, May 2018.

[15] Yuichi Tadokoro, Tatsuya Ibuki, and Mitsuji Sampei. Maneuverability analysis of a fully-actuated hexrotor uav considering tilt angles and arrangement of rotors. *IFAC-PapersOnLine*, 50(1):8981 – 8986, 2017. 20th IFAC World Congress.

[16] John R. Silvester. Determinants of block matrices. *The Mathematical Gazette*, 84(501):460467, 2000.

[17] S. Salazar, H. Romero, R. Lozano, and P. Castillo. Modeling and real-time stabilization of an aircraft having eight rotors. *Journal of Intelligent and Robotic Systems*, 54(1):455–470, Mar 2009.

[18] R. Voyles and G. Jiang. Hexrotor uav platform enabling dextrous interaction with structures; preliminary work. In *2012 IEEE International Symposium on Safety, Security, and Rescue Robotics (SSRR)*, pages 1–7, Nov 2012.

[19] Sujit Rajappa, Markus Ryll, Heinrich H. Bulthoff, and Antonio Franchi. Modeling, control and design optimization for a fully-actuated hexarotor aerial vehicle with tilted propellers. *Proc. - IEEE Int. Conf. Robot. Autom.*, 2015-June(June):4006–4013, 2015.

[20] R. Rashad, P. Kuipers, J. Engelen, and S. Stramigioli. Design, modeling, and geometric control on se(3) of a fully-actuated hexarotor for aerial interaction. *ArXiv e-prints*, sep 2017.

[21] Y. Lei, Y. Ji, C. Wang, Y. Bai, and Z. Xu. Aerodynamic design on the non-planar rotor system of a multi-rotor flying robot (mfr). In *2017 IEEE 3rd International Symposium in Robotics and Manufacturing Automation (ROMA)*, pages 1–5, Sept 2017.

[22] D. Toratani. Research and development of double tetrahedron hexa-rotorcraft (dot-hr). In *ICAS2012, 28 TH INTERNATIONAL CONGRESS OF THE AERONAUTICAL SCIENCES*, pages 1–8, 2012.

[23] Alexandros Nikou, Georgios C. Gavridis, and Kostas J. Kyriakopoulos. Mechanical Design, Modelling and Control of a Novel Aerial Manipulator. *IEEE Int. Conf. Robot. Autom.*, pages 4698–4703, 2015.

[24] Antonio Franchi at LAAS-CNRS RIS team. Omnidirectional aerial vehicles with unidirectional thrusters. `https://www.youtube.com/watch?v=PHZz_hTrN_w`,0:45. Accessed: 26-10-2018.

[25] Dario Brescianini and Raffaello D'Andrea. Design, modeling and control of an omni-directional aerial vehicle. In *2016 IEEE Int. Conf. Robot. Autom.*, pages 3261–3266. IEEE, may 2016.

[26] Sangyul Park, Jongbeom Her, Juhyeok Kim, and Dongjun Lee. Design, modeling and control of omni-directional aerial robot. In *2016 IEEE/RSJ Int. Conf. Intell. Robot. Syst.*, pages 1570–1575. IEEE, oct 2016.

[27] Daniel R. McArthur, Arindam B. Chowdhury, and David J. Cappelleri. Design of the I-BoomCopter UAV for environmental interaction. *Proc. - IEEE Int. Conf. Robot. Autom.*, pages 5209–5214, 2017.

[28] M. Ryll, H. H. Blthoff, and P. R. Giordano. Modeling and control of a quadrotor uav with tilting propellers. In *2012 IEEE International Conference on Robotics and Automation*, pages 4606–4613, May 2012.

[29] Sherif Badr, Omar Mehrez, and A. E. Kabeel. A novel modification for a quadrotor design. In *2016 Int. Conf. Unmanned Aircr. Syst. ICUAS 2016*, pages 702–710. IEEE, jun 2016.

[30] Pau Segui-Gasco, Yazan Al-Rihani, Hyo-Sang Shin, and Al Savvaris. A Novel Actuation Concept for a Multi Rotor UAV. *J. Intell. Robot. Syst.*, 74(1-2):173–191, apr 2014.

[31] M. Ryll, H. H. Blthoff, and P. R. Giordano. A novel overactuated quadrotor unmanned aerial vehicle: Modeling, control, and experimental validation. *IEEE Transactions on Control Systems Technology*, 23(2):540–556, March 2015.

[32] Marcin Odelga, Paolo Stegagno, and Heinrich H. Bulthoff. A fully actuated quadrotor UAV with a propeller tilting mechanism: Modeling and control. In *IEEE/ASME Int. Conf. Adv. Intell. Mechatronics, AIM*, volume 2016-Septe, pages 306–311. IEEE, jul 2016.

[33] ETH Zurich. Voliro, an omnidirectional hexacopter, focus project final report. `https://spectrum.ieee.org/automaton/robotics/drones/eth-zurich-omnicopter-plays-fetch`, 2017. Accessed: 28-10-2018.

[34] Mina Kamel, Sebastian Verling, Omar Elkhatib, Christian Sprecher, Paula Wulkop, Zachary Taylor, Roland Siegwart, and Igor Gilitschenski. Voliro: An omnidirectional hexacopter with tiltable rotors. *CoRR*, abs/1801.04581, 2018.

[35] Markus Ryll, Davide Bicego, and Antonio Franchi. Modeling and control of FAST-Hex: A fully-actuated by synchronized-tilting hexarotor. In *2016 IEEE/RSJ Int. Conf. Intell. Robot. Syst.*, number 644271, pages 1689–1694. IEEE, oct 2016.

[36] Yangbo Long, Lu Wang, and David J. Cappelleri. Modeling and global trajectory tracking control for an over-actuated mav. *Advanced Robotics*, 28(3):145–155, 2014.

[37] Florentin von Frankenberg and Scott Nokleby. Disturbance rejection in multi-rotor unmanned aerial vehicles using a novel rotor geometry. 08 2017.

[38] Fpv models. Turnigy graphene professional 10000mah 4s 15c lipo pack w/ xt90. https://hobbyking.com/en_us/turnigy-graphene-professional-10000mah-4s-15c-lipo-pack-w-xt90.html. Accessed: 9-11-2018.

[39] A. Oosedo, S. Abiko, S. Narasaki, A. Kuno, A. Konno, and M. Uchiyama. Flight control systems of a quad tilt rotor unmanned aerial vehicle for a large attitude change. In *2015 IEEE International Conference on Robotics and Automation (ICRA)*, pages 2326–2331, May 2015.

[40] Drone4agro. http://drone4agro.com/. Accessed: 20-7-2018.

[41] Shutterbug. Crop duster flying low over a palouse wheat field. https://www.shutterbug.com/content/crop-duster-0. Accessed: 28-10-2018.

[42] Agricultural Retailers Association. House to debate npdes bill. https://www.aradc.org/blogs/brian-reuwee/2016/05/24/house-to-debate-npdes-bill. Accessed: 28-10-2018.

[43] Colorado Department of Agriculture. Chemigation. https://www.colorado.gov/pacific/agconservation/chemigation. Accessed: 28-10-2018.

[44] J.U.Rao. Andhra pradesh and telangana suffer from high pesticide residues. https://www.deccanchronicle.com/nation/current-affairs/181016/andhra-pradesh-and-telangana-suffer-from-high-pesticide-residues.html. Accessed: 28-10-2018.

[45] Yamaha. Precision agriculture. https://www.yamahamotorsports.com/motorsports/pages/precision-agriculture-rmax. Accessed: 28-10-2018.

[46] JW Miller. Report on the development and operation of an uav for an experiment on unmanned application of pesticides. *AFRL, USAF*, 2005.

[47] Herbst A Langenakens J. He X K, Bonds J. Recent development of unmanned aerial vehicle for plant protection in east asia. *Int J Agric & Biol Eng*, 10(3):1830, 2017.

[48] Joyance. 15l precision agriculture spraying drone(jt15l-608). http://www.wecanie.com/html/sprayer/products/15L_precision_agriculture_pesticide_spra.html. Accessed: 28-10-2018.

[49] Bejing TT aviation technology. M8a pro. https://www.ttaviation.org/pro/m8a-pro. Accessed: 28-10-2018.

[50] Spraying drone. Efficiently spray your fields and reduce environmental harm. http://sprayingdrone.com/models.html. Accessed: 28-10-2018.

[51] Y. Lan W. Wu B. K. Fritz Y. Huang, W. C. Hoffmann. Development of a spray system for an unmanned aerial vehicle platform. *American Society of Agricultural and Biological Engineers*, 25(6):803809, 2009.

[52] M. Mann. A canadian startup wants to replace drone batteries with a gas engine. https://motherboard.vice.com/en_us/article/wnxjaq/a-canadian-startup-wants-to-replace-drone-batteries-with-a-gas-engine-pegasus, May 2016. Accessed: 30-10-2018.

[53] Thangaraj Kandasamy, S Rakheja, and A K W Ahmed. An analysis of baffles designs for limiting fluid slosh in partly filled tank trucks. 4, 01 2010.

[54] Wang Weiliang. Shaking-preventive liquid storage device of unmanned plant protection machine, 08 2014.

[55] Q. Zhou, P.C.H. Miller, P.J. Walklate, and N.H. Thomas. "prediction of spray angle from flat fan nozzles". *"Journal of Agricultural Engineering Research"*, 64(2):139 – 148, 1996.

[56] Matworks. fmincon. https://nl.mathworks.com/help/optim/ug/fmincon.html. Accessed: 28-10-2018.

[57] Ben Franzluebbers. Drag coefficients of inclined hollow cylinders: Rans versus les. *Worchester Polytechnic Institute*, April 2012.

[58] Sujit Rajappa, Heinrich Blthoff, and Paolo Stegagno. Design and implementation of a novel architecture for physical human-uav interaction. *The International Journal of Robotics Research*, 36(5-7):800–819, 2017.

[59] F. Augugliaro and R. D'Andrea. Admittance control for physical human-quadrocopter interaction. In *2013 European Control Conference (ECC)*, pages 1805–1810, July 2013.

[60] S. Rajappa, H. H. Blthoff, M. Odelga, and P. Stegagno. A control architecture for physical human-uav interaction with a fully actuated hexarotor. In *2017 IEEE/RSJ International Conference on Intelligent Robots and Systems (IROS)*, pages 4618–4625, Sept 2017.

[61] KDE direct. Kde2304xf-2350. https://www.kdedirect.com/collections/uas-multi-rotor-brushless-motors/products/kde2304xf-2350. Accessed: 28-10-2018.

[62] Banggood. 2 pairs gemfan flash 6042 6.0x4.2 pc 2-blade propeller 5mm. https://www.banggood.com/2-Pairs-Gemfan-Flash-6042-6_0x4_2-PC-2-blade-Propeller-5mm-Mounting-hole-for-RC-FPV-Racing-Drone-p-1246562.html?rmmds=buy&ID=3868&cur_warehouse=CN. Accessed: 28-10-2018.

[63] R. Naldi, F. Forte, A. Serrani, and L. Marconi. Modeling and control of a class of modular aerial robots combining under actuated and fully actuated behavior. *IEEE Transactions on Control Systems Technology*, 23(5):1869–1885, Sept 2015.

[64] Microcopter. Mk3638 mk3538. http://wiki.mikrokopter.de/MK3538. Accessed: 9-11-2018.

[65] Hobbyking. Carbon fiber propeller 12x6 black. https://hobbyking.com/en_us/carbon-fiber-propeller-12x6-black-cw-ccw-2pcs.html?___store=en_us. Accessed: 9-11-2018.

[66] T-Motor. Mn3508 kv700. http://store-en.tmotor.com/goods.php?id=356. Accessed: 9-11-2018.

[67] Minicopters. 10x4.5 inch carbon propellerset. https://www.minicopters.nl/product/1386599/10x4-5-inch-carbon-propellerset. Accessed: 9-11-2018.

[68] Kamami. 4108-480kv turnigy multistar 22 pole brushless multi-rotor motor with extra long leads. https://kamami.pl/niedodane-/230751-4108-480kv-turnigy-multistar.html. Accessed: 9-11-2018.

[69] RC timer. Rctimer 15x5.5" carbon fiber cw ccw propellers. http://rctimer.com/?product-706.html. Accessed: 9-11-2018.

[70] Hobbyking. Ntm prop drive 28-36 1400kv / 560w. https://hobbyking.com/nl_nl/ntm-prop-drive-28-36-1400kv-560w.html?___store=nl_nl. Accessed: 9-11-2018.

[71] Hobbyking. 8 "propeller voor rubber powered models. https://hobbyking.com/nl_nl/8-2-blade-propeller-rubber-band-power-5pcs-bag.html?___store=nl_nl. Accessed: 9-11-2018.

[72] Hobbyking. Turnigy d2836 / 8 1100kv brushless motor outrunner. https://hobbyking.com/nl_nl/turnigy-d2836-8-1100kv-brushless-outrunner-motor.html?___store=nl_nl. Accessed: 9-11-2018.

[73] Drone Matters. Hqprop 1138 carbon composite propeller. https://www.dronematters.com/power-system/propellers/11-propellers/hqprop-1138-carbon-composite-propeller-black-1-ccw.html. Accessed: 9-11-2018.

[74] Quadrocopter. Mk3638 rc multi-rotor heavy lift motor. https://www.quadrocopter.com/MK3638-RC-Multi-Rotor-Heavy-Lift-Motor_p_360.html. Accessed: 9-11-2018.

[75] KDE direct. Kde2315xf-885. https://www.kdedirect.com/products/kde2315xf-885. Accessed: 9-11-2018.

[76] Master Airscrew. 3-blade - 10x7 propeller. https://www.masterairscrew.com/products/3-blade-10x7-propeller. Accessed: 9-11-2018.

[77] ServoDatabase. Hextronik mg14 - metal gear servo. https://servodatabase.com/servo/hextronik/mg14. Accessed: 9-11-2018.

[78] Hobbyking. Henge md260 260 degrees metal digital servo for fpv pan tilt control. https://www.fpvmodel.com/henge-md260-260-degrees-metal-digital-servo.html. Accessed: 9-11-2018.

[79] Servo city. Hs-7940th servo. https://www.servocity.com/hs-7940th-servo. Accessed: 9-11-2018.

[80] Servo city. Hs-5055mg servo. https://www.servocity.com/hs-5055mg-servo. Accessed: 9-11-2018.

[81] O. Gur and A. Rosen. Optimizing electric propulsion systems for unmanned aerial vehicles. *JOURNAL OF AIRCRAFT*, 46(4):1340–1352, July-August 2009.

Appendix A

Hybrid Fully Actuated UAVs

There are many different hybrid drone concepts available. The addition of fixed wings to a multirotor has the advantage that the fixed wings produce lift with no power consumption, only some added weight, thus increasing flight efficiency. Although these concepts might be very advantageous for certain applications, they are not taken into account in this comparison. The reason for this absence is that these concepts are so fundamentally different from the multirotor concepts, that they cannot compared to them based on the given criteria. One hybrid concept, however, is mentioned here. This concept uses variable tilt fixed wings to change direction similar to the variable tilt concepts use variable tilt rotors.

A.1 Vaned Ducted Fan Multirotor

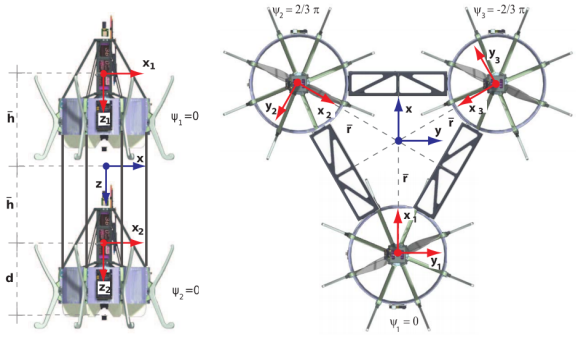

Figure A.1: Vaned ducted fan multirotor

This concept (figure A.1) is designed by Naldi et al. [63], who increased the amount of DoFs of a single rotor from one to four by placing fixed wing control vanes under the rotor. These vanes act like airfoils, producing a lift force in the direction lateral to the rotor thrust direction. These vanes can be used to eliminate the drag torque from the rotor, as well as to produce torque. The rotor is placed inside a duct to direct all thrust airflow toward the vanes. A single rotor can thus produce vertical force, pitch, roll and yaw. By connecting multiple vaned rotors the torque created from the vaned rotors can be transformed into horizontal actuation. A fully actuated drone can be made with very limited amount of rotors: two vaned rotors placed above each other or three rotors placed next to each other, which is much less then required for unvaned rotors. This concept is comparable to variable tilt rotors where instead of the rotor, the vanes are tilted. The vanes do require a lot more actuation than a variable tilt rotors; the eight control vanes are independently actuated, increasing the amount of actuators per rotor to nine (including the rotor itself). Since the vanes have a limited allowed angle, the possible horizontal acceleration is limited. Due to the low translational actuation, very high design complexity and aerodynamic complexity of the vanes this concept is not considered in the further comparison.

Appendix B

Rotors and Tilt Actuators Used in Concepts

In table B.1, an overview of the motor and propeller type and mass is shown. These specifics are used to determine the rotor thrust to weight ratio.

	Motor		Propeller		
Concept	Type	Mass [g]	Diameter [in]	Mass [g]	Total mass [g]
Quad4Hor	-	-	-	-	-
HexC	-	-	-	-	-
HexCD	Microcopter MK3638[64]	125	12	19[65]	144
CoHexC	-	-	-	-	-
HexDTet	-	-	-	-	-
HeptF	-	-	-	-	120
HeptW	-	-	11	-	-
OctCu	RTF2208[25]	45.5	-	10.5[25]	56.0
OctB	T-Motor MN3508-KV700[66]	104	10	12(2×)[67]	128
Tri1Hor vert.	Turnigy 4108-480 Kv[68]	111	15	14[69]	125
Tri1Hor hor.	NTM Prop Drive 28-36 1400 Kv[70]	86	8	5[71]	91
QuadvC	Turnigy D2836/8 1100kv[72]	70	11	19[73]	81
QuadvD	Turnigy D2836/8 1100kv[72]	70	11	19[73]	81
QuadvCD	MK3638[74]	125	11	45	170
QuadvCDc	-	-	-	-	-
HexvC	KDE2315XF-885[75]	75	9	12	87
HexvCc	-	-	-	-	150
PentvD coaxial	BP-U2212/10	47	10	28[76]	75
PentvD variable	AEO 55 mm EDF	58	-	-	58

Table B.1: Rotors used for the concepts

Appendix C

Tilt Actuators for Variable Tilt Concepts

In table C.1, the tilt actuators of the variable tilt rotors are given. Note that in the dynamic comparison of the variable tilt concepts, the maximum rotation of the tilt actuators is generalized at $360°$. This table shows that the mass difference between the servo motor, which have limited rotation, and brushless motor, which have unlimited rotation, is negligible, which validates the assumption of generalizing the maximum rotation.

Concept	Actuator type	Mass [g]	Max rotation [°]
Tri1Hor	Hextronik MG14[77]	14	120
QuadvC	Hnege MD260 [78]	12	260
QuadvD	Hnege MD260 [78]	12	260
QuadvCD	HS-7940TH[79]	66	120
QuadvCDc	-	-	-
HexvC	Faulhaber 1226...B	13	720[34]
PentvD	HS-5055MG[80]	10	120

Table C.1: Tilt actuators used for the variable tilt rotors

Appendix D

Motor Comparison

The thrust-to-weight ratio of rotors depends on the type of propeller and the motor type. For this comparison the motor type is limited to brushless motors. For the propeller type there are a number of considerations: the amount of blades, the blade geometry (the diameter, the blade canting etcetera). The optimal blade geometry depends on the motor size. The theoretical highest thrust can be achieved by large blades. However, the propeller size is limited by the available motor torque to rotate it. Brushless motor manufacturers often give a proposal of the maximum possible propeller size.

The thrust-to-weight ratio depends on the motor choice. There has been done a lot of research into the performance of brushless motors depending on the mass. Gur and Rosen [81] compared the power output to the mass for different motors. The results are shown in figure D.1a.

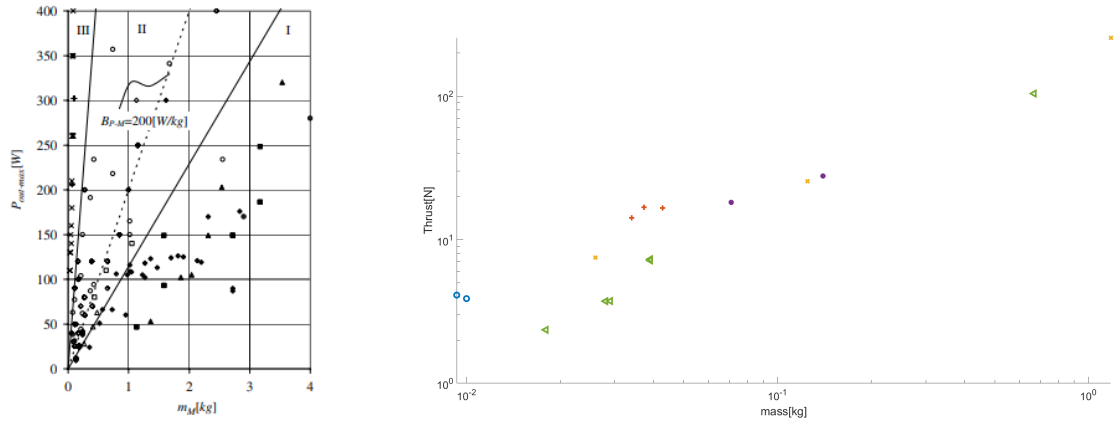

(a) Mass versus power for brushless motor

(b) Mass versus thrust for rotor

Figure D.1: Motor and rotor comparison

In this figure, the results are ordered by manufacturer with different markers. It can be seen that for some manufacturers, the power-to-mass ratio (B_{P-M}) remains equal at different scale. However, for generally B_{P-M} varies in the range of:

$$110 \text{ W/kg} < B_{P-M} < 800 \text{ W/kg} \tag{D.1}$$

According to Gur, the differences in B_{P-M} between manufacturers, or between different series of the same manufacturer, probably emerge from different technologies, design concepts, or manufacturing methods. To see if this difference is also present for the thrust to mass ratio, a number of thrust tests from motor manufacturers has been compared. The results are shown in figure D.1b, where the thrust is plotted against the mass. The results have again been ordered by different manufacturers with a different marker. The results resemble the results in figure D.1a, where there is resemblance in thrust to mass ratio for some manufacturers, while for the most there is no clear relation. This appears to mainly result from the difference in brushless motor quality.

Appendix E

Inertia Approximation

To validate whether the inertia of the UAV can be approximated with sufficient accuracy, the approximated inertia is compared to the measured inertia for a concept for which the inertia is given: the hexarotor canted/dihedral. According to Rajappa [19], the inertia of this UAV is:

$$I = \begin{bmatrix} 0.12 & 0 & 0 \\ 0 & 0.11 & 0 \\ 0 & 0 & 0.19 \end{bmatrix} \tag{E.1}$$

The rotational inertia of the rotors given as mass points, defined is chapter 2.4, is given by:

$$I = \begin{bmatrix} 0.07 & 0 & 0 \\ 0 & 0.07 & 0 \\ 0 & 0 & 0.14 \end{bmatrix} \tag{E.2}$$

The inertia from the reference is quite a bit higher than the approximation, which makes sense since the frame and battery actually add quite a lot of inertia. To see how this difference in inertia influences the results, the rotational acceleration with the measured inertia tensor is compared to the rotational acceleration with the estimated inertia in table E.1.

	Maximum Acceleration		
	x-rotation $\left[\frac{1}{s^2}\right]$	y-rotation $\left[\frac{1}{s^2}\right]$	z-rotation $\left[\frac{1}{s^2}\right]$
Actual inertia	175.0	227.8	141.5
Estimated inertia	313.8	362.4	196.5

Table E.1: Rotational accelerations based on measured and estimated inertia

It is clear that the difference in inertia yields a large difference in the results. For that reason an effort has been done to increase the accuracy of the approximation. First of all the Inertia of the Frame will be added. The frame has been simplified to 6 cylindrical bars, that connect the rotors to the CoM. The inertia of a these bars(I_t), rotated around the end of the bar is given by:

$$I_t = \frac{1}{3}\frac{\pi}{4}(D1^2 - D0^2)\rho l^2 \tag{E.3}$$

$$\tag{E.4}$$

where l is the length of the tube, D_1 and D_0 the outer and inner tube diameter respectively and ρ the density of the material. Here l = 0.4 m, D_1 and D_0 are estimated based on drawings from the articles and drones with similar frames to be 30 mm and 29 mm respectively. The density of the aluminium bar is 2800 kg/m^3.

In order to obtain the inertia of the tube in the $\mathcal{F}_{\mathcal{W}}$, it has to be rotated around the z-axis using the rotation matrix:

$$I_b^* = R_z I_b R_z^T \tag{E.5}$$

$$R_z = \begin{bmatrix} cos(\psi) & -\sin(\psi) & 0 \\ \sin(\psi) & \cos(\psi) & 0 \\ 0 & 0 & 1 \end{bmatrix} \tag{E.6}$$

Summing the rotated inertia's of the 6 tubes yields the total frame inertia I_F :

$$I_F = 10^{-3} \begin{bmatrix} 8.3 & 0 & 0 \\ 0 & 8.3 & 0 \\ 0 & 0 & 16.6 \end{bmatrix} \tag{E.7}$$

As shown the inertia of the frame is not very high compared to the inertia from the rotors. Another influence on the inertia to be considered is the battery. The battery is assumed as a solid cuboid placed at the CoG. This yields the inertia:

$$I_x = \frac{1}{12} m(w^2 + h^2) \tag{E.8}$$

$$I_y = \frac{1}{12} m(l^2 + h^2) \tag{E.9}$$

$$I_z = \frac{1}{12} m(w^2 + l^2) \tag{E.10}$$

where m is the mass of the battery and l, w and h the length, width and height of the battery. As the battery used is not specified in the article, the size and mass of the battery is overestimated at a mass of 1 kg and dimensions 150$\times$150$\times$50 mm, which is a large sized battery for a hexarotor. This yields the inertia of the battery I_B:

$$I_B = 10^{-3} \begin{bmatrix} 2.1 & 0 & 0 \\ 0 & 2.1 & 0 \\ 0 & 0 & 3.7 \end{bmatrix} \tag{E.11}$$

When the frame and battery are included, the inertia becomes:

$$I = \begin{bmatrix} 0.08 & 0 & 0 \\ 0 & 0.08 & 0 \\ 0 & 0 & 0.15 \end{bmatrix} \tag{E.12}$$

This inertia is still much lower than the measured inertia. It can be concluded that the approximation does not sufficiently describe the inertia of the UAV, even if the frame and battery are included.

Appendix F

Visualization of Rotated Human Interacting UAVs

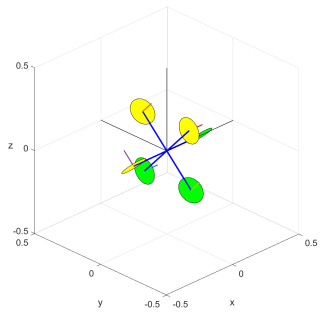

(a) Case 6.1/6.4

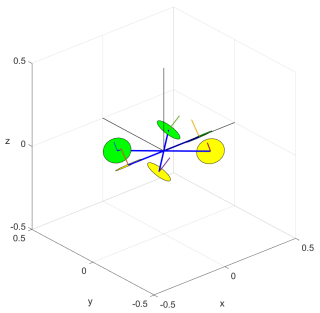

(b) Case 6.5

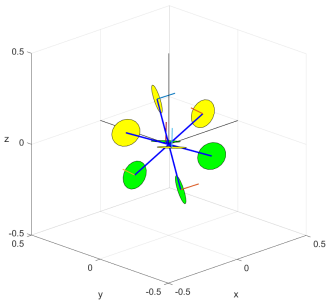

(c) Case 8.1

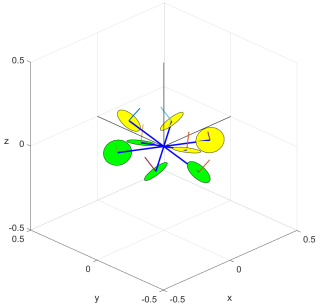

(d) Case 8.2

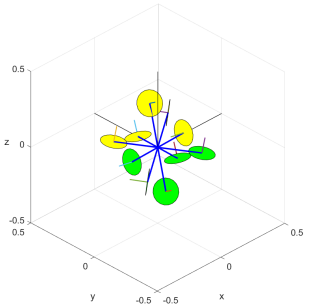

(e) Case 10.1

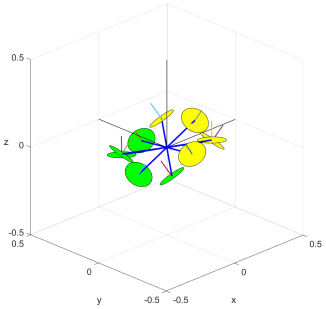

(f) Case 10.2

Figure F.1: Rotated concepts with the maximum force in vertical direction and the maximum horizontal force in x-direction

Appendix G

Additional Results for Human Interacting UAVs

G.1 Brute Force Method Volumes of Translational and Rotational Accelerations

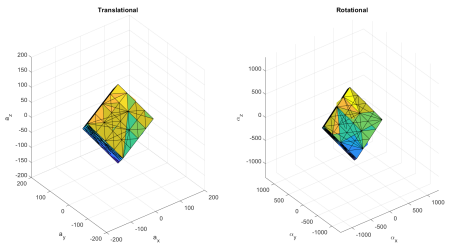

(a) Case 6.1/6.4

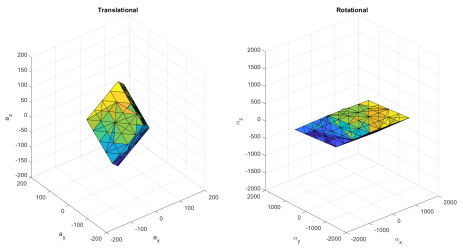

(b) Case 6.2/6.3*

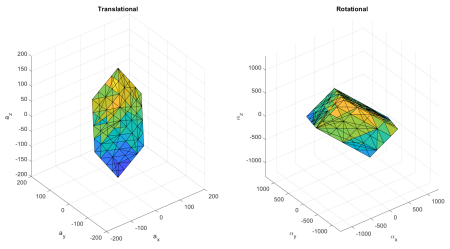

(c) Case 6.5

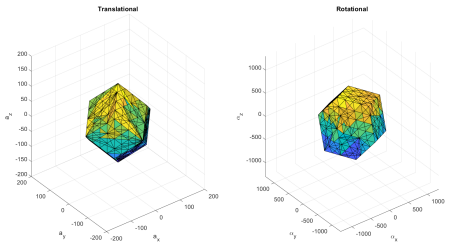

(d) Case 8.1

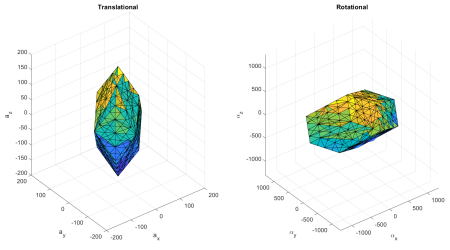

(e) Case 8.2

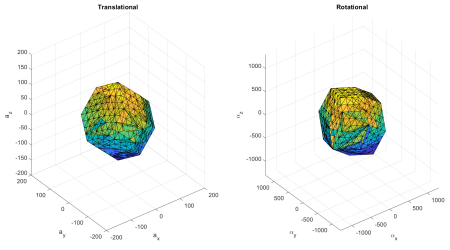

(f) Case 10.1

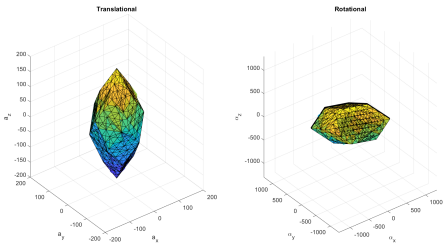

(g) Case 10.2

Figure G.1: Brute force method accelerations for human interaction UAV concepts (*note that the scale for the rotational acceleration for case 6.2/6.3 is higher than the others)

G.2 Comparison of Volume between Brute Force Method and Dynamic Manoeuvrability

The maximum possible acceleration based on the brute force method is given in table G.1. These are the maximum coupled accelerations in each direction and can be used to estimate the volume of the translational and rotational acceleration to validate $w_{D,t}$ and $w_{D,r}$. This is done for the translational part of case 8.1. The volume can be approximated by a sphere, since the acceleration in all directions is equal. The volume of a sphere with radius 131.6 N is $9.5 \cdot 10^6$ m/s^2, where $w_{D,t}$ = $1.00 \cdot 10^5$ kg^{-3}. Note the difference in units, which is a result of the multiplication with the unit vector $\vec{\lambda}$ for the brute force method. The estimation of the volume is much higher than the supposed actual volume $w_{D,t}$. However, it was expected that the volume of the sphere would be slightly higher than $w_{D,t}$, since the sphere is not perfectly round and defined for the maximum radius and this difference is too high to be contributed to this. Despite the small difference, this result is considered proof that $w_{D,t}$ actually yields the volume of attainable translational accelerations for case 8.1. For case 6.1, the volume can be estimated by the volume of a cube of length 152.0, based on the volume of the brute force method, resulting in a volume of $3.51 \cdot 10^6$ m/s^2. Again a small difference in volume is expected due to the estimation of a cube for the volume, but the difference is much higher.

Based on these two examples, it can be concluded that either this brute force method or the dynamic manoeuvrability does not yield the correct volume of the attainable accelerations. To conclude which of these measures does yield the correct volume, more research is required.

	Maximum acceleration					
Case	Longitudinal [N]	Lateral [N]	Vertical [N]	x-rotation [Nm]	y-rotation [Nm]	z-rotation [Nm]
6.1/6.4	124.1	107.4	131.6	774.2	644.7	810.6
6.2/6.3	128.0	89.0	140.9	825.2	1929.1	614.7
6.5	95.2	75.3	182.3	894.9	1066.0	515.4
8.1	131.6	131.6	131.6	683.8	789.7	683.8
8.2	96.7	96.7	182.3	1187.1	866.2	434.9
10.1	126.1	112.3	129.5	723.5	646.8	651.0
10.2	88.5	84.2	182.3	843.5	920.0	453.7

Table G.1: Maximum accelerations (coupled) based on brute force method